PhD Dissertation

COMPUTER-ASSISTED ANALYSIS OF THE DEVELOPING BRAIN MOTOR SYSTEM AND COORDINATED LOCOMOTION IN THE FOAL

Ferenc Szalay DVM

Supervisor: Ferenc Hajós, MD, PhD, DSc

Department of Anatomy and Histology
Faculty of Veterinary Science
Szent István University

Budapest, Hungary

2001

CONTENTS

1.1. SUMMARY

The purpose of the present study was to correlate the structural maturation of the horse brain with the development of coordinated locomotion of the animal.

A newly emerging method of gait analysis is being based on computerized measurements of recordings of the horse moving on a treadmill. However, information collected this way is still scarce in the literature and lacks a reliable basis of evaluation. We assumed that the development of the major motor centres and pathways of the brain may serve as safe reference for evaluating gait measurements.

Equine brains from 14 days before expected birth to adulthood were fixed in formaldehyde and embedded in paraffin. After taking the outer parameters of the brains, full series of large-area coronal sections were prepared on a special microtome and stained with Nissl's cresyl violet and Haidenhain's iron-haematoxylin. Microscopic images of sections were digitized and were subjected to computer-aided image analysis. Recordings of the moving foal and adult were made either with the CODA-system or, with our newly developed computer program, based on VHS recordings.

The gross morphology of the brains and the image analysis of histological preparations suggest that in the perinatal period studied there is no substantial increase in brain size and mass, while the amount of Nissl-substance and myelin grows rapidly till postnatal day 45. Then a relative decrease of both is observed till adulthood accompanied by a doubling of brain size and mass.

In monitoring the moving horse, our home video analysis system proved to be comparable to CODA. Computer-generated curves of different joint angles during walk and trot allow a clear distinction between immature and mature types of locomotion. The same was observed for the temporal variables of stride phases.

Maturation of gait, as indicated by the above objective measurements was parallel to the structural maturation of the perinatal brain.

It is concluded that during the maturation of the equine brain, decisive changes of the motor system such as synaptogenesis and the full myelination of motor tracts may coincide with the onset of economic, target-oriented, coordinated locomotion of the developing foal.

Our studies may contribute to world-wide efforts to develop objective tools for predictions as to the future performance of the foal.

1.2. ÖSSZEFOGLALÁS

(Csikók agyi mozgató rendszerének és a mozgáskoordináció kialakulásának számítógépes elemzése)

Jelen munkánk célja az volt, hogy összefüggést találjunk a ló agyának strukturális érése és az állat összehangolt mozgásának kifejlődése között.

A számítógépes méréseken alapuló, jelen tanulmány céljaira kifejlesztett mozgásanalízis rendszer futószalagon mozgó lóról készült felvételeket dolgoz fel. A szakirodalomban rendelkezésre álló vonatkozó irodalom szegényes, megbízható értékelésre nem ad lehetőséget. Feltételezésünk szerint a főbb motoros központok és pályák fejlődése megbízható támpontot szolgáltat a mozgásanalízis eredményeinek objektív megítéséhez.

Hét ló agyat vizsgáltunk a várható ellés előtti 14 napos kortól a felnőtt korig, amelyeket formalinban való fixálást, majd az agyak külső paramétereinek felvételét követően egyben ágyaztunk paraffinba. A teljes agy keresztmetszeti preparátumokat speciális mikrotómmal metszettük le, majd Nissl krezilibolyával és Haidenhain vas-haematoxylinnak festettük meg. A metszetsorokat digitalizáltuk és komputeres képanalízis technikával vizsgáltuk. A csikó és a felnőtt ló mozgását párhuzamos CODA és VHS felvételek alapján elemeztük. A digitalizált VHS felvételeket saját fejlesztésű szoftverrel analizáltuk.

Az agyvelő átfogó morfológiai és részletes szövettani vizsgálata azt mutatja, hogy a vizsgált perinatális időszakban nincs jelentős növekedés az agyvelő méretében és tömegében, viszont a Nissl-anyag és a myelin mennyisége növekszik a 45 napos korig. Azt ezt követő, felnőtt korig tartó időszakban az utóbbi két paraméter értéke relatíve csökken, ugyanakkor ezt az agyvelő méretének és tömegének megkétszereződése kíséri.

A video felvételek alkalmazása a mozgásanalízis területén a CODA rendszerrel való összehasonlításban megbízhatónak bizonyult. Az ízületi szögeket leíró komputeres görbék, amelyeket lépésnél és ügetésnél vettünk fel, eltérést mutatnak a fejletlen és fejlett mozgásformák között. Hasonló eredményeket hoztak a lépés fázisainak megoszlására irányuló vizsgálataink is.

A fentiek alapján megállapíthatjuk, hogy párhuzamosság áll fenn a perinatális agy fejlődés és a mozgásanalízis objektív eredményei között.

Megállapítható továbbá, hogy a ló agyának maturációs időszakában a motoros rendszerben olyan döntő változások zajlanak, mint pl. teljes a myelinizáció kialakulása, a synaptogenesis, stb., amelyek egybeesnek a mozgás célorientáltságának, koordináltságának megjelenésével a fejlődő csikóban.

Eredményeink remélhetően hasznosan járulnak hozzá azokhoz világszerte folyó kutatásokhoz, amelyek a csikók felnőttkori teljesítményének korai megítélését célozzák.

2. INTRODUCTION

„A horse! a horse! my kingdom for a horse!"
(Shakespeare: Richard III. Act 5, Scene 4)

The distinguished position of the horse among domestic mammals dates back to the origins of Eurasian civilizations. Ever since the horse has been domesticated, its usefulness in locomotion, transport and warfare was realized. Particularly people living on plain areas could make use of the power, speed, and endurance of this animal. Without the horse the migration of people, the encounter of cultures and civilizations, the development of trading could not have happened as they did. But beyond all utilitarian aspects, locomotion and (alas!) wars were always important incentives for human actions. Hence all sophistication in animal breeding and husbandry, all experience and skills accumulated in dealing with animals, all efforts to ensure animal health and welfare were concentrated on this species.

The body of knowledge collected developed into a separate field of animal sciences called hippology. Hippology had its climax in the 18-19th centuries particularly when horse racing was institutionally introduced in a number of countries as a means to further improve the efficiency of horse breeding and to produce horses bred with the purpose to satisfy best the most special needs of economy as well as of imperial armies. Looking back from our times, hippology can also be viewed as a science underlying a kind of arms race that mobilized human energies. Nevertheless, the results was a close, almost intimate relationship between horse and man for which this noble animal was worth not only for its physical traits but also for its intelligence and affection to its master.

Hippology, quite understandably, focused on horse gait. Its ultimate goal was to analyze the function of equine locomotor apparatus to an extent which would allow to select the best horses for a given purpose on one hand, and to obtain a full and perfect control over the animal's behaviour on the other. The unconditional and immediate execution of instructions to make quick movements, turns, jumps or even some movements unusual for the untrained animal such as reversing, turning around lying down, etc. was a general requirement of the military horse.

These abilities were life-saving under circumstances of a fight with hand-weapons and could increase enormously the value of a horse. The military training was a crucial moment of preparation for wartime. Beside warfare, the best trained horses were also used in equestrian competitions in peacetime. These competitions require extraordinary movements, postural positions and subtle moments of the locomotor apparatus.

As it is known from Xenophone's writings the written history of the art of horse riding has started as early as in 400 b.c summarized by Magyar and Győrffy-Villám (1988). The trainers of antiquity already required different gait types from their freely moving and saddled horses. Nevertheless, a major drawback of development in riding techniques was that in the antiquity the stirrup was unknown in Europe. It was not until after the repeated attacks of nomadic armies against the borders of the Roman empire that the significance of this accessory has been realized. In the middle ages but particularly in the Renaissance the majority of European equestrian schools were established mostly in Italy. Federico Grisone has published his fundamental work "Ordini di Cavalcare" ("The rules of horse riding") in 1550 which formulated high requirements for both the rider and the horse. Parallel to the development of training techniques saddlery and harness also went through changes. From the 17th century horse riding and training schools have shown up in written accounts from Germany, England, Holland and France. After the Napoleonic wars the accent was put rather on preserving the military conventions and developing the athletic skills of horses. This transformation had a selective effect on schools but some of them are still working such as the "Cadre Noire" in Saumur, France or the Spanish riding school in Vienna. Now the "Haute Ecole" means the top of equestry grown from the base of military riding.

Hippology, however, could never develop beyond the confines of mere observation. Around the middle of the 19th century pioneer efforts were taken in cinematography which had, among other things, a dynamical impact on the development of motion analysis. Several attempts have started in different technical directions. The first scientific descriptions and notations of the equine gait were published from the 1870's. The very first correct step succession at walk

have been illustrated in hoof diagrams by Wilhelm Baumeister in 1870 (Baumeister, 1870).

Three years later Etienne-Jules Marey introduced his pneumatic device previously used in human gait experiments. As a result detailed hoof diagrams with accurate phase duration signs of each limb were generated. The principle of this device is still used in recent accelerometers. Marey, however, earned his fame from the own constructed photographic gun (Fig. 1.). This gun made 12 exposures of 1/72th of a second each and this time resolution was high enough for studying details never seen before with the human eye. In 1882 the firstly published series of images of flight of birds has focused public interest on his works. He used a single camera for recording serial images onto a single photo plate. In his pioneering studies all images appeared overlapping each other giving thereby a montage effect (Fig. 2.) but later he could separate them into series suitable for the purposes of analysis. Marey has recognized the scientific importance of his devices and expanded his observations in several directions such as biomechanics of humans and animals, aviation, aerodynamical observations of smoke trails in a wind-tunnel (Marey, 1873). His serial photographs taken of a falling cat proved the presumption that the cat during falling is able control the maneuver of limbs to face the ground by the moment of touch. This short movie earned for Marey world fame immediately. He also had several fundamental inventions and devices with respect to circulation, electrocardiography, respiration, muscle function, etc.

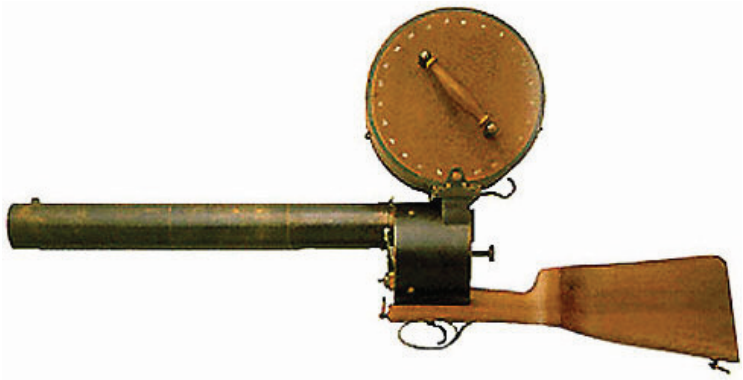

Fig. 1. Marey's photographic gun

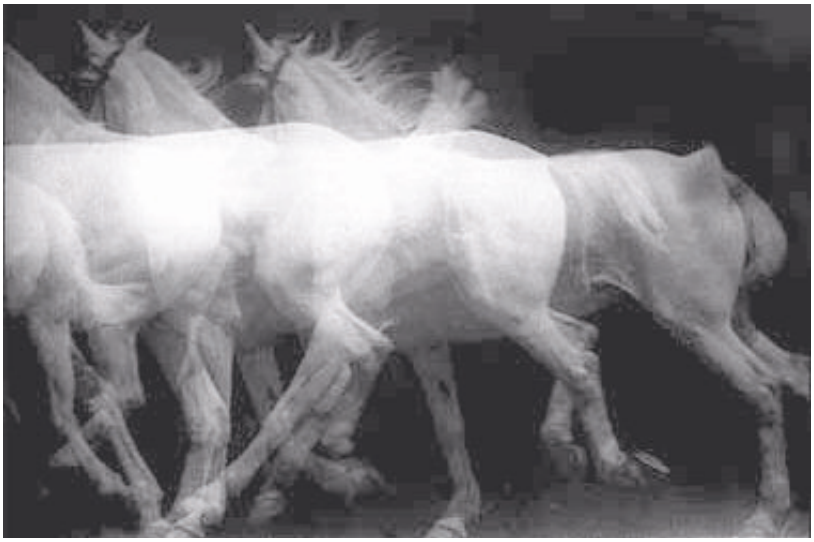

Fig. 2. Marey's serial photographs describing a horse in motion resulting a montage

Parallel to Marey's investigations Eadweard Muybridge's "movies" appeared with his still sequences taken of a running horse. This observation aimed to clarify Leland Stanford's (the owner of the horse) idea whether there is a moment of suspension when no hooves are touching the ground. Originally he used a row of still cameras and took images in a synchronized way. These images mounted on a band were called "zoetrope bands". The theory of the zoetrope bands and their appropriate display equipment the stroboscope, was established by Simon Stampfer in 1833. These bands were fixed on the inner surface of a cylinder and were viewed through apertures on the circumference. When the cylinder was mechanically rotated, still images seemed as if they were animated. Muybridge was studying different gait types, everyday movements and sport actions of humans and several animals. His films are renowned as artistically valuable works and became world-wide known.

It is noteworthy that the Hungarian historical painter, Bertalan Székely (1835-1910) was one of the pioneers in preparing zoetrope bands which were recently recovered (Szőke and Beke, 1992) from the cellar of the Budapest Academy of Fine Arts together with the artist's superb anatomical drawings of the equine skeleton (Fig. 3.). As a teacher of artistic anatomy he also made studies on the locomotion of man and animals. His "engineering" approach to anatomy and

motion analysis did not meet too much of understanding by his contemporaries. His abstractions in comparative motion analysis required detailed knowledge in anatomy from his students which did not rise his popularity. From over a hundred year distance, however, his descriptions still exceed the quality of today's publications on motion analysis. For an example, Székely described the positions and proportions of centres of gravity according to skeletal segments of the horse which is still poorly studied in today's research (Fig. 4.). He made precise sketches on the extended pendular movement of limb segments whose importance is still unknown in hippology. His calculations based on hoof diagrams are still satisfactory to be applied in the diagnosis of equine lameness. Of course, his major field of interest was the artistic representation, dynamism awaking in moments of movements. He also put an emphasis on the proportions and averages of measures of the body. As we learned from his demonstration drawings he even distinguished the proportions of different horse breeds. It was interesting to see the change of his mind as a painter in the judgment of introduction of photography. In his opinion dated from 1863, the "brightness of movement" cannot be reflected by photographs thus photography should not be accepted in art. Undoubtedly, Marey's and Muybridge's works made a deep impact on his appreciation in this matter after the 1870's. An extensive correspondence with Marey has been explored and exhibited with his other works in Budapest in 1992.

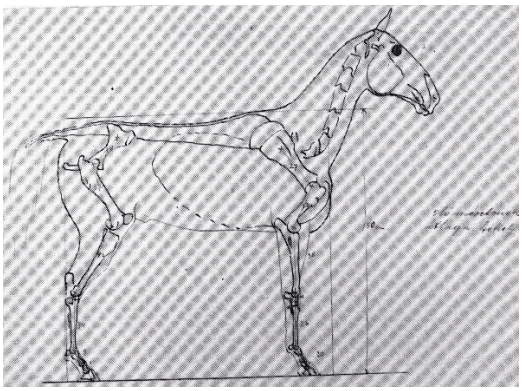

Fig. 3. Skeleton and boundaries of the horse by Székely

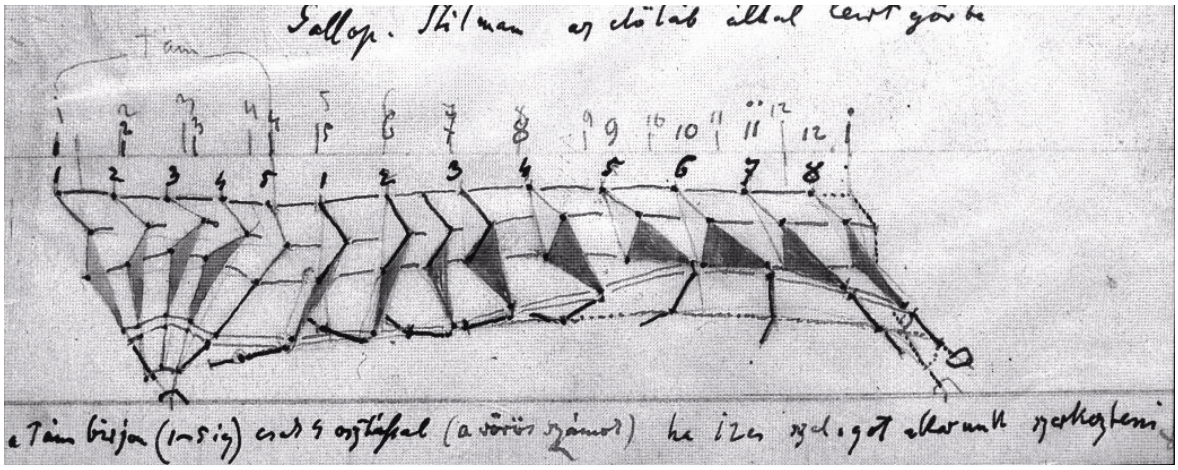

Fig. 4. Sketch of Székely displaying moments of limb segments at gallop

Nevertheless, the period of application of revolver-equipped snapshot gun and other tricky equipment was just a short prelude to the movie camera which became for the next decades the exclusive device of recording.

Films made with the conventional movie camera having the speed of 24 pictures per second could reproduce horse gait in a quality that appeared perfect for the human eye. The slow motion analysis of these recordings proved to be particularly useful in learning more about the details of different gait forms. In our times methods reached an even higher sophistication using various video cameras, including the extra high-speed CCD-cameras. The appearance of high-speed photography enabled application of high speed cameras in motion analysis (Kobluk et al., 1989; Martinez del Campo et al., 1991). After the 1970's when electronic devices have been introduced in the everyday life, special shutter systems, highly accurate synchronization of moving mechanical parts were developed for cameras. Advances in photochemical techniques enabled highly sensitive films to be produced industrially. All these improvements allowed to take pictures in the fractions of milliseconds or movies recording over 10,000 images per second.

A further major development was the introduction of the treadmill. While filming free-moving animals, unpredictable elements cannot be excluded. On the treadmill, however, animals can be kept in one place even during the fastest gait, the strategic points of limbs can be labeled with conspicuous tags to facilitate

further analysis and measurements. Of course animals must be trained to perform in the treadmill (Althouse and Auer, 1987; Fredericson et al, 1983) so that results obtained have to be critically compared to those derived from the natural free motion or motion during other tasks (Ingen Schenau, van 1980; Corley and Goodship, 1993). Nevertheless, the monitoring of the horse gait in a treadmill and the subsequent analysis of recordings, provided valuable information as to the mechanics of joints and proved to be extremely useful in the diagnosis of lameness (Stashak, 1987).

An important objective, however, of normal gait analysis was to allow a prediction of future performance in young animals, in other words, to enable the assessment of the military and sports value of foals as early as possible (Clayton, 1989; Grant, 1989, 1992; Back, 1994b). This goal, however, has never been achieved. Unfortunately, what looks even worse, up to now there appeared to be no coherent conclusion whatsoever that could have emerged from the wealth of data collected during the past 150 years. These data did not inspire any new training methods and were of no help in predictions. After all, the advantage of an instrumental scientific analysis can be accepted only if it produces predictions of higher accuracy than simple experience-based inspection. It has to be stated that , this is still not the case. When this situation is compared with the state-of-art in human biomechanical research the contrast is obvious. Human sports medicine provided a rapid development in coaching and boosting physical skills and performance. For example, in high-jumping the idea of leading through the centre of gravity of the human body mass under the bar by the flop-technique, a style of jumping developed on the basis of predictions made by motion analysis, led not only to a spectacular sequence of world records but also to an increase of the average starting height in international competitions. Thus an extension of frontiers of human physical capabilities has been achieved. Nothing of the kind can be said about horse gait analysis. The reasons may lie in the differences in the underlying knowledge of locomotion control by the central nervous system. While human neurosciences have for long clarified the pathways of skeletal muscle innervation both in the central and peripheral nervous systems, the equine central nervous system is practically unexplored. Lacking detailed information on the topography and development of the motor pathways of the horse there is no biological basis of

assessment, consequently no objective methods of improvement or selection can be introduced. Veterinary textbooks describe the gross surface anatomy of the horse brain and spinal cord but when considering the internal structure of the brain of domestic mammals they rely on descriptions derived from other species, usually small domestic mammals. This has practical reasons. The brains of the cat, dog, sheep, etc. are small enough to be fixed and embedded as a whole and cut with a conventional microtome. The method of tract-tracing is based on series of sections through the entire brain from where the course of specially stained fibres can be reconstructed. In addition to inconveniences caused by the huge body mass, the high costs of keeping and the fact that the horse is much too valuable to be sacrificed for experimental purposes, all experience suggests that the sampling of horse brains of given ages is a long and cumbersome procedure. Moreover, the size of the equine brain matches with that of the young human brain giving no chance for serial sectioning either in a conventional microtome or a cryostat.

In the veterinary clinical practice several reflexes are known and used to check the integrity of the central and peripheral nervous system (PNS, CNS). As compared to human neurology only a few of these techniques can be applied in the veterinary practice because of the limited manifestation of reactions. The anatomical and physiological background of these clinical examinations are more or less explored but there is no available information on the development of these phenomena. The theoretical description and clinical application of these examinations are already involved in the curriculum of veterinary schools which shows its importance. The exact appearance of these reflexes in ontogeny and its relationship to the maturation of the PNS and CNS is still a white spot in veterinary neurology. The development of a child can be easily controlled by performing neurological tests and comparing their result to protocols based on extensive investigations (Beck et al., 1981; Clark et al., 1988). In the infancy and early childhood these test are simple reflexes and provoked reactions as listed in Table 1. (Mumenthaler, 1989). Some of them are present only for a short period of time such as Moro's and Landauer's reflexes which vanish after a certain age. In the veterinary neurology there is no similar reflex palette and moreover the development of the known reflexes from birth till adulthood has not been clarified.

Table 1. Primitive reflexes of human infants

Name of reaction	**Age**
Postural reflexes	
Doll's eye	0-10 d
Stepping reflex	first weeks
Crossed extensor reflex	abnormal
Crossed flexor reflex	0-7-12 m
Postural reactions	
Stance response	0-4-6 m
Placing reflex	first weeks
Tonic palmar grasping response	0-3 m
Tonic plantar grasping response	0-12 m
Tonic spine reflex	first moths
Tonic neck reflexes	0-5-6 m
Tonic labyrinthic reflex	unsure
Positioning reflexes	
Head positioning reflexes	2-6 m
Landau's reflex	4-18 m
Head-to-trunk positioning reflexes	0-14 m
Moro's reflex	0-6-7 m
Balancing responses	
Support responses	7- m
Parachute reflex	6-9 m

d.: days
w.: weeks
m.: months
y.: year

Taken together, it can be said that lacking any firm reference, to date the results of gait analysis cannot be interpreted in biological terms. This uncertainty has both theoretical and technical reasons.

Surveying the theoretical gaps in knowledge the question boils down to the poor understanding of the topography and development of the major motor pathways in the horse.

Our objective was therefore to describe the motor system of the adult horse brain and to correlate it with brains from various developmental periods of horse embryos and foals.

Tract-tracing is based on the demonstration of bundles of myelinated fibres. A number of staining technologies have been developed to visualize the myelin sheath (see Pannese, 1994). On the other hand, formation of the myelin sheath around an axon is a process taking place in the late embryonic and early postnatal period (Río Hortega, 1930). There are, however, wide interspecies variations in the timing of myelination. Some animals are born with an almost unmyelinated central nervous system, while others in differently advanced stages of myelinization. Some pathways are notorious by their late myelination being protracted into early adulthood. This applies particularly to the motor system. It is also important to note that the acquisition of the myelin sheath also means the functional maturation of an axon since it becomes only then capable of a full velocity (saltatory) impulse conduction (Lillie, 1925; Huxley and Stämpfli, 1949). This is clearly reflected by the pattern of movements of the newborn. Species with more advanced myelination of their motor pathways at birth develop earlier their independent locomotion than the ones with neonatally poorly myelinated motor tracts.

This parallelism between the degree of neonatal locomotion and the advance of myelination of the motor pathways encouraged us to take myelination as a major morphological reference to compare motion patterns with.

Recent advances in microtome technology – initiated primarily by the demand to cut series of sections from whole adult human brains – led to the construction of a special high-performance microtome on which large-size sections can be readily cut. This was completed with the manufacturing of large-size slide glasses and special coverslips, as well as with the modification of the specimen stage of the microscope such that it can carry large area preparations. This equipment, particularly when joined through a video camera to a computer was thought to be suitable to map the adult and young horse brains.

3. AIMS AND SCOPE

Our primary aim was to provide a morphometric analysis of the adult and developing horse brains. By this we hoped to obtain some basic reference data for further functional morphological studies. To this end, we attempted

(i) to monitor the cytoarchitectonic maturation of motor centres, particularly the motor areas of the neocortex, striatum, brainstem and the cerebellar cortex

(ii) to follow the course of myelination of motor centres and pathways in areas of the brain which may be instrumental in the innervation of the skeletal musculature and in the control of motor coordination.

(iii) to get an objective measure of brain growth from late fetal to young adult age, including size and volume increase, surface increase and the degree of gyrification.

Secondly, efforts were made to correlate histologically defined maturational states of the motor centres and pathways with the development of motion patterns as distracted from video recordings of animals either performing on a treadmill or moving free.

Finally, we decided to express our findings both histologic and functional, in terms of an objective, automated method, the computer-assisted image analysis which needed a substantial development to be adaptable for these purposes.

The present work is an endeavor to open up new possibilities in the prediction of future sport value of foals. Results may be also relevant to equine neurology.

4. MATERIALS AND METHODS

4.1. Histology

Equine brains were removed from the skull in the late prenatal and the postnatal period up to 2 years of age. The following brains from half/quarter-bloods were used in this study:

- Brain 1. Fourteen days before calculated birth
- Brain 2. Seven days before calculated birth

Fetal brains were obtained from newborns lost in premature births

- Brain 3. Newborn,

Newborn brain was obtained from an animal born in due time but lost.

- Brain 4. Four-day-old
- Brain 5. Six-week-old
- Brain 6. One and a half-year-old
- Brain 7. One and a half-year-old

Postnatal brains were obtained from animals in which infectious and/or neurological diseases were excluded. Lost animals were kept at 4 C° temperature. Sampling was carried out 2-4 hours after death. After sawing-off the calvaria, the brains were carefully lifted, cranial nerves and hypophyseal stalk were transected, and the medulla was truncated at the level of C2. Then the brain could be removed from the skull without major surface damages. Brains were cleaned from the meninges, weighed (14 days before birth: 305 g, 7 days before birth: 303 g, newborn: 312 g, 4-day-old: 311 g, 6-week-old: 326 g, 545-day-old: 608 g, 560-day-old: 615 g) and their rostrocaudal extent was measured.

Whole brains were fixed in 4-10% formaldehyde buffered at pH 7.4 with phosphate buffer. The duration of fixation was 3-8 months depending on the size of the brain. Following fixation, the rostrocaudal extent of brains was measured again, photographed (Fig. 5.) and immersed for a week into 1% eosin solution. Then they were dehydrated in graded ethanol, each phase lasting 2-5 days, and embedded through chloroform in paraffin. Twenty-micron thick serial sections (full series) were cut in the frontal plane from the entire specimen with a TETRANDER

Large-Section Microtome. In 500 µm distances, three subsequent sections were mounted on large-area slide glasses. Every first section was processed for Nissl's cresyl violet staining to reveal cytoachtecture, every second for Haidenhain's iron-haematoxylin for the demonstration of myelin sheath, and every third was left blank. The rest of the sections were stored on special plates covered with foils. They were kindly archived by the specially air-conditioned section-store of the O. and C. Vogt. Institute for Brain Research at the Heinrich Heine University of Düsseldorf (Germany).

The blanks, due to the pre-embedding eosin treatment showed in light pink the section contours helping to remove excess paraffin from the slides which greatly facilitated of further processing.

Fig. 5. Lateral view of an adult horse brain followed by fixation

4.2. Image analysis

The comparison of results in biological and medical research requires a strong emphasis on objectivity. Visualization of results is biased by a number of factors but detailed description of the applied equipment, technique and protocols makes production of results easier and improves objectivity. Nowadays, when several parameters are provided by international industrial standards, scientific data are more compatible. Notwithstanding, a high degree of subjectivity burdens evaluation. Standardization of evaluation of biological features and phenomena is now a routine in applied mathematics.

When images are produced as a result of scientific research, computer based image analysis can be applied in the evaluation phase of work. Photographs, microphotographs, even motion pictures have to be translated into a language understandable for computers. There are two major approaches in this translation methods of image understanding: shapes can be described mathematically as vectors thus all shapes of an image including background, surface pattern, etc. can be given as a set of functions. Images containing this sort of data are called vector graphics. The other method accounts image as a cluster of points arranged in a matrix where x and y coordinates of the matrix correspond to the width and height of the image. Basics of matrix calculations has been established already in the 70's (Rosenfeld and Kak, 1976) and theoretical importance of them in image understanding has been recognized. After the 90's, calculating capacity of computers especially in the field of floating-point calculations enabled us to carry out high performance computations. Nowadays, a personal computer of an average performance is suitable for processing medium size biomedical images. This processing technique includes measurements of area, perimeter, length, elliptic axes, XY-coordinates, determination of centre of gravity, etc. Beside these parameters density of colours or gray values can also be expressed.

A "black and white" image in informatics consists of pixels (elements of a bitmap image) organized in a matrix and represented by a value in a gray scale ranging from 0 to 255 (Figs 6, 7). Mathematically this corresponds to a three-dimensional matrix where x and y values are equal to x and y coordinates of the image and z values are given by the gray scale density (Figs 8, 9).

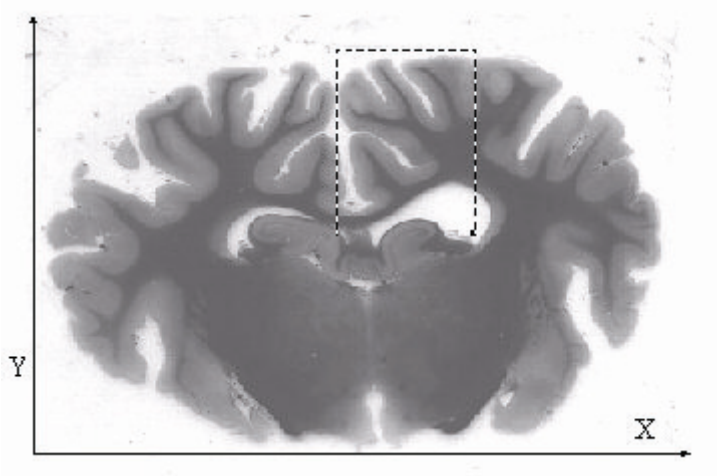

Fig. 6. A section from an equine brain with a selection in the right hemisphere. Square within the dashed line is converted into a 3D enlarged diagram in Fig. 7.

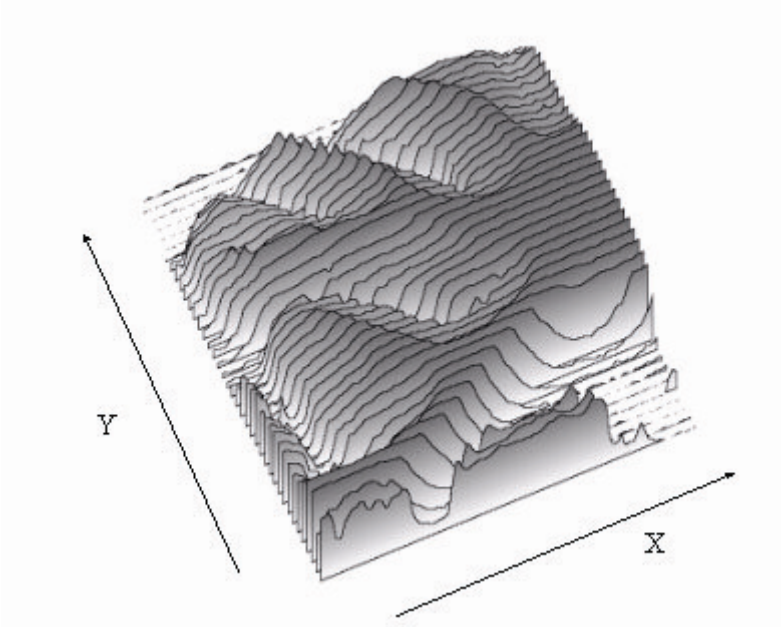

Fig. 7. (see Fig. 5.)

In most of the cases 256 grades of gray scale are sufficient to visualize features of interest. In informatics this image file is characterized as an 8 bit depth gray scale image. The depth of an image is given with an exponent of two which gives the range of possible values (2^8=256) where 0 represents white and 255 represents black. This is the image quality of recent MRI, CT, or ultrasound equipment used for clinical purposes.

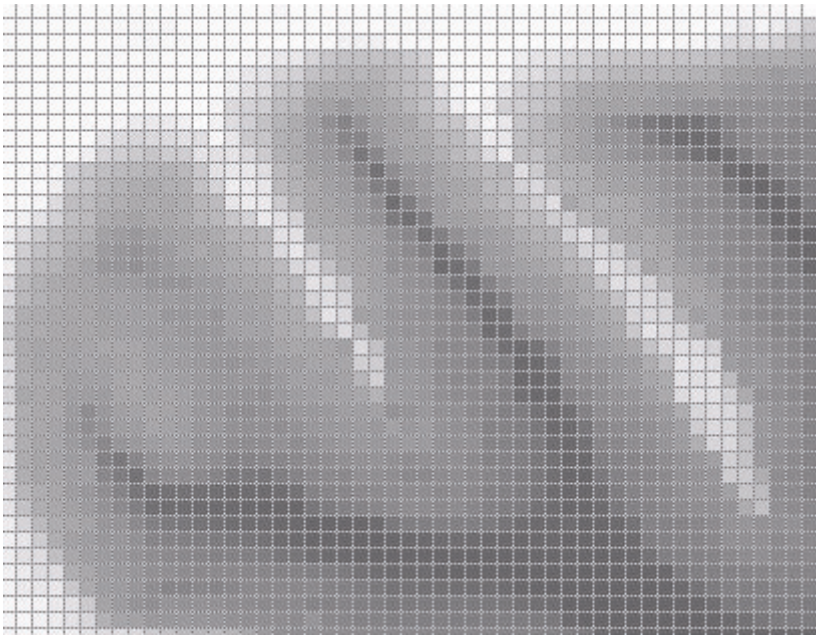

Fig. 8. Pixel level magnification of the brain surface.

,0,0,0,0,0,15,0,15,15,15,15,0,0,0,0,0,0,0,0,0,0,0,0,0,0,0,15,15,15,15,15,15,0,15,0,0,0,0,0,0,0,0,0,0,0,15,0,15,0,0,0,0,0,0
,0,0,0,0,0,0,0,15,0,15,0,0,15,0,0,0,0,0,15,0,15,15,15,15,16,16,31,31,31,31,31,31,16,16,16,16,0,0,0,0,0,0,15,15,15,15,15,16,16,16,16,16,16,16,16,16
,0,0,0,0,0,0,15,0,0,0,0,0,0,0,0,0,0,0,0,0,15,15,16,31,31,47,48,63,64,63,64,63,63,48,47,15,15,0,0,15,15,15,15,31,31,32,32,47,48,48,63,63,63,63,63,63
,0,0,0,0,0,0,0,0,0,15,0,15,0,0,0,0,0,0,15,15,31,31,32,47,47,63,64,64,64,79,79,64,64,63,48,16,15,15,0,15,15,31,31,47,47,48,48,63,64,64,64,79,64,79
,0,0,0,0,0,0,0,15,0,0,0,0,0,0,0,0,15,16,31,32,47,48,63,64,79,79,80,79,80,79,64,64,63,31,16,15,0,15,16,32,47,48,48,64,79,79,79,80,80,80,80,80
,0,0,0,0,0,0,0,0,0,0,15,0,0,0,0,0,15,15,31,32,47,48,63,64,80,95,95,95,95,80,80,79,64,63,47,16,15,15,16,32,47,48,63,63,79,80,80,95,95,95,95,96,96
,0,0,0,0,0,0,0,15,15,15,15,15,15,0,15,16,32,47,48,63,79,79,95,96,96,111,95,95,80,79,79,64,48,32,16,16,16,32,48,48,64,64,80,80,95,95,96,96,96,111,111
,0,0,0,0,0,15,15,16,16,31,31,16,16,15,15,31,32,47,63,64,79,80,95,111,112,112,111,96,95,95,80,79,63,63,48,31,16,31,47,64,64,80,80,95,96,111,111,127,127,128,143
,0,0,0,0,0,15,31,32,32,32,32,32,31,32,16,16,31,48,48,64,79,80,96,96,112,112,127,96,96,80,80,80,79,64,63,47,16,31,48,64,64,79,80,95,96,96,111,111,112,128,143
,0,0,0,15,15,31,32,47,48,48,48,47,48,32,31,31,31,47,48,64,79,80,95,96,111,127,127,112,96,95,95,80,79,79,64,48,32,31,48,63,64,79,80,95,95,96,111,111,112,112,127
,0,0,15,16,31,47,48,63,63,64,63,64,63,47,32,32,31,32,47,63,79,80,95,96,96,112,127,128,112,96,95,95,80,79,79,63,48,47,48,48,64,79,80,80,95,95,96,96,111,111,112
,15,15,15,47,48,63,64,64,79,79,79,79,79,63,48,31,31,31,31,48,64,79,95,95,96,111,112,128,127,111,111,96,95,80,79,79,64,64,48,47,48,79,79,79,80,95,95,96,96,111,111
,0,15,16,47,63,64,79,79,80,80,80,79,80,64,48,47,16,16,31,47,79,79,80,95,96,96,112,127,128,127,111,96,95,95,95,80,64,79,48,47,47,63,79,80,80,80,95,95,96,96,111
,15,15,32,63,64,64,79,80,80,80,80,80,80,79,64,48,31,31,31,32,63,79,80,95,95,96,96,112,128,128,112,111,96,95,80,80,79,64,63,63,47,47,80,79,80,80,80,80,95,96,96
,16,31,32,63,64,64,80,80,80,95,80,80,80,79,79,64,48,32,31,32,47,63,80,80,95,96,96,111,127,128,128,127,96,95,95,80,80,79,64,64,63,47,63,64,79,79,80,80,95,96,96
,31,47,48,64,64,79,79,95,95,95,95,95,95,80,80,79,79,63,63,48,32,32,47,79,80,95,95,96,96,112,128,128,128,111,111,96,96,95,80,80,64,64,63,48,48,64,79,80,80,80,95,96
,47,48,64,79,79,80,95,96,111,96,96,95,95,95,80,80,79,79,79,48,32,32,64,79,80,80,95,96,111,111,127,128,128,127,111,96,96,95,80,80,79,79,48,47,47,48,79,80,80,80,95
,48,64,64,79,80,95,96,96,111,111,96,96,96,95,80,95,80,80,79,64,63,32,31,48,64,80,80,95,95,111,111,112,127,143,128,127,111,96,96,95,80,80,79,79,48,47,47,47,79,79,95,95
,63,64,79,80,80,95,96,111,111,111,96,96,96,95,95,80,80,80,79,64,63,32,47,48,79,80,95,96,96,111,112,112,143,143,128,112,96,96,95,95,95,80,79,64,48,32,47,48,79,80,80
,64,79,80,80,95,95,96,96,96,96,111,96,96,96,96,96,95,80,80,80,79,64,63,32,47,48,79,80,95,96,111,111,111,112,127,128,143,128,112,111,96,96,96,95,80,79,63,47,32,47,47,64
,79,80,80,95,95,95,95,95,96,96,96,96,96,96,96,95,95,95,80,79,79,48,32,32,63,80,95,96,96,111,111,111,112,127,127,143,143,128,112,111,96,96,96,95,80,79,64,47,32,47,48
,80,80,80,80,80,95,96,95,95,95,95,96,96,96,96,96,95,95,95,95,80,79,64,47,32,48,95,95,96,111,111,111,112,112,127,128,143,143,112,111,111,111,111,96,95,95,80,79,47,47,32,48
,80,80,95,95,95,95,95,95,96,95,96,96,96,96,96,111,96,95,95,95,95,80,80,79,64,47,48,64,95,96,96,111,111,112,112,112,127,144,143,128,112,111,111,96,96,95,95,80,63,32,32,47
,80,95,80,95,80,95,80,95,95,95,95,96,96,96,96,96,96,96,95,95,80,80,80,79,64,48,64,95,96,96,111,112,112,112,127,128,143,143,128,127,112,111,111,96,95,95,79,63,47,32
,80,95,95,95,95,95,95,80,95,95,95,96,96,96,96,111,96,96,96,95,95,95,95,95,95,79,47,63,80,96,111,111,111,112,112,112,127,128,143,143,143,127,112,111,96,96,96,95,79,63,48
,80,95,80,95,95,95,95,95,80,95,95,95,95,96,96,96,111,96,96,96,95,95,95,95,95,80,48,48,80,96,96,111,111,112,112,112,127,127,127,143,144,144,128,112,111,111,111,96,96,95,79,63
,80,80,95,95,95,95,95,95,95,95,95,95,96,96,96,96,111,96,96,111,96,96,96,95,95,95,80,79,95,96,96,96,111,96,111,111,112,112,112,127,127,128,144,144,143,127,112,112,111,111,96,96,95,79
,80,80,95,95,96,111,111,96,96,95,95,95,95,95,96,96,111,111,111,112,111,111,111,96,111,96,96,96,96,96,96,96,111,96,111,111,111,112,127,127,127,128,143,144,143,128,127,112,112,111,111,111,96
,80,95,95,96,111,111,111,96,96,95,95,95,96,96,111,96,111,111,112,111,111,111,96,96,96,96,96,96,96,96,96,96,111,111,111,112,112,112,127,127,128,128,144,143,143,127,112,112,112,111,111,111
,80,95,95,95,96,112,112,111,111,96,96,95,96,96,111,111,112,112,112,111,112,111,111,111,111,96,96,96,96,96,96,96,111,111,111,111,112,127,127,127,128,128,143,144,143,128,127,112,112,112,111,111
,80,95,95,96,96,111,127,128,112,112,111,111,96,111,112,112,112,112,112,112,112,112,111,111,111,111,111,111,111,111,111,111,111,112,112,127,127,127,143,143,144,144,128,127,127,112,112,112,111
,80,95,95,95,96,96,127,127,128,127,112,111,111,112,112,127,127,128,128,128,127,127,112,112,112,112,111,111,112,112,112,112,112,112,112,112,127,127,128,128,143,144,144,143,127,127,127,127,112,112
,79,80,95,95,96,96,112,127,128,128,127,127,127,128,128,143,128,143,128,128,128,112,127,112,112,111,112,112,111,111,112,112,112,111,112,112,112,127,127,127,128,128,143,143,144,144,143,128,127,127,112,112
,79,80,95,95,96,111,112,112,128,143,143,143,143,143,143,144,143,144,144,143,143,127,127,127,127,112,112,112,111,111,112,112,112,112,127,127,128,128,143,144,143,144,144,143,128,127,127,112,112
,64,79,80,95,96,96,111,112,127,128,143,143,143,144,143,144,143,144,144,144,144,144,144,143,128,127,127,127,127,127,112,112,112,112,112,112,112,127,127,127,128,128,143,143,144,144,144,143,143,128,127,127,127,112
,48,79,80,80,95,95,111,111,111,127,128,128,143,143,143,143,143,143,143,143,143,144,143,143,143,144,144,143,143,128,127,127,127,127,127,127,127,128,128,143,143,144,143,144,144,144,144,144,128,128,112,127
,47,63,79,95,95,96,96,111,111,112,127,127,127,128,128,128,128,143,143,143,144,144,144,144,144,144,144,144,144,143,143,143,143,128,143,143,143,143,143,143,144,143,144,144,144,144,144,144,144,143,144,128,127,127
,32,48,64,80,95,96,96,96,111,112,112,112,127,127,127,127,128,128,128,128,143,143,143,144,144,144,144,144,144,144,144,144,144,144,144,144,144,144,144,144,144,144,144,144,144,144,128,128,127
,31,32,63,79,95,95,96,96,111,111,112,112,112,112,127,127,127,127,128,128,128,128,143,143,143,144,144,144,144,144,144,144,144,144,144,144,144,144,144,144,144,144,144,144,144,144,144,144,144,143,143,127
,31,32,32,64,80,95,96,96,96,111,111,111,112,112,112,112,112,112,127,127,127,127,127,128,128,143,143,143,143,143,143,144,144,144,144,144,144,144,144,144,144,144,144,144,144,144,144,144,144,144,144,144
,31,31,31,48,64,95,96,96,96,111,112,127,112,112,127,112,112,112,112,112,112,112,112,127,127,127,127,128,128,143,143,143,143,143,143,143,143,143,143,144,144,144,144,144,144,144,144,144,144,144,144,144,144,144
,16,16,31,32,48,64,95,96,111,111,111,111,112,112,111,112,112,112,112,112,127,112,112,112,127,127,127,127,128,128,128,128,128,143,128,143,143,143,143,143,144,144,144,144,144,159,144,144,144,144,144
,15,16,16,31,47,63,80,95,96,111,111,111,96,111,111,111,111,112,112,112,112,112,112,112,112,127,127,127,127,128,127,128,128,128,128,127,128,128,127,128,143,128,143,144,144,144,144,144,144,144,144,144,144,144
,15,16,16,31,32,47,79,79,79,80,95,95,95,95,96,96,96,96,111,111,111,111,112,111,112,112,112,127,127,127,127,127,127,127,127,127,127,127,127,127,128,128,143,143,144,144,144,159,144,144,144
,15,15,16,16,31,32,32,32,47,48,63,63,79,79,79,79,79,95,96,111,111,111,112,111,112,112,112,112,112,112,112,112,112,127,127,127,127,127,127,127,127,127,128,143,143,144,144,144,144,144,159
,15,15,15,16,16,16,32,47,63,79,80,80,95,95,96,95,95,95,79,80,95,96,111,111,112,111,112,112,112,112,112,127,127,127,112,112,127,127,127,127,127,127,127,128,143,143,144,144,144,144
,16,16,16,16,16,31,47,79,79,95,95,95,96,96,96,96,96,96,95,80,80,96,111,112,111,111,112,112,112,112,112,112,127,127,112,112,112,112,127,127,127,128,143,143,143,144,144,144
,16,16,16,16,16,32,64,80,95,95,96,96,111,96,111,111,111,96,96,96,96,95,95,96,96,95,96,111,111,111,111,112,112,127,112,112,112,112,112,112,112,112,112,127,127,127,128,143,144,144,144
,16,15,16,16,31,47,80,80,96,96,111,111,111,111,111,111,111,111,111,111,111,96,96,96,96,95,79,80,96,96,111,111,111,111,112,112,112,111,112,112,112,112,112,112,112,127,127,127,128,143,143,144
,15,16,15,16,31,47,80,95,96,96,111,111,111,112,112,111,111,111,111,111,111,111,96,96,95,80,79,80,96,96,111,111,111,111,111,111,112,111,111,112,111,112,112,112,112,127,127,127,128,143,144
,16,15,15,16,32,63,80,95,96,111,111,112,112,112,111,112,112,111,111,111,111,111,111,96,111,96,96,95,64,64,79,95,96,96,111,112,111,111,112,112,112,111,112,112,127,112,127,128,127,128,143,143
,15,16,15,31,32,63,95,95,96,111,111,111,112,112,112,112,112,112,112,111,111,111,111,96,111,96,96,79,64,64,80,96,96,111,111,111,111,111,111,112,111,112,112,112,112,112,127,127,127,127,128,143
,16,15,16,31,32,64,95,96,96,111,112,112,112,127,112,127,112,112,111,112,111,111,111,111,96,96,96,95,80,64,79,80,80,80,95,95,96,111,112,112,112,112,112,112,112,127,127,127,127,128,143
,16,16,16,31,47,63,95,95,111,111,112,112,112,127,128,127,127,112,112,112,112,111,111,111,111,111,96,96,80,64,63,63,63,79,95,111,111,111,112,112,112,112,112,127,127,127,127,127,128,128,128
,16,31,31,31,47,64,95,96,96,111,112,112,112,128,128,128,128,127,127,112,112,112,111,111,111,96,96,111,95,95,80,63,48,63,63,80,111,111,112,112,112,127,127,127,127,127,127,128,127,128

Fig. 9. The numerical matrix of the pixel values of Fig. 8.

Images gained from biomedical research should reflect sizes, proportions, shades or colours in an undistorted way. Optics of research microscopes and cameras should meet this requirement as well as digital imaging tools. During the purely digital processing of images further distortion may not occur. When images are present as a set of numeric data, each element of the set should be handled equally. This means that values of pixels can be increased or decreased linearly or non-linearly but in any case equally. For instance, adding a constant value to each pixel, darkens the entire image, multiplying with a constant enhances contrast by a more intense increasing of darker pixels. These operations correspond to data transformations in mathematics which are permissible techniques from the statistical point of view.

It is important to note, however, that linear change of gray values is not followed by linear change of density of an image due to the loss of illumination in the transmitting medium. The recognition of this logarithmic correlation is expressed by Beer's low:

$$OD = \text{Log } 10 (I_0/I) \qquad (1)$$

where OD: optical density

I_0: incident light

I: transmitted light

In recent frame grabbers and CCD cameras used for digitization of biomedical images this logarithmic relationship has been approximated to linearity. Nevertheless, when absolute values are measured calibration of the complete set of applied equipment is required. For instance, when a series of proteins on a gel is investigated a standard gel is also to be measured. When staining intensity of an image is measured the unstained area can be used as a zero point reference. All the measurements of the same image can be expressed with respect to the reference area as a proportion or percent of it.

Selection of regions in a digital image called segmentation can be performed manually of automatically. Manual circumscription of features in an image file is usually precise enough but it is time-consuming when it has to be done on a series of images. Automatic selection of parts of an image is based on pixel level

operations. Automatic measurement of the stained area in a tissue means that the area has an increased density related to the environment (background) which can be delineated by isolating a range of values on the gray scale. This region of interest may be a polygon or any irregular shape. The size of the segmented area is strongly influenced by the density relationships of features of an image. Staining techniques in histology cannot be standardized to reach the quality of automatic segmentation, therefore, modification of the gray value range is needed image by image. In other words, if a section is darker or lighter than the adjacent one, differences can be eliminated by additions or subtractions of pixel values. Indifferent areas of sections such as tissue-free fields can be used as reference fields within one specimen. In computer-based image analysis, area measurement means the addition of number of pixels covering the selected area. Apparently, this is a linear method with quadratic measurements but all operations of area measurements of classical geometrics can be applied in one to one like in integral calculations.

In length measurement also the number of pixels are calculated along the selected line. When measuring the perimeter of a shape the problem of pixel relationship might occur. The major question of neighborhood analysis is how the contour pixel should touch the perimeter of the shape: with one or two sides or with the corner. Especially in case of small shapes the particles touching only the edge with their corner can multiply the number of pixels calculated when perimeter is measured. In most of the image analysis softwares the parameter "particles touching the edge" can be switched on or off. Both settings can be applied but it is not recommended to switch within one series.

Histological slices were digitized with a flatbed scanner at 150 dpi resolution as 8 bit gray depth. In the NIH Image 1.62 image analysis software (Wayne Rasband, National Institutes of Health, USA) the size of digitized images was readjusted to the same proportion to meet the requirements of comparison of dimensions.

4.3. Measurements

4.3.1. Contour and area measurements and related calculations

The sharpest contours were seen in the Nissl-stained material. A rough contour of each section defined at segmentation of low magnification gave the outer perimeter (C_{out}). At higher magnification all the sulci became clearly identifiable and their total perimeter (C_{tot}) could be drawn. The relationship of the outer perimeter to the total perimeter is similar to the arachnoid and pial surfaces. The depth of the sulci defines the amount of gray substance or gyrification in other terms. The quotient of C_{out} and C_{tot} is the gyrification index (GI; Wosinski et al, 1996) (Fig. 10.).

$$GI=C_{out}/C_{tot} \qquad (2)$$

Beside the perimeter, the area of each section has been determined. Principal elements of the brain such as the hemispheres, cerebellum and the brainstem were measured discretely. Where principal elements join each other (cerebellum and brainstem, hemispheres and mesencephalon), the line connecting the dorsal and ventral end-points of the full hemispheric surfaces showed the demarcation line between brainstem and hemispheres. The quotient of area and perimeter of demarcated parts was calculated in each section (see Appendix). The value of this quotient varies depending on the degree of convolution of the surface: it is smooth and low in the brainstem and high at the hemispheres.

Fig. 10. Summarizing figure of two kinds of contours. The outer contour (C_{out}) is represented by dashed line, the continuous line corresponds to the total contour (C_{tot}).

4.3.2. Measurement of territorial amount of myelin

4.3.2.1. Total sections and demarcated units

The total area of each section was measured on the Nissl-stained sections, while myelin stained sections were segmented for defining the total territory of myelin by sections. This way the sum of the myelin amount could be calculated and related to the entire brain size by adding the values obtained in the individual section.

Since areas of hemispheres, cerebellum, brainstem and mesencephalon have been quantified discretely, the same myelin determination was performed on each demarcated unit. The highest grey-value territory within the section was taken as 100 (the most advanced region of myelination), and the rest was expressed as percent of the total.

4.3.2.2. Circumscribed motor tracts and areas

Within the sections the tracts which may play important role in the execution and coordination of functions of the locomotor system were segmented manually.

We concentrated our attention on the following areas:

- internal capsule
- the brainstem portion of the pyramidal (corticospinal) tract
- the extrapyramidal nuclei and tracts
- the corpus callosum

The territory of the measured regions and the amount of myelin related to the reference areas were calculated. The two major reference areas were the cerebral cortex as a minimum and the optic nerve as a maximum density of myelination. In equines the optic pathway appears to be fully myelinated by birth (Froriep, 1891; De LaHunta 1997) therefore it seems to be an appropriate reference area in sections where it occurs. In specimens where no optic fibres were available amount of myelin was related to the portions of the best myelinated regions (see Chapter 5.3.).

4.3.3. Cytoarchitectonics of motor centres

The cytoarchitectonics of the primary motor cortex (Brodman 4 - precruciate gyrus) and the secondary motor cortex (Brodman 6 - postcruciate gyrus) was studied. Density of pyramidal cells of layers 3 and 5 was measured by segmentation of their cell bodies and expressed as percentage of total cortical area.

In the cerebellum, the perinatal migration of granular cells was investigated from the external granular cell layer through the ganglionic layer to the final (internal) granular layer. The amount of cells was determined with densitometric segmentation in the external granular and molecular layers.

The density of Purkinje cells was estimated by calculating the number of cells intersecting a line drawn along the layer of Purkinje cells.

4.3.4. Observation of brain slices on MRI sequences

Series of MRI images were taken from both of the two adult brains. After the removal from the skull a 6 months long period of fixation followed. MRI sequences consisted of 256 coronal sections. A three-dimensional reconstruction of sequences was made in NIH Object Image 1.62 software (Wayne Rasband,

National Institutes of Health, USA) in order to assist identification of anatomical features. Unlike in histological sequences, positioning of slices following each other was correctly adjusted in the MRI series, therefore their three-dimensional reconstruction could be easily performed. The benefit of the MRI reconstruction - as compared to surface pictures of the brains (Fig. 5.) - was the possibility to define the relationship of features to the inner structures which are not visible in the surface pictures (such as the primary motor cortex to the corpus callosum).

4.3.5. Gait observations using a VHS home video camera

Pilot studies have been made on the comparison of commercially available VHS video cameras to specially developed CODA-3 (Cartesian Optoelectronic Digital Apparatus, Charnwood Dynamics, Loughborough, UK) motion analysis system (Mitchelson, 1988; Schamhardt et al., 1992; Back et al., 1993) in order to confirm accuracy of the non-professional VHS cinematography.

In order to compare results of both systems, parallel recordings were taken. Motion of a 5-year-old Dutch warm blood gelding recorded followed by a 5 minutes warming up exercise on a treadmill. Recordings have been taken from a left lateral view at 8 m distance. The observed gait types were walk, trot and left lead canter at 1.6, 4 and 7 m/s speed, respectively. For the sake of comparison the same stride of each gait types has been measured in both systems. Fore- and hindlimbs were investigated in different recordings. In the accuracy checkup, moments of each video frame of 13 strides of a trot at 4 m/s have been identified and compared in the dataset of CODA system. Identification of the same event recorded by both systems was assisted by a timer device connected to CODA.

In the CODA recordings 11 photodiodes have been glued to the skin (van Weeren et al., 1992) on the forelimb and 10 on the hindlimb at the anatomical features indicated in Table 2. In order to separate strides from each other, signals of an accelerometer (Lanyon, 1971; Schamhardt et al., 1994) fixed on the hoof have been used (Back et al. 1995a, 1995b).

Table 2. Anatomical positions of markers on the limbs

	Forelimb	Hindlimb
1	heel	heel
2	toe	toe
3	coronary band	coronary band
4	distal end of the metacarpus	distal end of the metatarsus
5	proximal end of the metacarpus	proximal end of the metatarsus
6	lateral styloid process of the radius	lateral malleolus
7	attachment of the collateral ligament of the elbow	attachment of the collateral ligament of the stifle
8	lateral epicondyle of the humerus	lateral epicondyle of the femur
9	caudal part of the greater tubercle on the humerus	cranial part of the greater trochanter
10	distal end of the spine of the scapula	tuber coxae
10a	a marker in between	
11	proximal end of the spine of the scapula	

The same skeletal markers have been visually emphasized by gluing 40x80 mm size light yellow TESA (Beiersdorf AG, Hamburg, Germany) adhesive tape strips perforated in the centre allowing light transmission for the CODA photodiodes. The markers could easily be distinguished on the still images of video recordings.

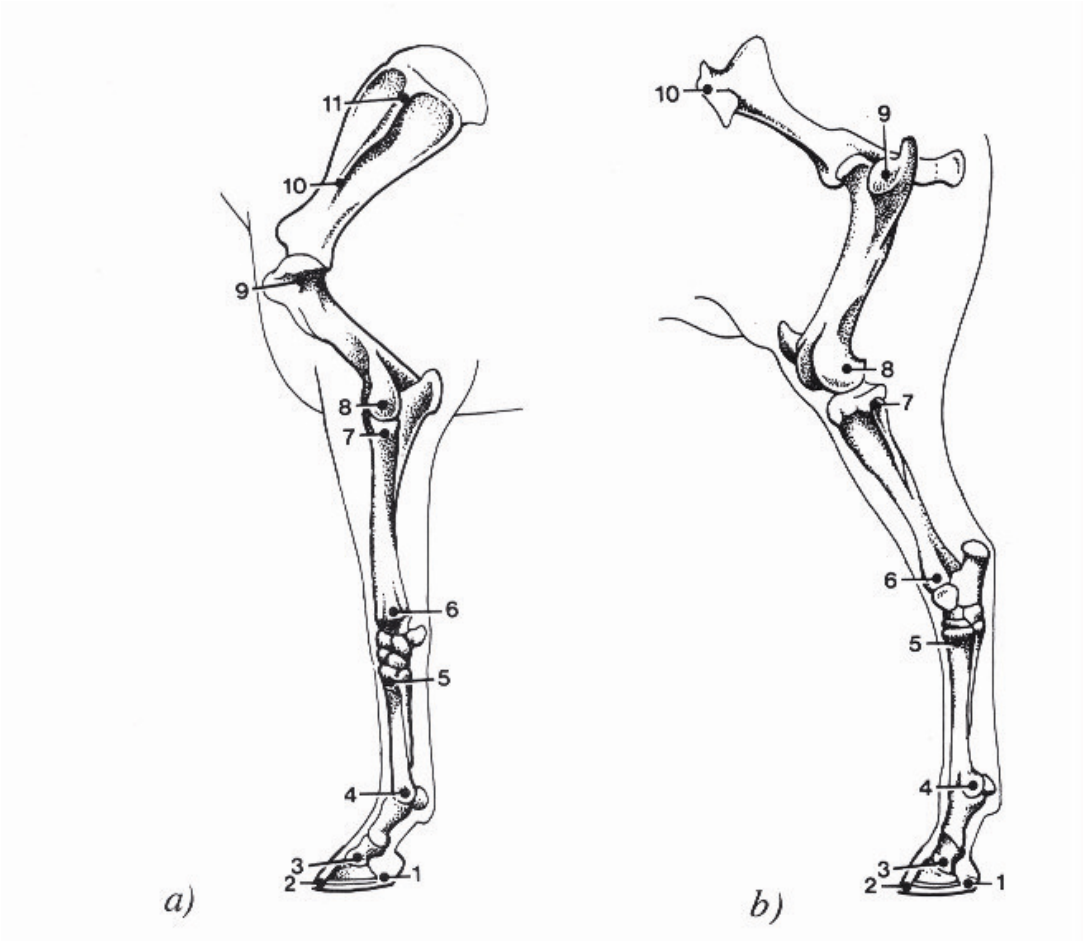

Fig. 11. Anatomical features visualized by markers

4.3.5.1. Treadmill

Video recordings have been taken by an MS1 Panasonic CCD VHS camcorder (Matsushita Electric Industrial CO., Ltd., Japan) under normal daylight circumstances. At indoor recordings 1000-1500 lux of illumination has been measured by illuminometer (Model 5200, Kyoritsu Electrical Instruments Works, Ltd., Japan). The horse was running on a treadmill and video recordings have been taken from 8 m distance on the left side. Autofocus has been switched off, shutter value has been set to 1/500 sec and the diaphragm has been adjusted according to actual illumination. Because of the parallel recording with both systems, usage of an extra artificial light source had to be avoided. In cases when the accuracy was compared the timer device was connected to CODA which has been recorded in video images. The digital timer device displayed thousands of seconds of elapsed time as digital characters and flashing LEDs at the same time.

In still video images both the digital characters and LEDs were recognizable with the exception of the ones displaying thousands of seconds.

4.3.5.2. Computer image processing system

Video recordings were played back on a SONY VCR (SONY Corp., Tokyo, Japan) used in freeze-frame mode. Digitization was carried out frame by frame and temporarily stored on hard disk. Digitization has been performed using a Macintosh 8100/80 AV computer with a built-in digitizing board. Image files have been stored as 367x288 pixels of size at 24 bit depth. Image analysis was carried out with NIH Image 1.62 (Wayne Rasband, National Institutes of Health, USA) application. Sequence of digitized still images has been analyzed at 8 bit depth gray scale. Identification and position definition of markers was done manually. For calculations of segmental angles and positions macros were applied coded in a Pascal like macro language of the software developed for this purpose (see Appendix). Joint angles have been calculated as positive and negative values around 0 degree. Scapula rotation was computed as an angle between the axis of the scapular spine and the horizontal plane of the environment. Pelvic rotation was also related to the horizontal plane. The difference between the horizontal plane of the two systems was corrected by mathematical transformation of video data. The difference of averages of angular data was added to video data in averaged strides.

As a result an Excel compatible comma-delimited text file has been generated. For further data management and statistical analysis Microsoft Excel and StatView SE+Graphics™ (StatView® Abacus Concepts, Berkeley, California, USA) softwares were used.

Detection of moment of impact and lift-off was carried out by sight in video recordings. In the series of CODA data stance and swing phases could be distinguished by observing change of amplitude of the accelerometer signal and the fetlock data together. Strides were compared to each other by projected curves onto each other. According to higher sampling frequency of CODA (300 "frames" per second) its curves are smooth while video data are present as rare set of points oscillating around CODA data in both positive and negative directions. In numerical comparison, absolute values of differences were used.

Sequence of points of video data have not been averaged since they are representing individually different biological events and consequently different statistical variables.

Differences between the two recording systems may derive from the following reasons:

- biological error
- measuring error
- error of synchronization

4.3.5.3. Testing accuracy

For testing accuracy comparison of the same events observed at the same moment is required. In order to prove this condition signals of the timer device was applied in parallel recordings. Digital characters of the device displaying elapsed time of CODA recording (10 seconds) was recorded on each frame of video sequences. Digits of hundreds, tens and singles of seconds could be recognized in the digitized image and 0.04 sec duration could be measured between successive still images. This is the reciprocal of the 25 frames per second (fps), the sampling resolution of PAL video systems which ensure the confluent motion of a movie. During 10 seconds 13 strides have been recorded at trot. Synchronization was carried out with identifying individual CODA data by calculating with 1/300 fps as its sampling frequency. Regarded to this sampling rate ± 1/300 sec as error level was tolerated in identification.

For fitting data of systems having different sampling frequency a “grid” has been introduced which has filtered CODA data by passing every 12^{th} of video data through. The best fitting series of video data appeared at the same number of passes at each stride. This procedure has eliminated errors of synchronization. Since biological error has charged both systems, it can be neglected in the comparative investigations.

4.3.6. Statistical analysis

For statistical analyses the Student’s t-test and the χ^2-test were applied. For correlations between gait analysis data sets regression tests were used.

5. RESULTS

5.1. The development of cytoarchitecture and myelination

5.1.1 Plots of Nissl preparations

In computer plots of Nissl-stained sections the most important motor areas were compared in rostrocaudal series of prenatal, early postnatal and young adult brains. As early postnatal samples, brains of fetuses 14 days before the expected birth were taken, the early postnatals were 45-day-old and the young adults were 545 and 560 days old. The motor areas studied were the primary motor area of the cerebral cortex, the corpus striatum, the motor nuclei of cranial nerves in the upper and lower brainstem, and the cerebellum.

The primary motor cortex (Fig. 12) showed in the prenatal brains (Fig. 12a) an advanced gyrification. The superficial, cell-poor layer (stratum zonale, lamina I) was well visible, while the cell-rich layers (external granular, pyramidal, internal granular, and ganglionic layers, laminae II-V) appeared on the plot as a dark strip. The dimensional changes between prenatal and early postnatal cortices (Figs 12a and b, respectively) were negligible. Growth in size could be seen to occur after the early postnatal period (Fig 12c) This growth was substantial and as indicated by the measurements of diameters (Fig. 26), was fairly proportionate. In addition, the intensity of Nissl- staining increased till day 45, and then it decreased to the adult level.

When comparing the region of the striatum (Figs 13a, b, c), in the prenatal brain there was no internal cellular structure visible at all. By contrast, in the early postnatal (Fig. 13b) and adult (Fig. 13c) brains the cytoarchitectonic details of the striatum could clearly be distinguished. The caudate nucleus was distinct, the internal capsule was seen permeated by the typical striae, and the lentiform nucleus was well circumscribed. Also in the striatum, the strongest Nissl staining occurred in the 45-day old brain. The intensity of Nissl-staining declined thereafter. The midbrain (Fig. 14) displayed no internal structure in the Nissl-stained prenatal brains (Fig. 14a), whereas in the early postnatal midbrain the cytoarchitectonic

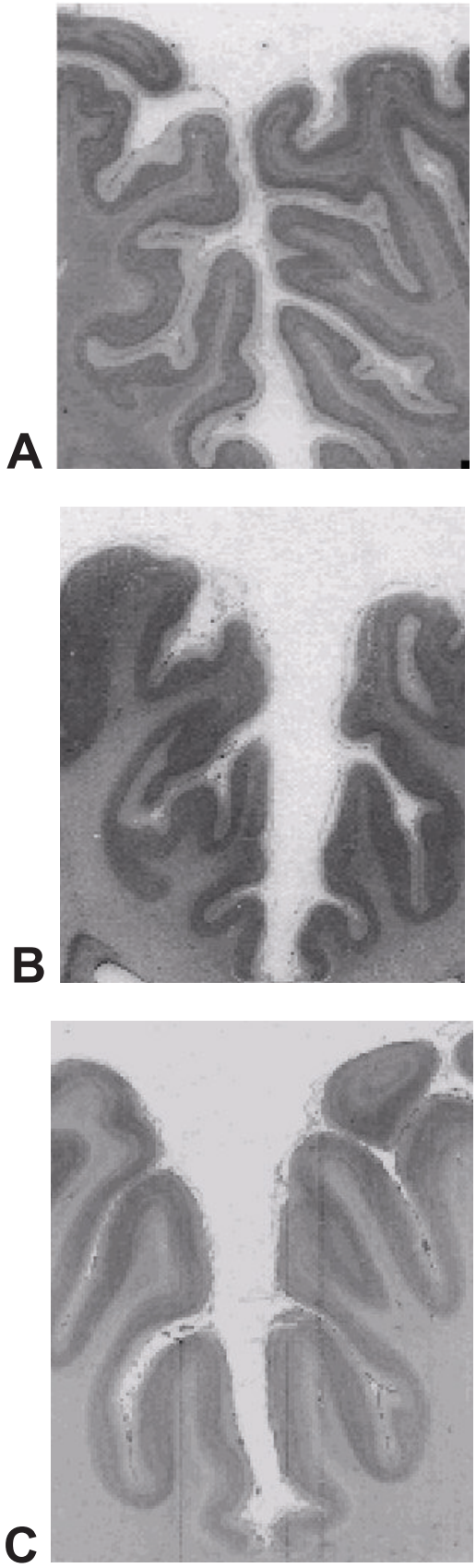

Fig. 12. Computer plots of Nissl-stained sections of the primary motor cortex. Mag: 2 ×
A: prenatal, B: early postnatal, C: adult

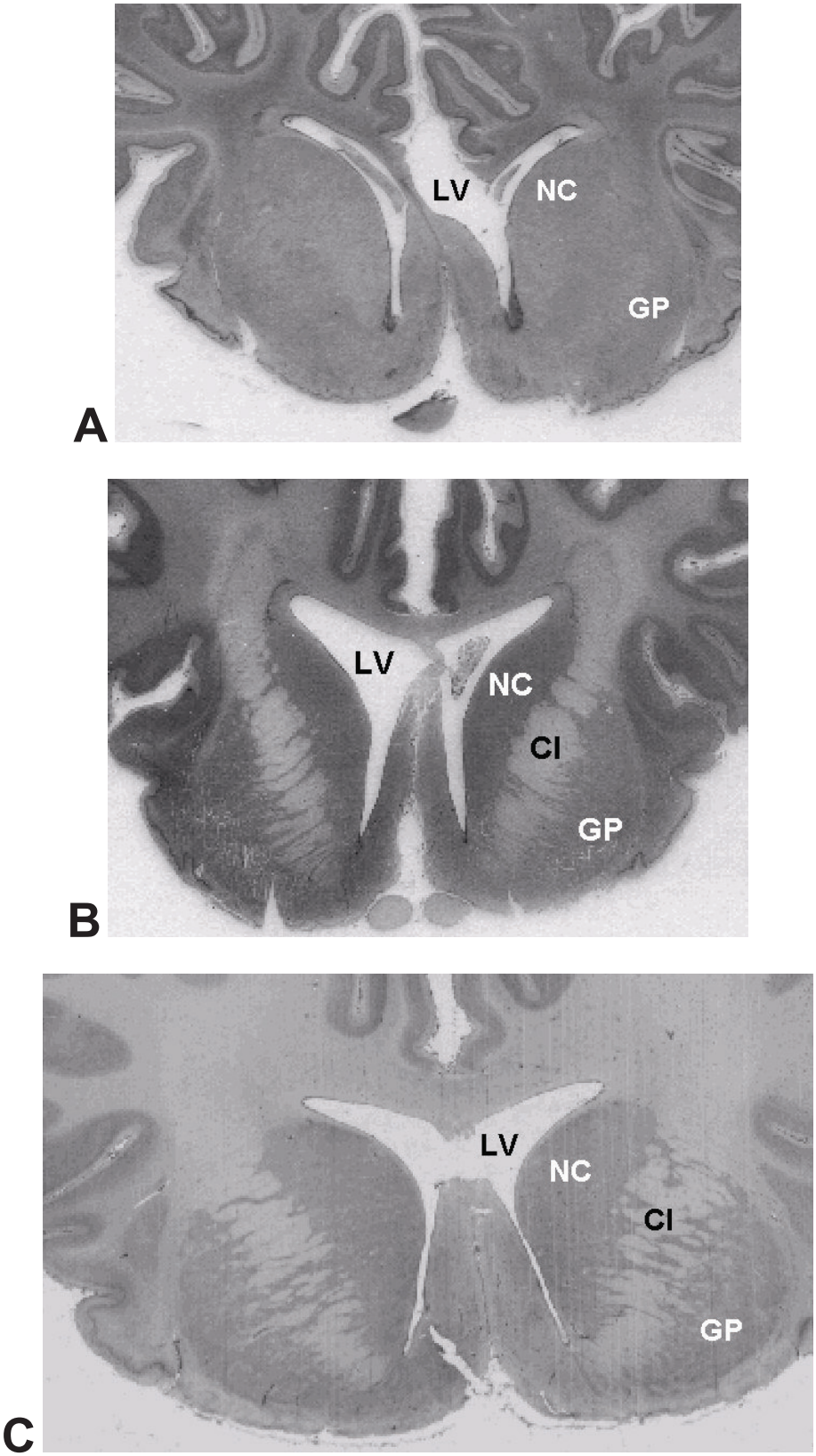

Fig. 13. Computer plots of Nissl-stained sections of the internal capsule.Mag: 2 ×

A: prenatal, B: early postnatal, C: adult

LV: lateral ventricle, NC: caudate nucleus, CI: capsula interna, GP: globus pallidus

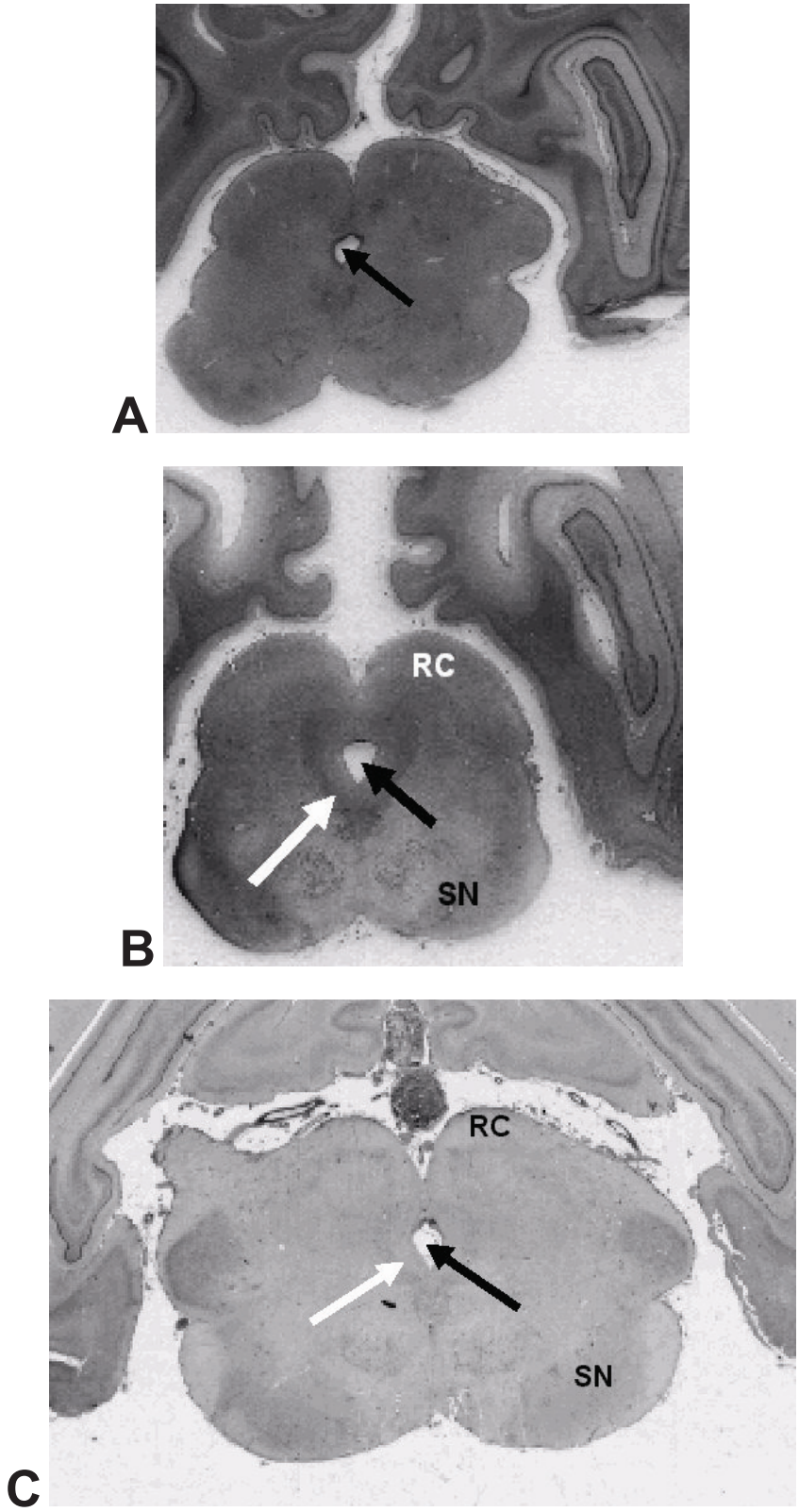

Fig. 14. Computer plots of Nissl-stained sections of the midbrain. Mag: 2 ×

A: prenatal, B: early postnatal, C: adult

Black arrow: cerebral aqueduct, white arrow: periaqueductal grey matter, RC: rostral colliculi, SN: substatntia nigra

parcellation was quite remarkable (Fig. 14b). The periaqueductal central grey matter was clearly delineated, the colliculi were darkly stained. The tegmental nuclear groups and the substantia nigra could also be recognized. An even more differentiated structure appeared in the adult (Fig. 14c) where the cellular layers of the rostral colliculus could be distinguished, the lateral geniculate body also appeared, moreover the substantia nigra and the tegmental nuclear groups were also evident. The periaqueductal grey was seen to continue ventrally into the raphe nuclei. It is noteworthy that also at this sectioning-level, the Nissl-staining of the adult was less intense than in the perinatal midbrains.

In the cerebellum (Fig. 15) it was interesting to observe that the external granular layer of the cerebellar cortex was almost absent already in the prenatal brain (Fig. 15a). Sporadic clusters of small cells were found under the pial surface (Fig. 15b) but these did not show the typical features of an external granular layer, i.e. mitoses were not encountered and the cells seemed to be aligned in a premigratory position. This was in good accordance with the fact that in the adult (Fig. 15c), apart from a substantial growth in the number of cerebellar folia which resulted in a massive volume increase of the entire cerebellum, there was no appreciable thickening of the internal granular layer, or any other layer of the cerebellar cortex or white matter. This suggested a prenatal cytoarchtectural maturation of the cerebellum supported by the fact that in this region there was no intensification of the Nissl staining during the developmental period covered by our studies.

The medulla (Fig. 16) again showed the typical temporal sequence of Nissl-staining intensification as observed for most motor areas having a peak intensity in the early postnatal brain. Whereas cytoarchitectural details could only be guessed in the prenatal medulla (Fig 16a), they were quite marked in the early postnatal preparation (Fig. 16b). This applies particularly to the spinal trigeminal nucleus, the vagal and hypoglossal nuclei and the caudal olivary nucleus. The layered structure of the caudal olivary nucleus was conspicuous in the early postnatal (Fig. 16b), and to a lesser extent in the adult oliva (Fig. 16c).

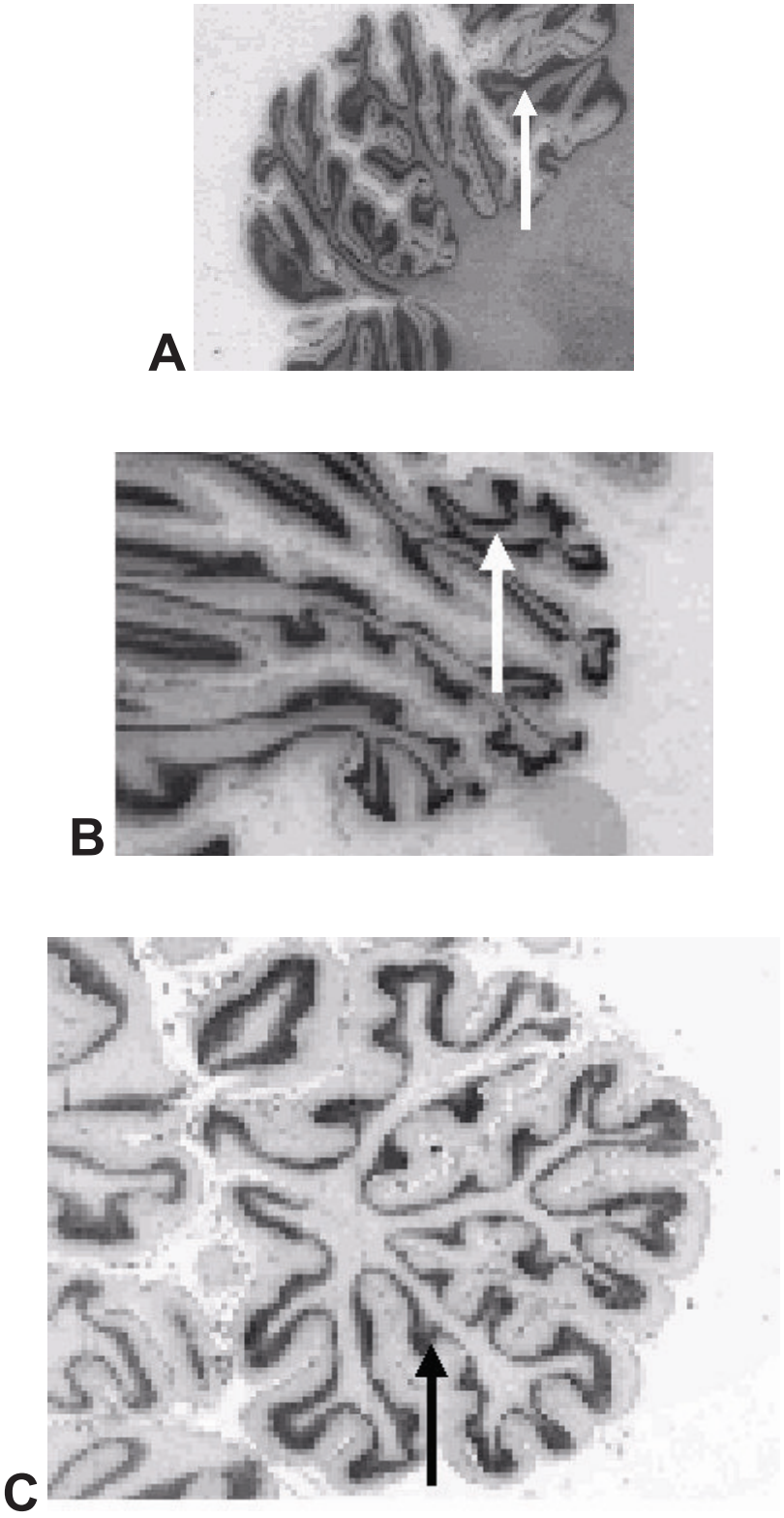

Fig. 15. Computer plots of Nissl-stained cerebellum (coronal plane). Mag: 3 ×
A: prenatal, B: early postnatal, C: adult
Arrow: granular layer

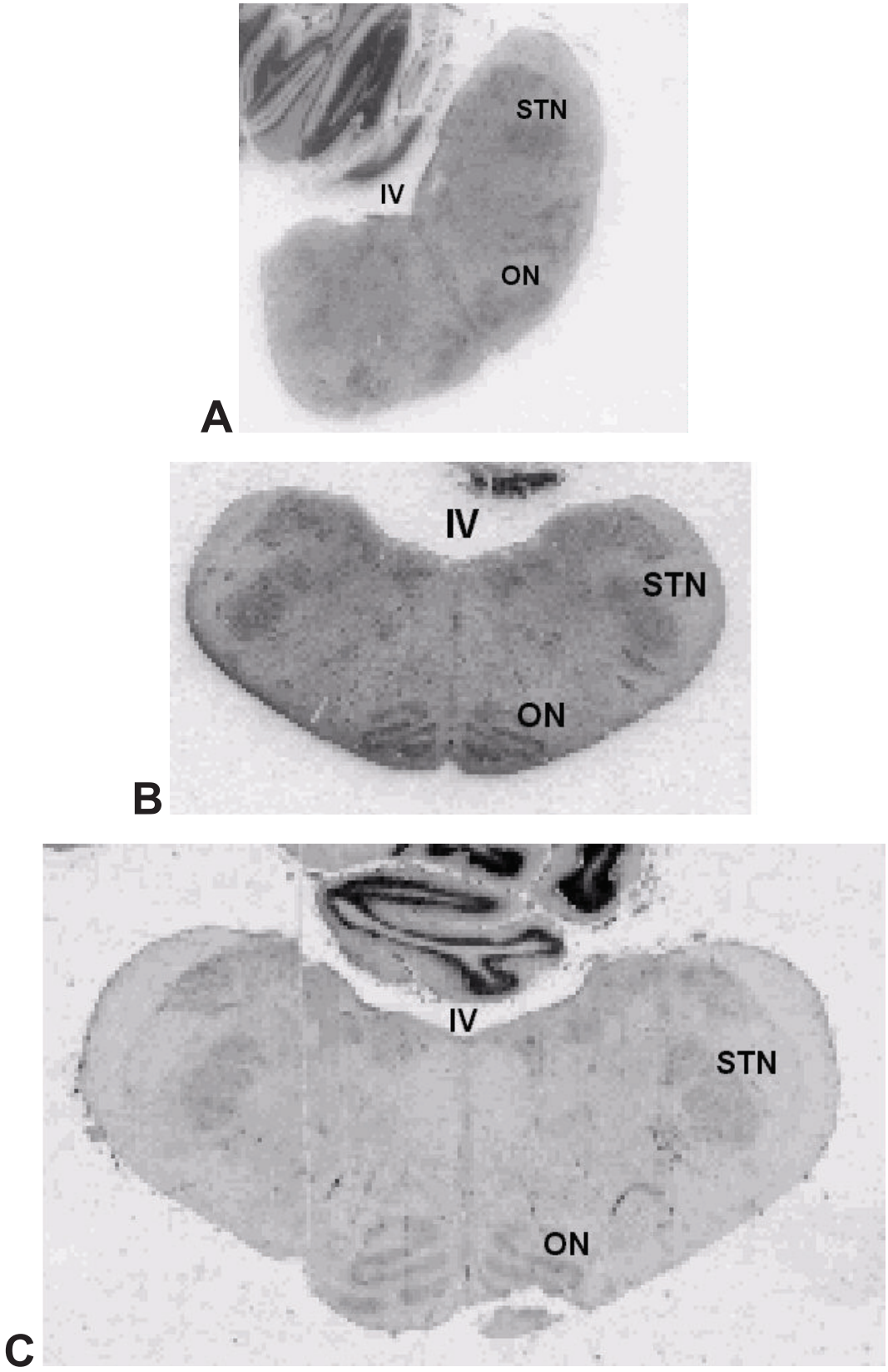

Fig. 16. Computer plots of Nissl-stained sections of the medulla. Mag: 2 ×

A: prenatal, B: early postnatal, C: adult

IV: floor of hte IVth ventricle, ON: olovary nucleus, STN: spinal trigeminal nucleus

5.1.2. Cytoplasmic maturation of motor cells

Taking into consideration that the Nissl-staining showed in all regions a similar tendency of intensification till postnatal day 45 from where it decreased till adulthood, we thought it necessary to examine under a higher microscopic magnification the cytoplasm of motor neurons. In agreement with the overall appearance of staining reflected by the computer plots. individual cells showed parallel differences in their content of Nissl-material. In the prenatal brain (Fig. 17a) motor neurons contained loosely packed, distinct Nissl-bodies in their cytoplasm. At postnatal day 45 (Fig. 17b) the cytoplasm of motor neurons was so densely packed with cresyl violet-stained material that at lower magnifications it gave the impression of a solid cytolpasmic staining and it was only under higher power that the rough granular nature of the cresyl-violet staining could be recognized. In the adult motor neurons (Fig. 17c) Nissl-bodies were again discernible as distinct cresyl violet stained blocks.

It is also worth of notion, that in the preantal brain the cells of brainstem motor nuclei are smaller and more densely packed than in the early postnatal brain. From this time, packing density of cells decreased till adulthood, while cell-size remained unaltered.

5.1.3. Plots of myelin-stained sections

In this series of observations the major motor pathways were looked at concentrating on the pyramidal tract, the extrapyramidal system, cerebellum and brainstem. The main commissural bundle, the corpus callosum was also investigated.

Between 14 days before and 45 days after birth, there was a significant increase in the amount of myelinated fibres in the white matter of motor cortex and particularly in the internal capsule (Figs 18a, b). Advance in myelination could be seen best in the ansa lenticularis which is still poorly myelinated on prenatal day 14 (Fig. 18a), whereas its myelination is substantial by postnatal day 45 (Fig. 18b). In addition, the grey matter strips which combine the caudate nucleus and the putamen to form the corpus striatum, are thinner at postnatal day 45 than prenatally.

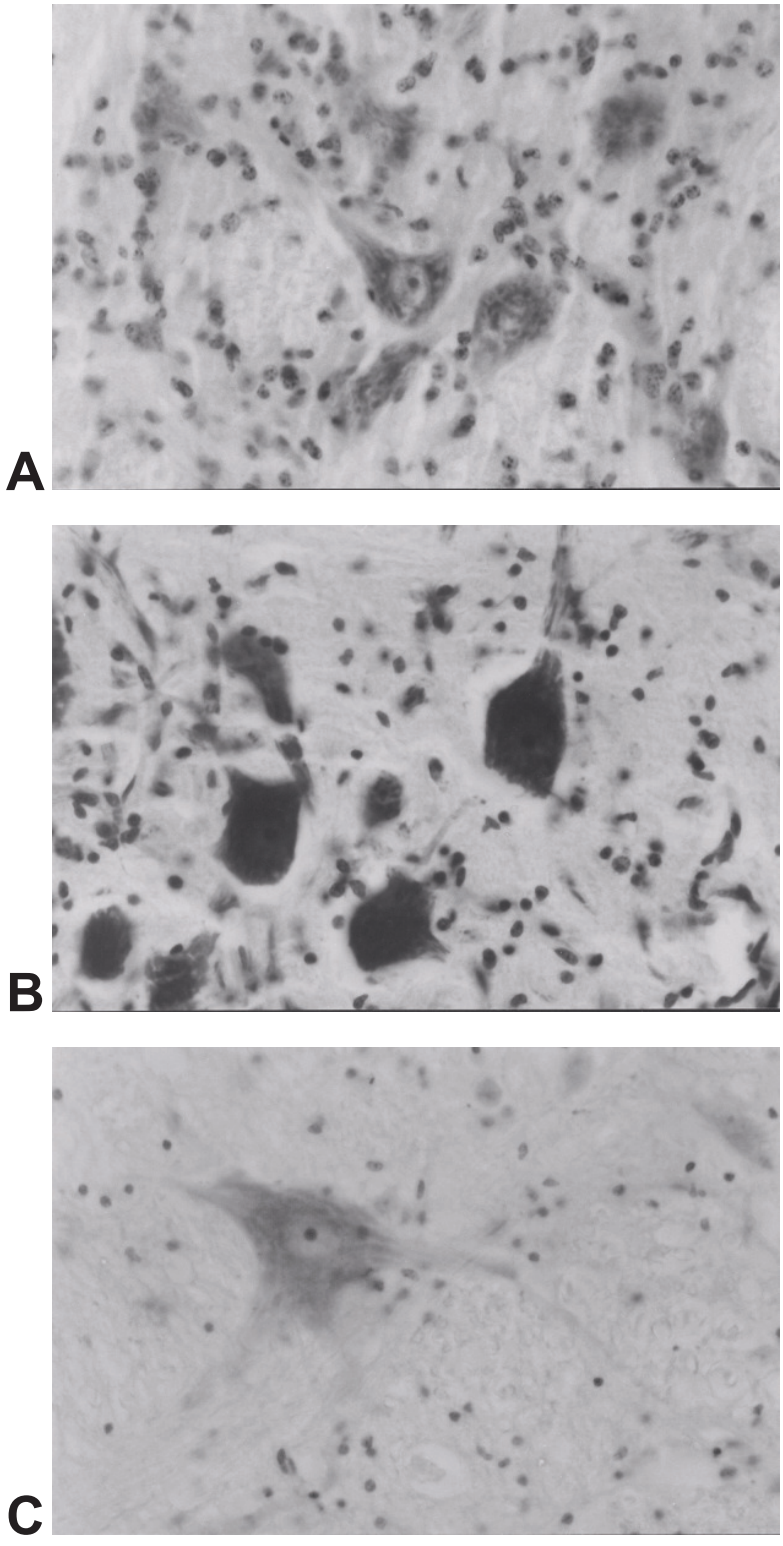

Fig. 17. Nissl-stained preparation of the medullary motor nuclei. Mag: × 360

A: in the prenatal (-14 day-old) brain the Nissl-bodies of motor neurons form distinct blocks in the cytoplasm, B: at postnatal day 45 the amount of Nissl-material is increased to an extent that is solidly fills the cytoplasm of motor neurons, C: in the adult motor neurons the Nissl-bodies are clearly visible

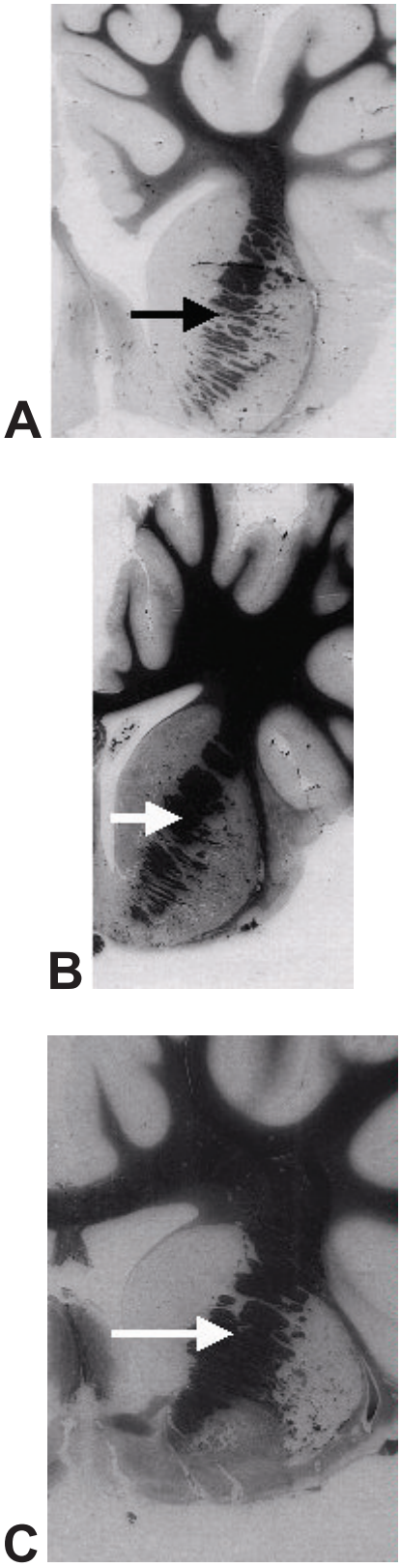

Fig. 18. Computer plots of myelin-stained sections showing the internal capsule (arrow). Mag: 2 ×
A: prenatal, B: early postnatal, C: adult

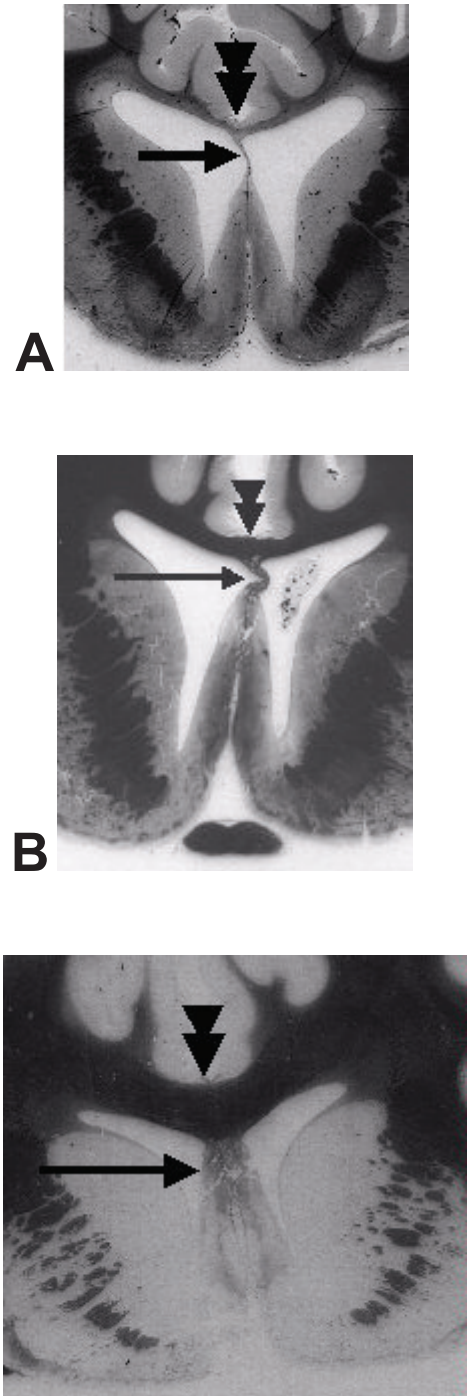

Fig. 19. Computer plots of myelin-stained sections at the level of the septum (arrow) showing the trunk of the corpus callosum (arrowheads). Mag: 2 ×

A: prenatal, B: early postnatal, C: adult

In the adult (Fig. 18c), due to a general growth of the brain the myelinated pathways are less compact and the putamen and globus pallidus can be distinguished on the basis of their myelin-content.

Cut at the level of the optic chiasma (Fig. 19), the septum and the corpus callosum could be observed bordering the rostral horn of the lateral ventricle from medial and above, respectively. While in the prenatal brain (Fig. 19a) the corpus callosum was a thin strip of transverse white matter, in the early postnatal brain (Fig. 19b) it appeared as a conspicuous cross-bundle, and in the adult (Fig. 19c) it was a thick, powerful commissure of myelinated fibres connecting the two hemispheres. It should be noted that in this series of preparations the development of the septum from a prenatal thin membrane to a thick, myelinated pathway-containing wall is evident. At this level, the growth of the striatum could particularly well be documented.

In the midbrain (Fig. 20), a peak accumulation of myelinated fibres was observed at postnatal day 45 (Fig. 20b) such that except for the periaqueductal central grey matter and the substantia nigra no internal detail were discernible. This was not the case in the prenatal and adult midbrains, where details such as the layers of colliculi, raphe nuclei, geniculate body, etc., could be percieved.

A gradual increase of myelinated area was observed in the cerebellar white matter (Fig. 21). In the myelin-stained medulla only the prenatal preparation allowed to distinguish details. At later stages myelinated fibre bundles became overwhelming and masked non-myelinated elements (Fig 21b). With the growth of the medulla in the adult, the myelin staining became less compact but it still covered evenly the entire section (Fig. 21c).

The white matter/grey matter ratio was followed within the devebpmental period studied (Fig. 22). Values are summarized in Fig. 29. From the comparison of ratios it appears that the bulk of myelin formation occurred in the period between prenatal day 14 and postnatal day 45. Myelinated territories became wider and more ramified. After this period there is an overall growth of the brain but apparently not followed by a further increase in myelinated fibres. This is reflected in a less intense myelin staining, because myelinated fibres are spread over a larger territory in the adult as compared to the perinatal brains.

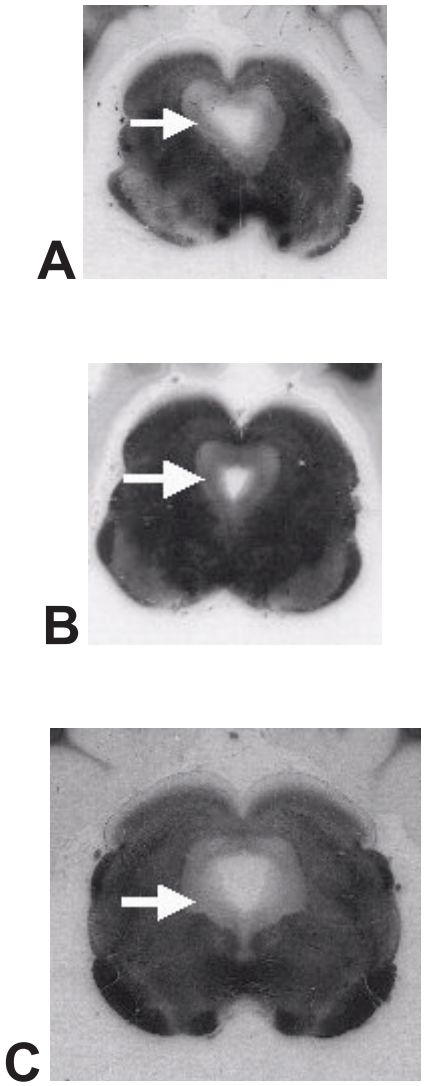

Fig. 20. Computer plots of myelin-stained sections of the midbrain. Arrow points at the periaqueductal grey matter. Mag: 2 ×

A: prenatal, B: early postnatal, C: adult

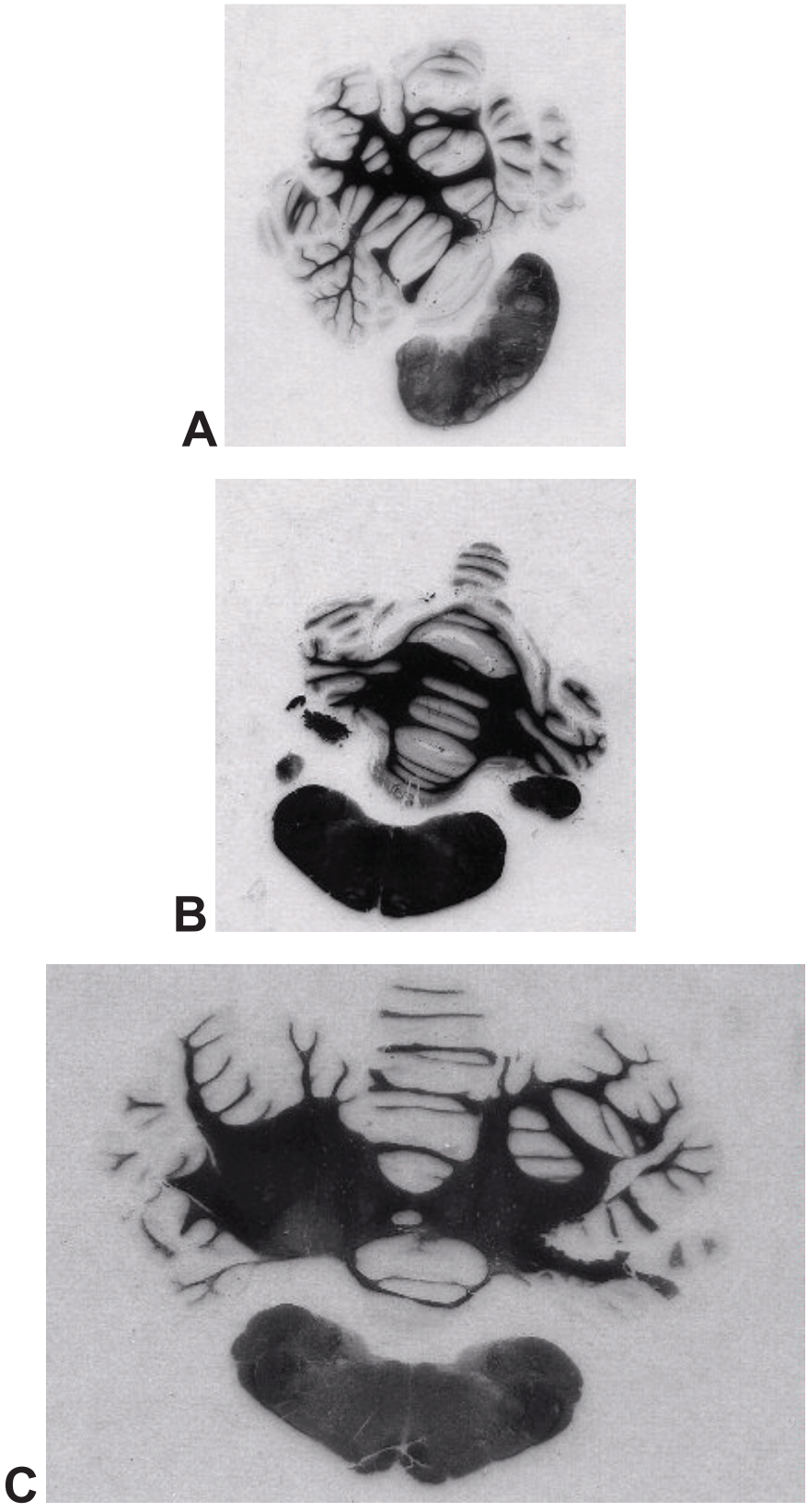

Fig. 21. Computer plots of myelin-stained sections of the medulla and the cerebellum. Mag: 2 ×
A: prenatal, B: early postnatal, C: adult

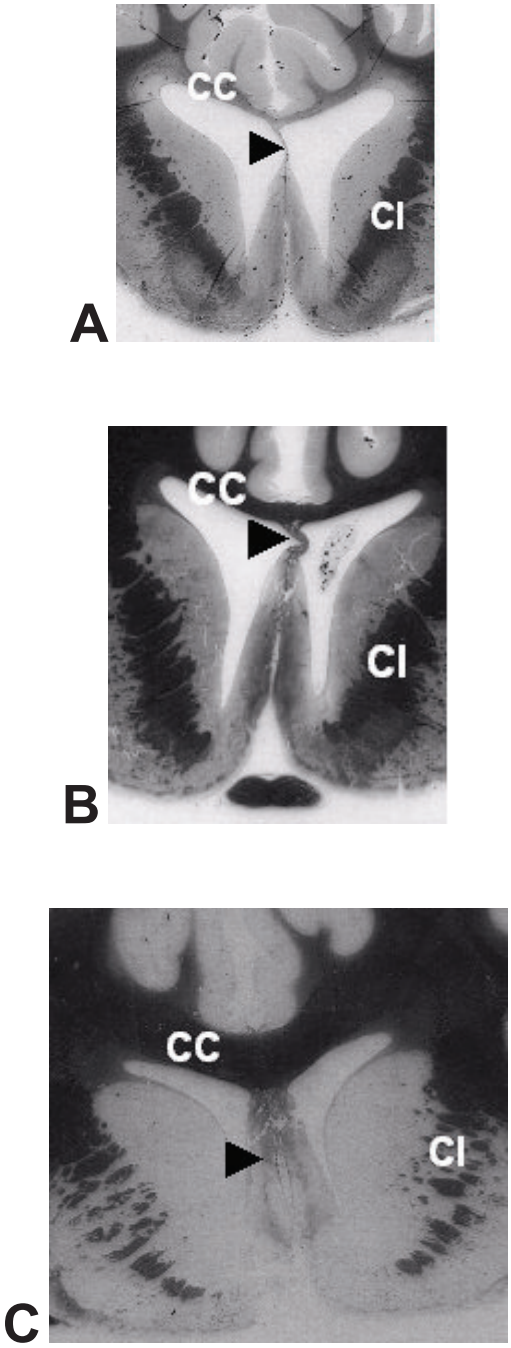

Fig. 22. Ratio of the white and grey matter of various developmental stages as seen in co mputer plots of myelin-stained sections. Observe the growth of corpus callosum (CC), capsula interna (CI) and septum (arrowhead). Mag: 2 ×

A: prenatal, B: early postnatal, C: adult

5.2. Contour and area measurements and related calculations

5.2.1. Dimensions of brains

The length of the entire brain and its units showed a doubtless increase with age (Fig. 23). The most prominent difference appears between the perinatal (pre- and early postnatal) and adult brains in all parameters measured. The data of the brain length in prenatal (D-14 – 14 days, D-4 – 4 days, D0 – 0 day before expected birth) and early postnatal ages (D4 – 4 days and D45 – 45 days after birth) showed a small degree of oscillation but this deviation did not exceed 6 mm. After one and half month this parameter reached its maximum. This oscillation reappeared in each data line: the hemispheres and the brainstem ranged between 74 – 94 mm and 61 – 72 mm, respectively in the prenatal and early postnatal ages. In the cerebellum the difference between minimum and the peak was only 12 mm.

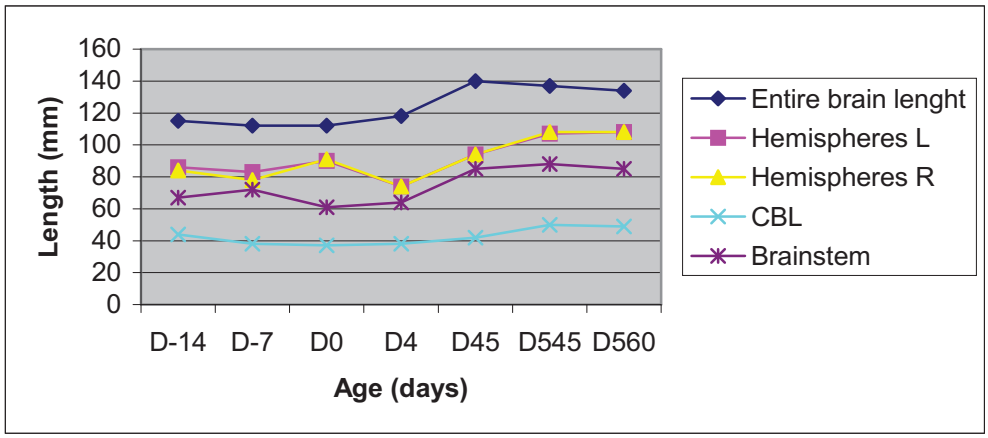

Fig. 23. Length of the brain and its parts in different ages

The marked volume increase between early postnatal and adult periods was due to the elongation of the entire brain was more pronounced in the hemispheres than in the cerebellum and brainstem. The sizes of the left and right hemispheral pairs are more or less identical.

In order to clarify the exact reason of volume increase we examined the area and the perimeter of the hemispheres, the cerebellum and the brainstem in each section (Fig. 24).

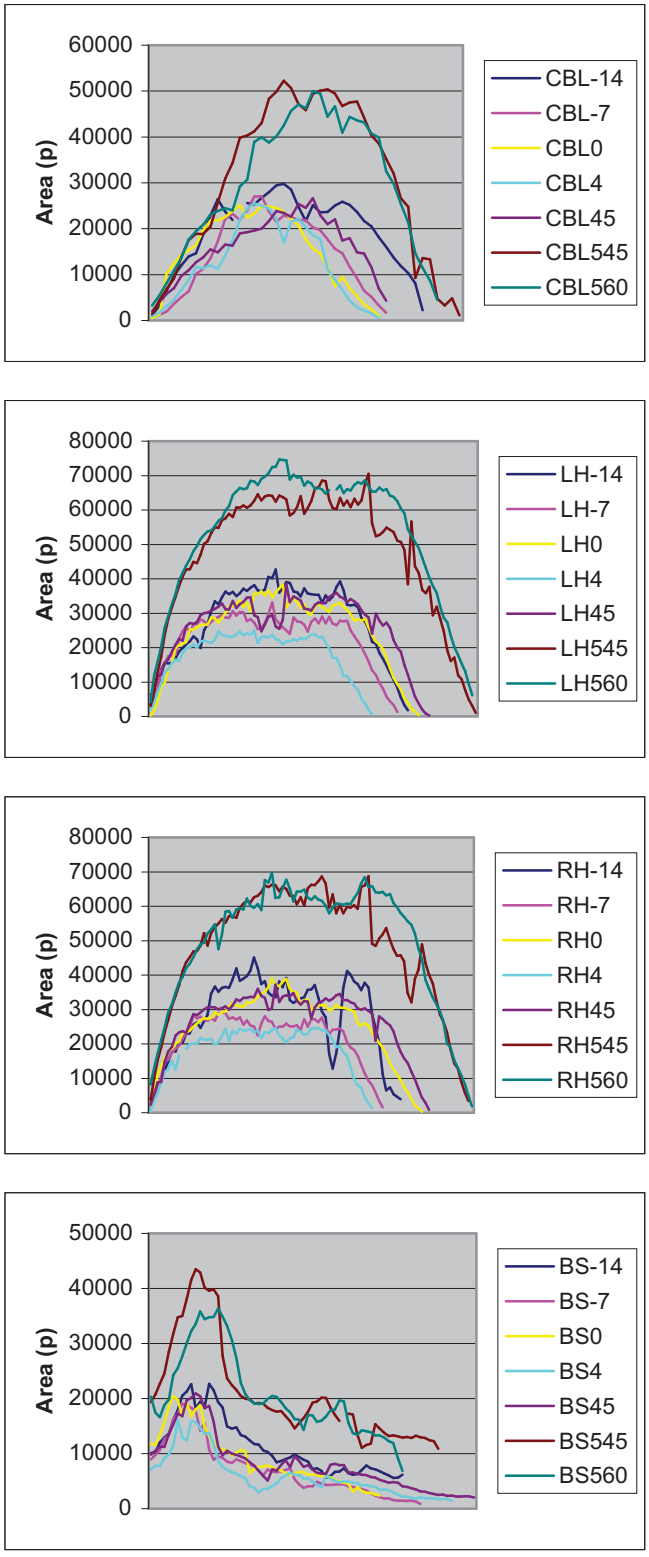

Fig. 24. Areal measurements of major parts of the brain of differe nt ages

Similarly to longitudinal parameters the most obvious changes appeared between the perinatal age and adulthood. Within the time period between days 14 prior to and 45 following birth, alterations did not exceed the level of individual differences. Data of each major part of the fully developed adult brains were also similar but the areal alteration from perinatal brains to the adults displayed remarkable increases. For comparison of the two groups averages of major parts were calculated

In Fig. 25 averaged perinatal and adult brains are compared. None of the differences within the perinatal period showed such a deviation which can be seen between the perinatal and adult groups.

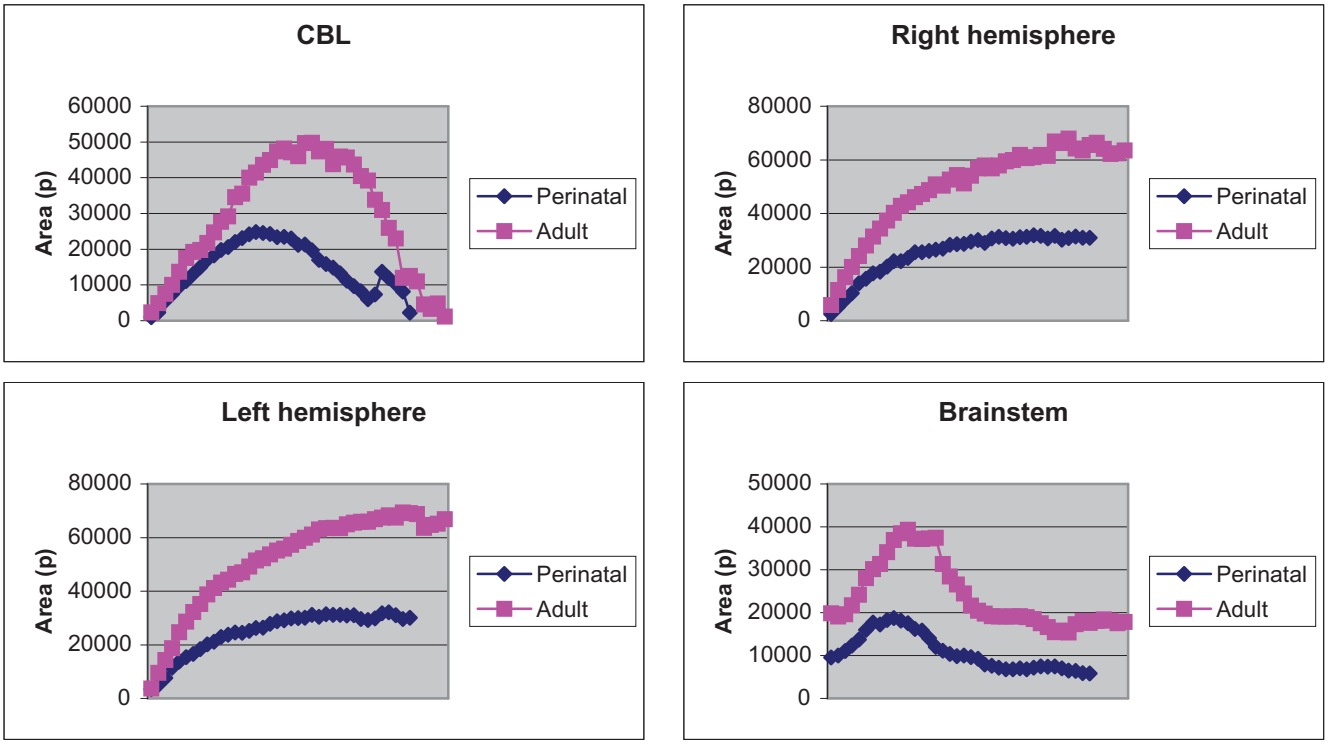

Fig. 25. Areal measurements of major parts of the averaged perinatal and adult brains

5.2.2 Maximum diameter of the hemispheres

Beside longitudinal parameters the maximum of transverse diameter was also analysed in the series of coronal sections (Fig. 26). This was measured across the caudal end of the tuber cinereum as it is illustrated in Fig. 27. Its values were

similar within the prenatal and adult groups with a small variance but the difference between them was already significant. This profile was similar to the data of longitudinal measurements, which suggests the proprortional growth of the entrire brain.

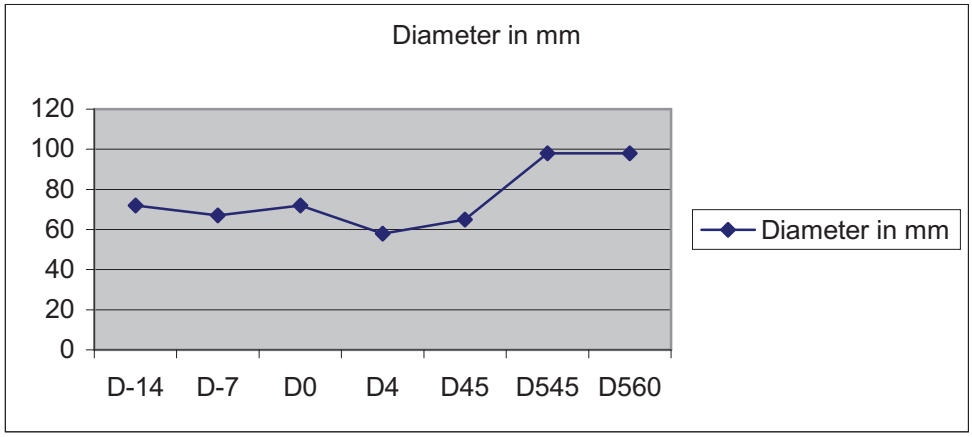

Fig. 26. Diagram of maxima of transverse diameters in different ag es

Abbreviations: D-14 = 14 days before birth, D-7 = 7 days before birth, D0 = at birth, D4 = 4 days after birth, D45 = 45 days after birth, D545 = 545 days after birth, D560 = 560 days after birth

Fig. 27. The maximum of transverse diameter was measur ed at the level of the optic decussation indicated by a black line

5.2.3 Gyrifacation index (GI)

The difference - more exactly the quotient - between the free and the convoluted surfaces of the brain reflects degree of convolution of the cortex. Depending on the depth of sulci this value, the GI value, varied between 0 – 1. At 1 there was no difference between the two contours at all, in other words: the cortex is flat. In our diagrams, however, there were some values exceeding the theoretical maximum of 1 because of some technical reasons. At some extreme areas (rostral and caudal poles) the convoluted contour crossed the way of the free contour, this way it decreased the value of the free countour which may result in values higher than 1 in our calculations.

As it is indicated in Table 3 the average GI value ranged between 0.64 – 0.766. This showed that there was no signifcant difference in the GI of the brains. In Fig. 28. GI of couples of hemispheres are shown. There is no common chararacteristic feature in the diagram. All data are oscillating around 0.6 – 0.7 forming an irregular curve.

Table 3. Calculated average of gyrification index of both hemispheres

	L. H.		R. H.		AVG of both
Age	**GI**	**SEM**	**GI**	**SEM**	
-14	0.671	0.074	0.608	0.104	**0.640**
-7	0.662	0.075	0.674	0.105	**0.668**
0	0.765	0.095	0.689	0.094	**0.727**
4	0.757	0.100	0.775	0.123	**0.766**
45	0.723	0.127	0.698	0.132	**0.711**
545	0.654	0.099	0.684	0.101	**0.669**
560	0.685	0.071	0.704	0.069	**0.694**

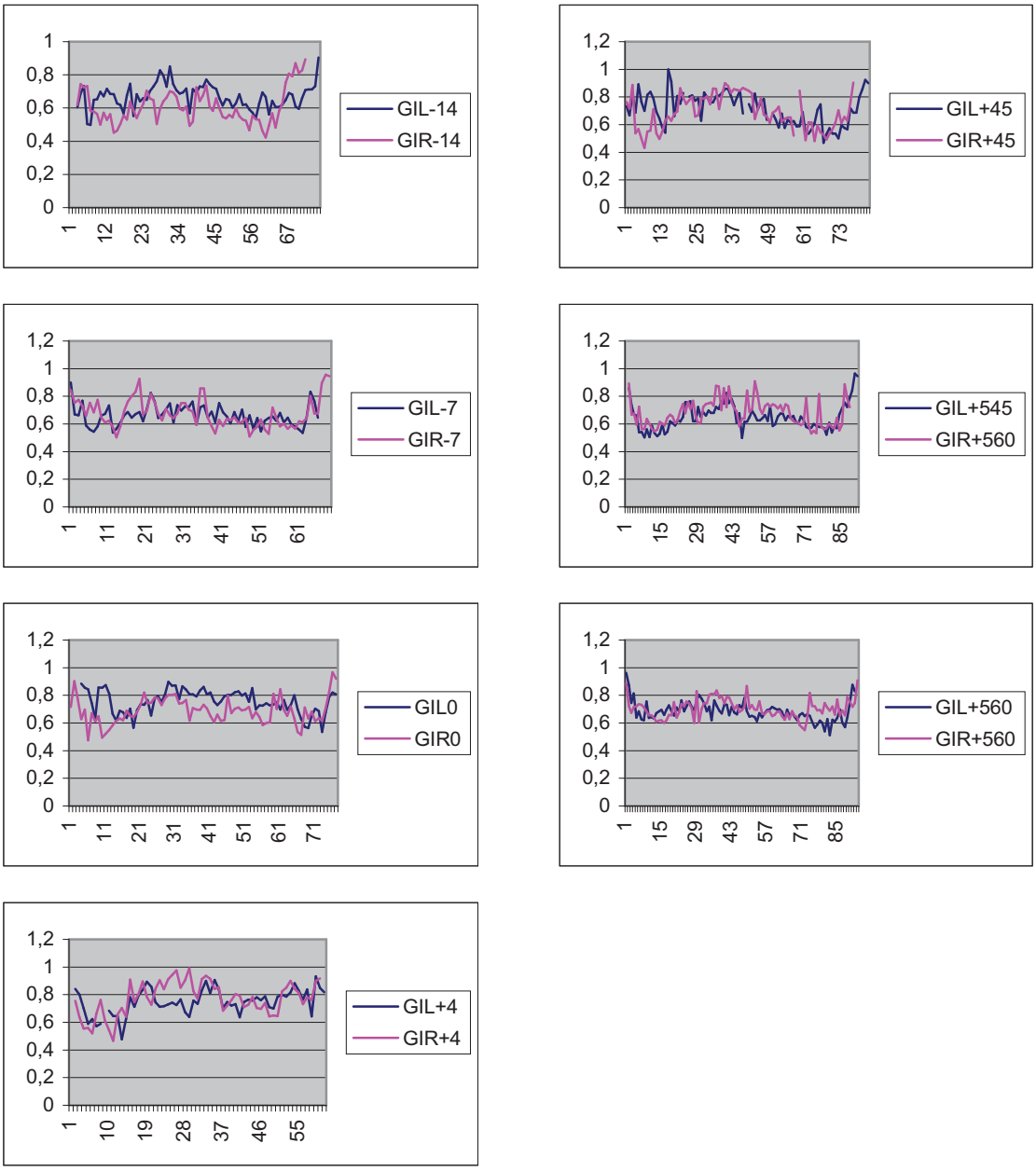

Fig. 28. Comparative diagrams of pairs of hemispheres at different ages

5.3. Total amount of myelin

Total amount of myelin was measured on the basis of segementation of digital images. The higher density of the myelinated tracts in the myelin sections stained specially for myelin made the segmentation obvious. The territory occupied by the darker (myelin) area was expressed as a percentage of the total area.

In the first rostral series of coronal sections until the level of corpus callosum, hemispheres were separated from each other by the interhemispheric fissure in the median line. At the occipital lobe sections contained the two hemispheres and the mesecephalic section. In the portion between them, the hemispheres were arbitrarily cut from basal ganglia and the thalamus by a line drawn from the top of corpus callosum to the lateral rhinal sulcus. This sulcus separates the neopallium from the rhinencephalon rostrally and the temporal cortex and the piriform lobe caudally.

Data are demostrated in Fig. 29. The profile of these curves contains one major peak in the mid-region where the optic and acoustic radiations are found in the continuation of the basal ganglia. The notch in front is due to the artificial separation of the hemispheres where the lateral part of the basal ganglia was also included. This technical error, however, is equally present in each brain, therefore they remain comaprable.

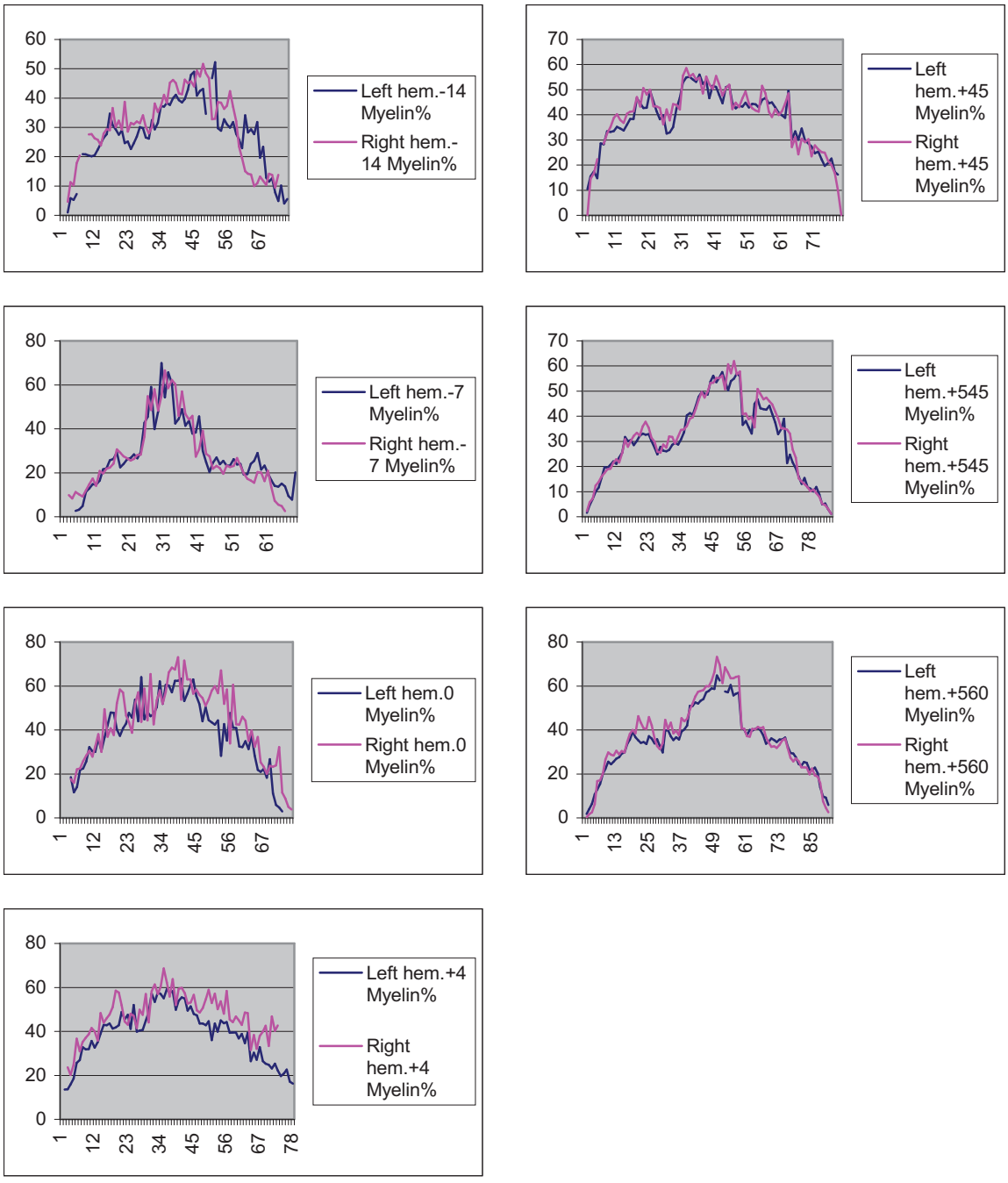

Fig. 29. Total amout of myelin expressed as % of total area in both hemispheres

In the cerebellum a more or less similar regular distribution of the myelin was observed. The curve profile of these distributions slightly changes from a hillock to a bell shape. This curve actually follows the areal profile of the cerebellum (Fig.

30). In the middle of the cerebellum the medullary body and the cerebellar peduncules give the majority of the tissue which seemed fully myelinated.

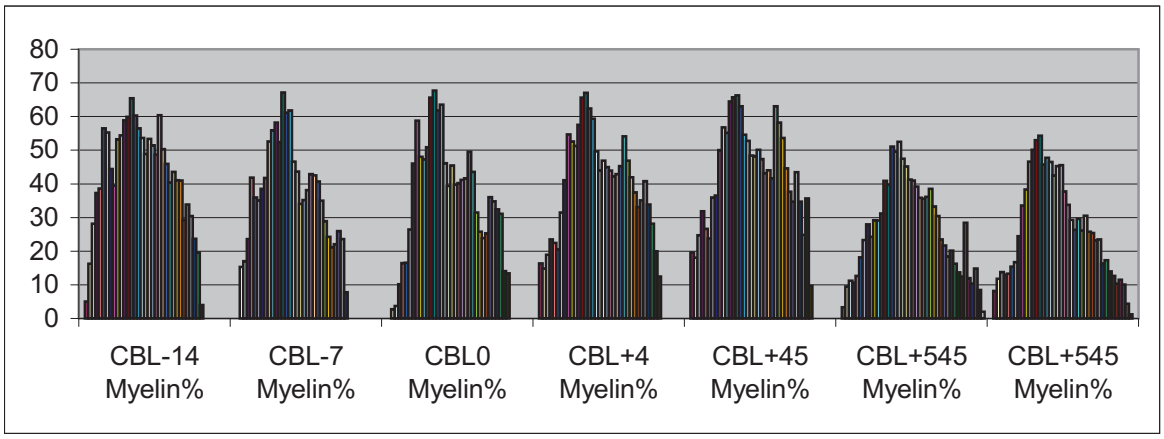

Fig. 30. Profile curves of myelin amount expressed as % of total area in each cerebellum

5.4 Circumscribed motor pathways and areas

As the total amount of myelin showed a significant increase between prenatal and early postnatal brains, in the following we focussed on certain pathways. Among the motor pathways which play an important role in the execution of different types of movements the internal capsule, the pyramidal tract, some parts of the extrapyramidal tract (rubrospinal, cerebellospinal tracts) and the corpus callosum were measured. In the myelin-stained section each of these pathways were evenly stained. Their myelination seemed to be normal. Detailed observations on their myelin sheath could not be performed because of the unusual thickness of the sections (20 µm).

For quantitative description constant sections of motor pathways were measured for an average diameter charaterizing the thickness of the pathway (Table 4).

Age (days)	CI (mm)	P (mm)	EP (mm)	CC (mm)
-14	22,30	2,06	1,68	0,96
-7	21,51	2,33	1,89	0,96
0	23,01	2,57	2,17	1,20
4	22,89	2,47	2,27	1,23
45	23,04	2,76	2,47	1,66
545	33,19	4,67	3,34	3,38
560	34,17	4,93	3,10	3,47

Table 4. Summarizing table of the diameter of circusribed myelinated motor pathways
Abbreviations: CI = capsula interna, P = pyramydal tract, EP = extrapyramidal tract, CC = corpus callosum

The internal capsule was measured at the level of the basal ganglia in a V shape from the corona radiata to the mesencephalic flexion. Its size varied within a narrow range in the young brains (from 14 prenatal days to 45 postnatal days) but substantially increased in the adults.

Data of the pyramidal tract were collected along the medulla oblongata on the ventral surface. In order to avoid addition of the height of the arcuate nucleus only the tract was meausred at the horizontal diameter. A moderate increase can be seen in the young brains and an approximate duplication can be identified in the adults.

The increase of the diameter of the extrapyramidal tracts is more even then in the previous two cases.

The most significant rise was measured in the corpus callosum. For reduction of technical errors only the trunk of the corpus callosum was measured. The growth of this pathway showed a continuous increase parallel with age.

5.5. Cellular parameters of the cerebella

5.5.1. The creation of virtual section with help of MRI

Since brains were cut coronally, we took the advantage of MRI in reconstructing a virtual series of sagittal sections. In both adult horse brains MRI image sequences were taken resulting a 256 cubic voxel image matrix. This matrix was used in a three dimensional reconstruction work in order to create a virtual longitudinal section along the median plane of the brains (Fig. 31). This longitudinal section

assisted us in identifing the folium of the vermis in our preliminary studies. The most prominent lobe of the vermis of the cerebellum in cross sections was the folium vermis.

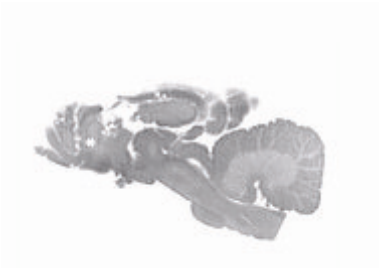

Fig. 31. Virtual longitudinal section of the cerebellum of an adult horse. The image was reconstructed from MRI cross-sections

5.5.2. Distribution of the Purkinje cells in the cerebellum

Each folium of the folium vermis was investigated and Purkinje cells were counted in each microscopic field measuring 200 μm^2. In the young animals the cell number varied between 36 – 64 while the Purkinje cells of the adults showed an evenly packed distribution with a more or less constant average. These data are collected in Table 5. It is worthy to note that the deviation of the cell counts are twice or even three times higher in the young brain than in the adults.

Age	N* (Purkinje cells)	S.E.M.
-14	36	± 8
-7	60	± 11
0	55	± 14
4	54	± 6
45	64	± 5
545	40	± 3
560	42	± 5

Table 5. *N = average number of Purkinje cells per territorial unit

5.5.3. Cells in the cerebellar molecular layer

In the late prenatal and even in the early postnatal age an intense cellular migration can be observed in the cerebellar molecular layer. Cells of a former external granular layer are migrating through the stratum moleculare presumably

along the glial processes (Altman and Bayer, 1985). This phenomenon is known in the most frequently studied species such as rodents and cat, and to some extent in man, but is less investigated in the horse.

The molecular layer contained migratory cells, however, no external granular layer could be demarkated in our specimens. A 200 μm^2 territoreal unit was observed and digitally segmented. The area of the dark, isolated particles corresponding to the cells were compared to the total microscopic field and expressed in percentage. This method, however, adds the number of “local” cells of the molecular layer such as basket and stellate cells to the total cell count, but this was considered as a constant in our measurements.

As it is summarized in Table 6 the number of migratory cells in the molecular layer is remarkably high in the prenatal brain, somewhat lower in the early postnatal foals and definitely low in adults. This decrease, however, is not linear due to an increase at 4 and 45 postnatal days.

Age	N*	S.E.M.
-14	1.42	± 0.2
-7	1.83	± 0.34
0	0.65	± 0.07
4	0.9	± 0.07
45	1.5	± 0.26
545	0.48	± 0.05
560	0.45	± 0.04

Table 6. Cell counts expressed in ‰ of territorial units of the cerebellar molecular layer.
N*= average number of cells

5.5.4. Proportions of the cerebellar cortical layers

Accoring to the active cell migration from the molecular to the internal granular layer in the young population a change in thickness of these layers and their proportions is expected. The quotient of the thickness of the moleclar and the internal granular layers is introduced in Table 7. Since the thickness data strongly deviate, 100 measurements were taken within the entire lobe in one section.

Age	Mol/IGL
-14	1.43
-7	1.03
0	1.65
4	1.19
45	0.98
545	1.02
560	0.93

Table 7. A quotient was calculated from the thickness of molecular (Mol) and internal granular layer (IGL)

5.6. Cellular measurements in the cerebral primary motor cortex

5.6.1. Average thickness of the primary motor cortex

Unlike in the most frequently studied species such as cat, laboratory rodents and dog the primary motor cortex of the horse is not around the cruciate sulcus. According to Breazile's works based on electrical stimulations (Breazile et al., 1966) this area is situated along the dorsal margin of the rostral half of the hemispheres (Fig. 32). In his opinion the entire rostral half medial to the suprasylvian sulcus corresponds to the primary motor area. The contralateral somatotopic representation of the limbs matches the medial surface aproximately at the level of the rosrum and the genu of corpus callosum.

Fig. 32. The dorsal margin of the right hemisphere. The primary motor cortex is indicated by the shaded area

The cross-section cortical thickness varied within a wide range depending on the plane of the section, therefore a well-defined area was measured situated immediately at the rostral tip of the genu of corpus callosum in the cingulate gyrus.

The difference in cortical thickness from the youngest to the adult brains is demostrated in Table 8. The linear increase of thickening can be observed.

Age	MC thickness (mm)	S.E.M.
-14	1.32	± 0.4
-7	1.23	± 0.41
0	1.31	± 0.5
4	1.62	± 0.39
45	1.93	± 0.35
545	2.17	± 0.2
560	2.29	± 0.21

Table 8. The thickness of the cortical primary motor cortex in mm

5.6.2 Qualitative characterization of the primary motor cortex

An obvious difference could be observed in the microscopic images at the appearance of granular and pyramidal layers between the young (late prenatal to early postnatal) and adult brains. The cellular layers mentioned above were conglomerated in a narrow zone below the superficial molecular (plexiform) layer. The cells of the external and internal granular and pyramidal layers were “condensed” (Fig. 33) in high number in a regular orientation as it is expected in the case of the motor cortex. It is difficult to compare the total cell number of a cortical segment in the young and in the adult brain but they appeared more or less equal. Altogether only their distribution seemed different within the available area.

Fig. 33. Primary motor cortex in the late prenatal (14 days prior to birth) age

5.7. Gait analysis

5.7.1. Motion of the adult horse

5.7.1.1. Angle - time diagrams (Fig. 33)

Scapula rotation

Markers were well recognized due to good illumination on the proximal segments of the forelimb. Flexions of these curves like indentations at the ascending (lower speed) and descending (higher speed) sides were followed by video data at higher speed.

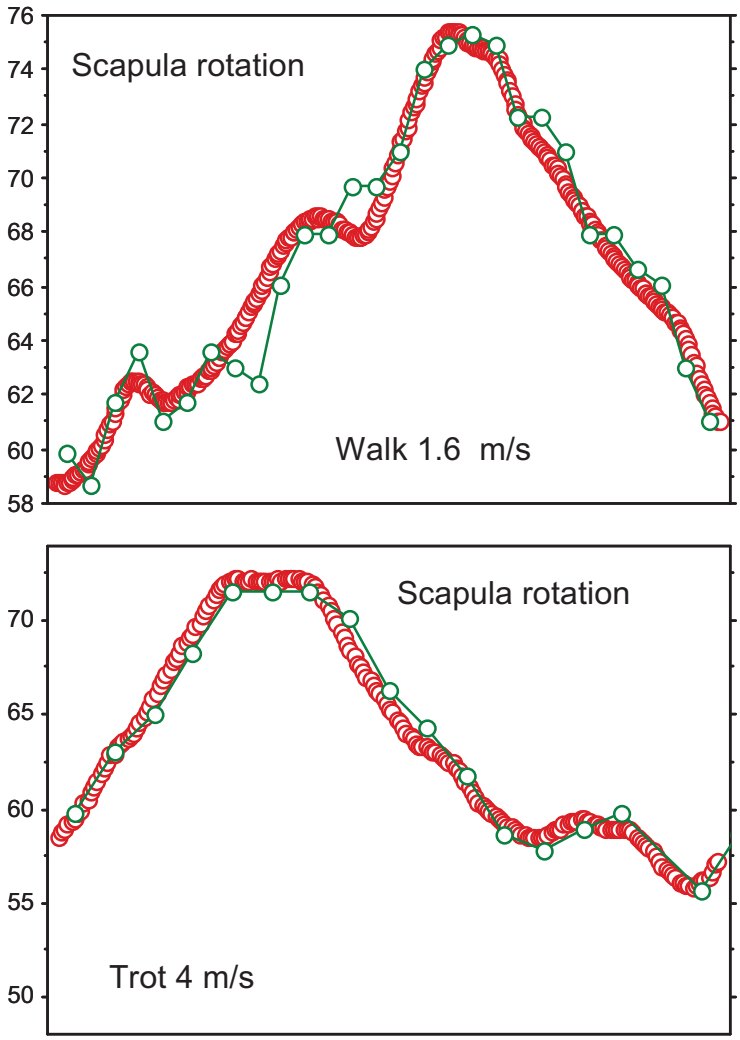

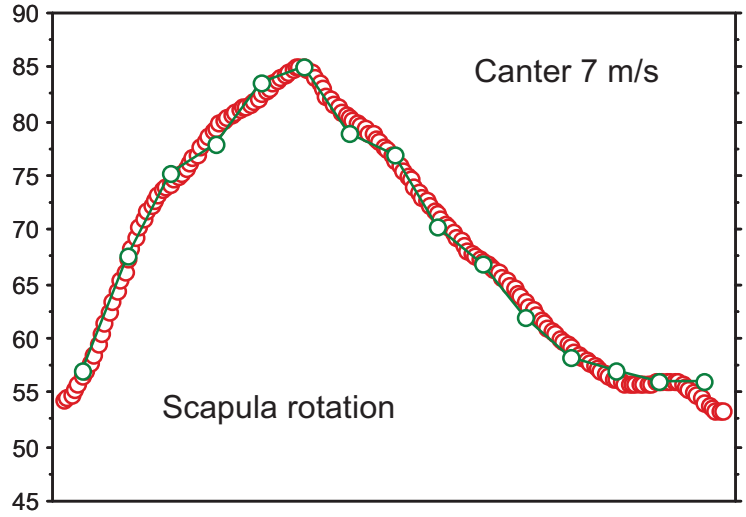

Fig. 33. Scapula rotation at each gait type

Elbow joint angle (Fig. 34)

Video data surpisingly fitted to CODA curve with a high accuracy. At walk and trot the initial negative and positive peaks were followed satisfactorily. A shift could be observed at trot and in a more expressed way at canter.

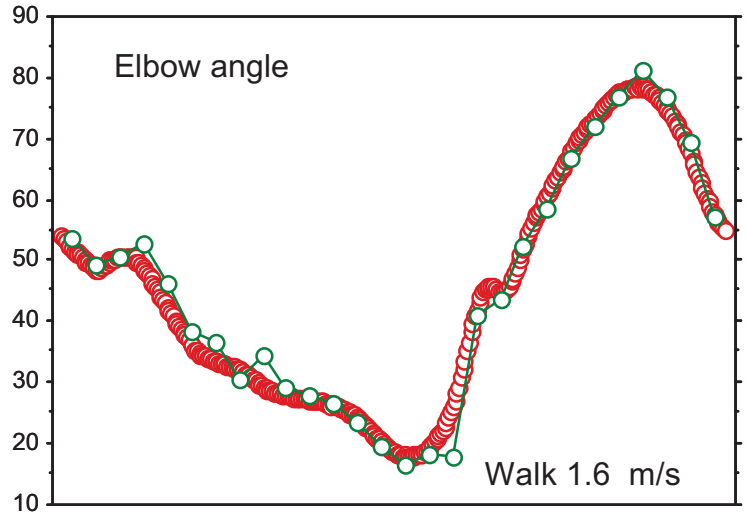

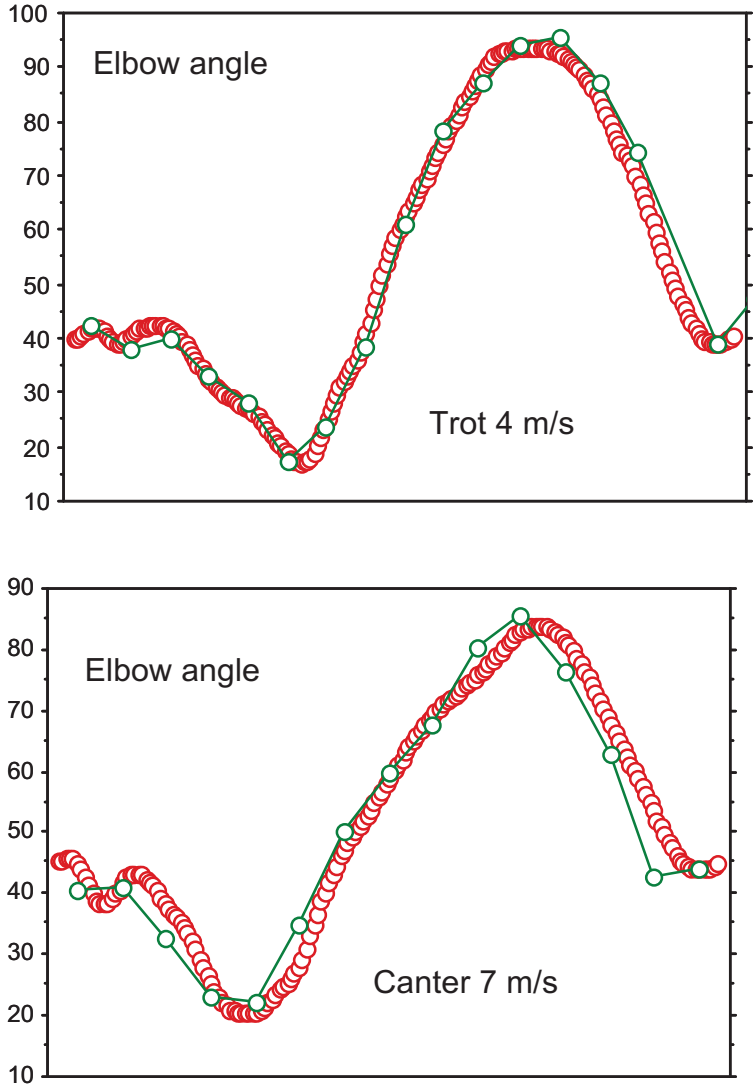

Fig. 34. Elbow angles at each gait types

Carpal joint angle (Fig. 35)

In the begining of the stride an oscillation around the zero degree during stance phase appeared with small measure of deviation. Shortly after the impact a hyperextension became visible on the curves - except for canter - the joint turned to flexion. The inflexion of the curve on the increasing part of joint flexion could be recognized. Absolute values of data looked more or less satisfactory in all gaits, but characteristics of curves turned out at walk and trot only.

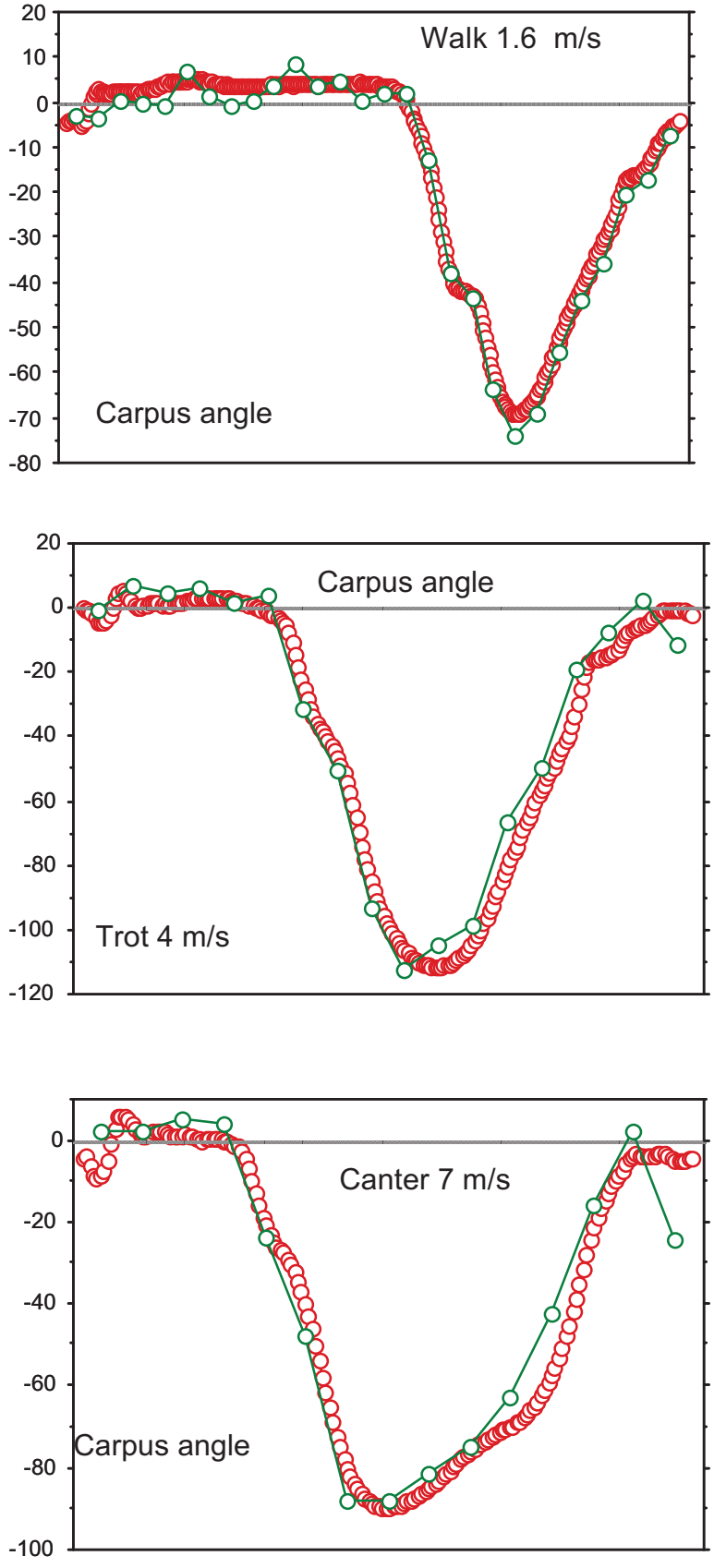

Fig. 35. Carpus angle at each gait type

Fetlock joint angle (Fig. 36)

Absolute values of data of CODA and VHS were fitting best at walk. At higher speed curves seemed to be shifted a bit. The inflexion on the ascending part at the begining of stance phase was followed. The plateau in the middle of the the stance phase showed oscillation. Characteristic details disappeared by increasing speed.

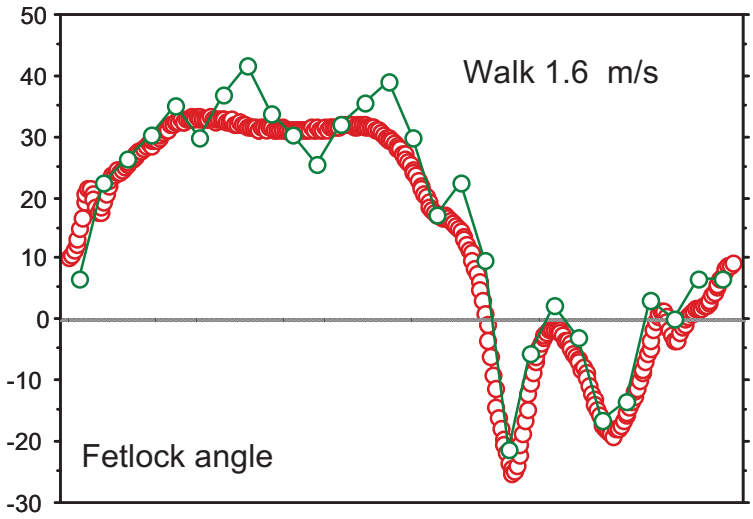

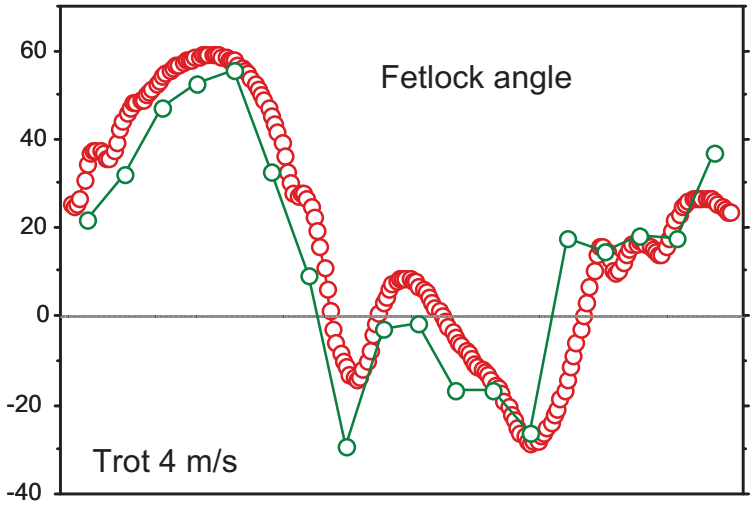

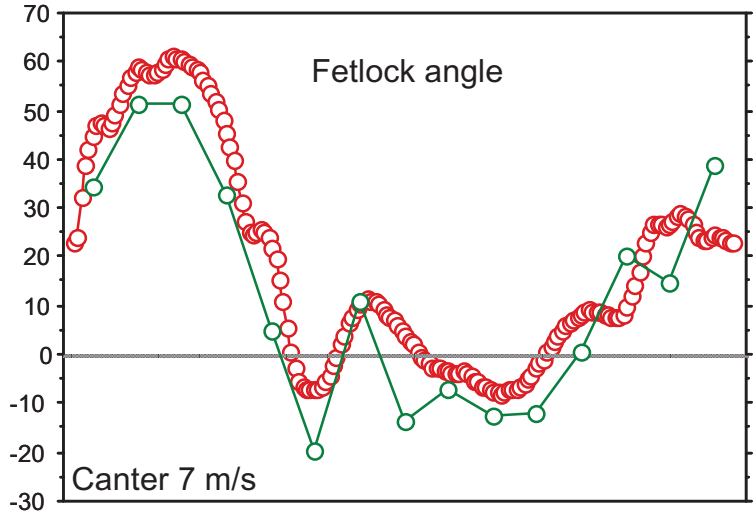

Fig. 36. Fetlock angle at each gait type

Hip joint angle (Fig. 37)

During stance phase the value of video data were definitely less than CODA data. However, at higher speed the ascending part of the curve showed higher values. At canter there were only two intersecting points of curves. Minimum of this curve could not be compared to missing CODA data, but the maximum point looked correct. Though the total curve did not follow CODA data finely because of a strong shift, trends of its portions were similar.

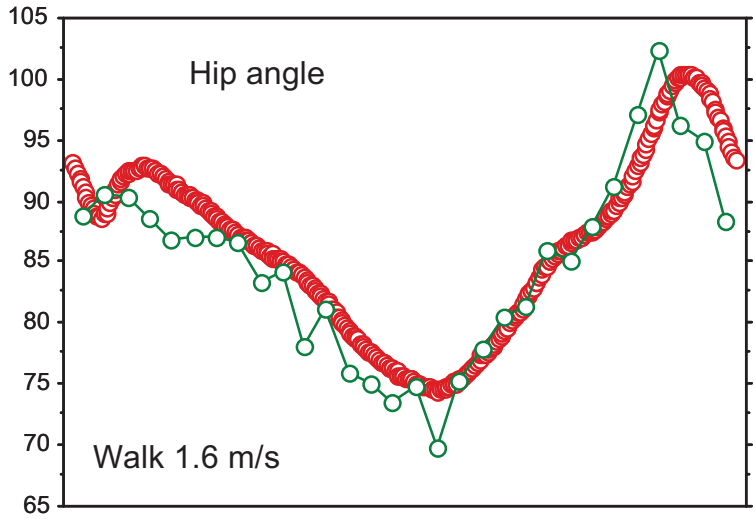

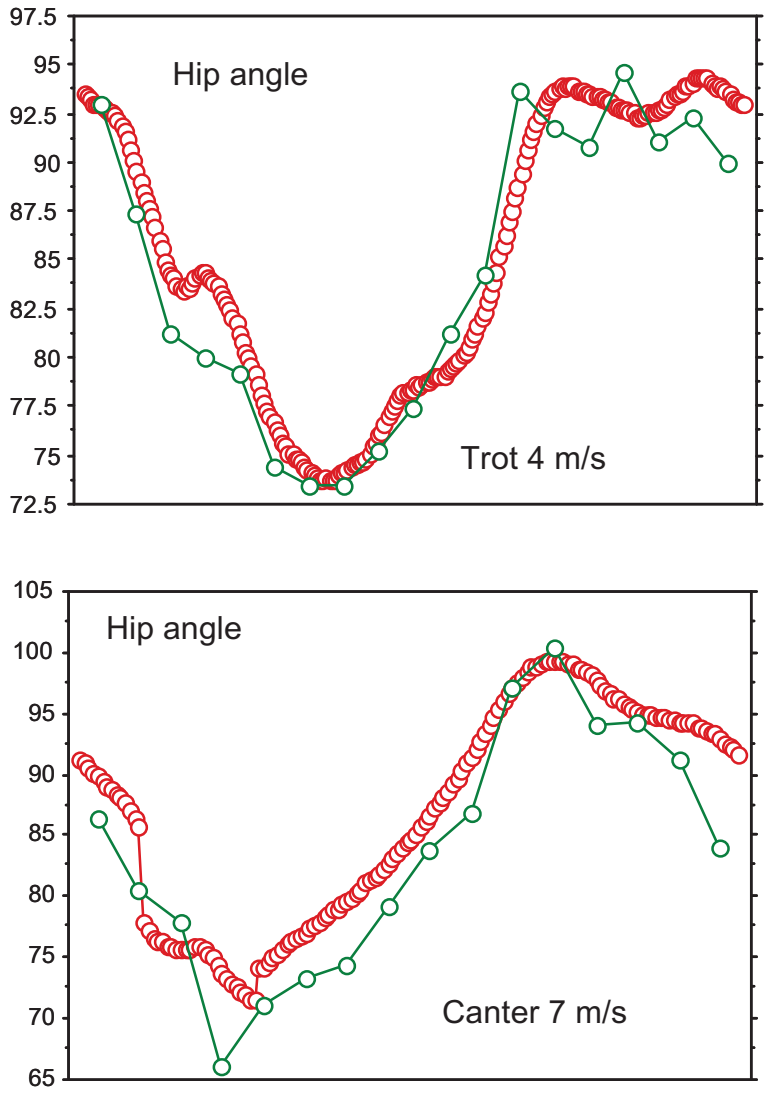

Fig. 37. Hip joint angle at each gait type

Stifle joint angle (Fig. 38)

During flexion of the stifle at least two peaks could be recognized in positive direction. Until getting maximum of flexion, curves were fitting. After this moment, elements of curves looked to be shifted. Canter seemed to be an exception. Its curve was strongly shifted.

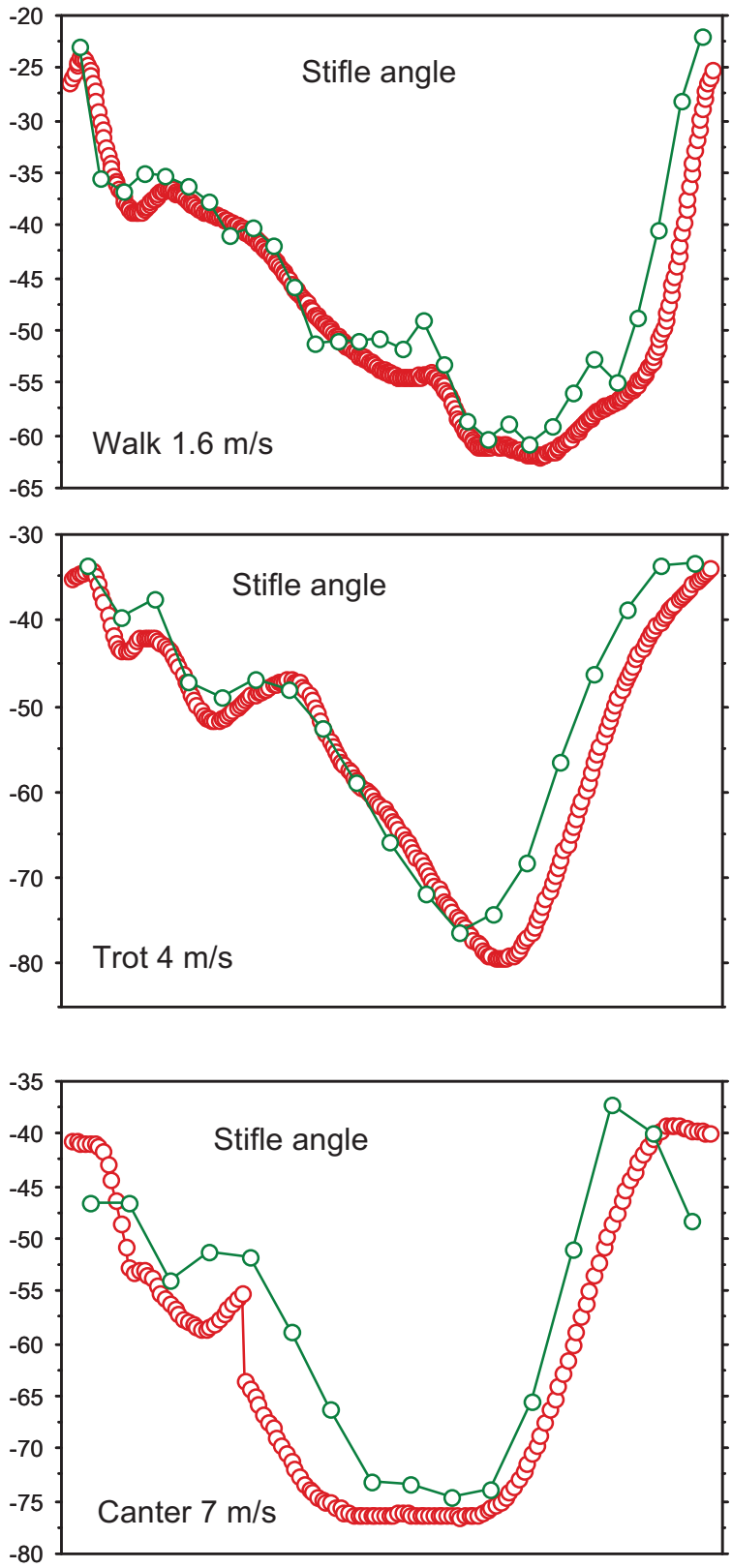

Fig. 38. Stifle joint angle at each gait type

Tarsal joint angle (Fig. 39)

Video data approximatelly followed CODA curves. The measure of maximum value was less in all gaits. All curves seemed to be shifted leftwards. The measure of shift was increasing with speed.

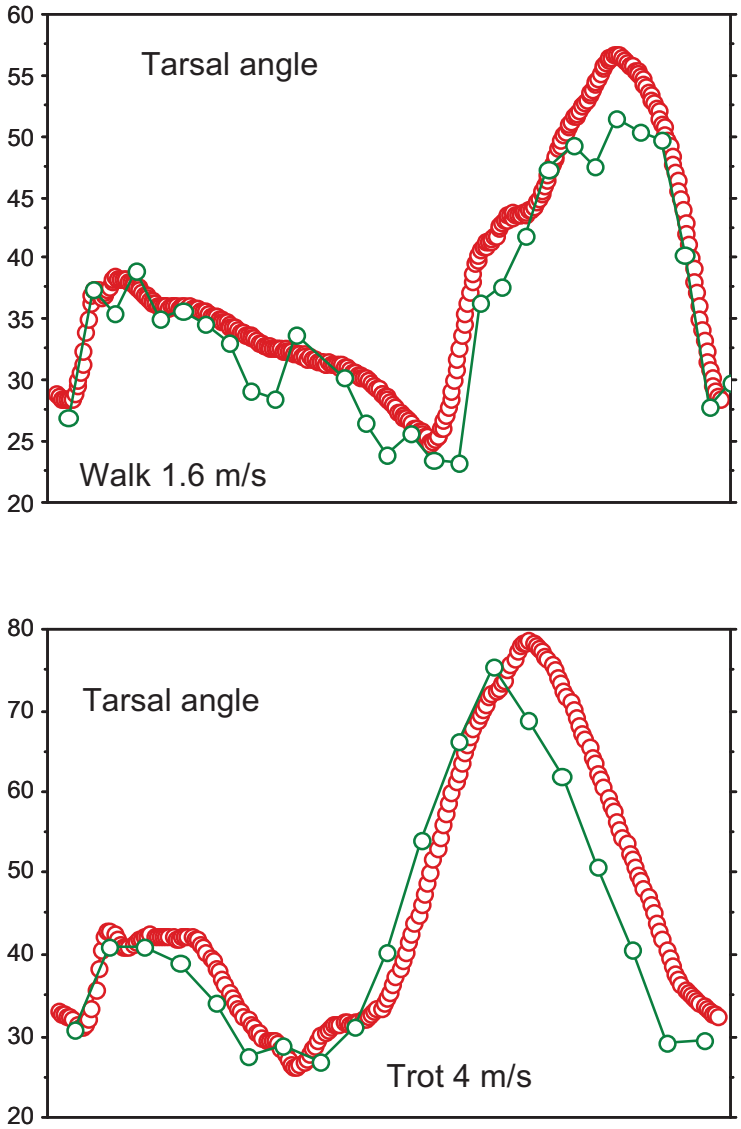

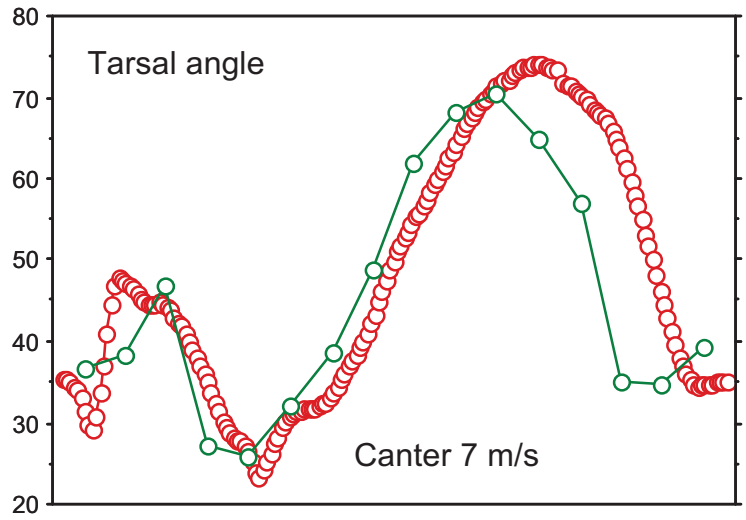

Fig. 39. Tarsal joint angle at each gait type

Fetlock joint angle (Fig. 40)

At walk, video data followed CODA curve with good accuracy. Inflexions of these curves could be also recognized. The first inflexion shortly after the impact could not be seen. By increasing speed, deviation was getting higher consequently.

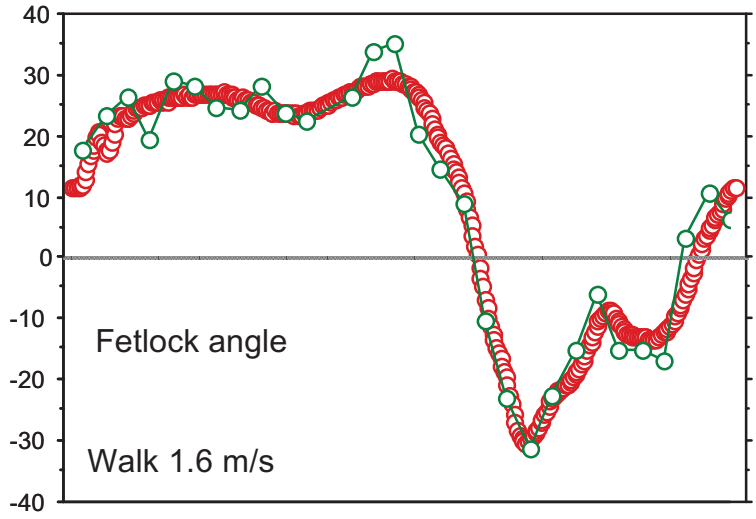

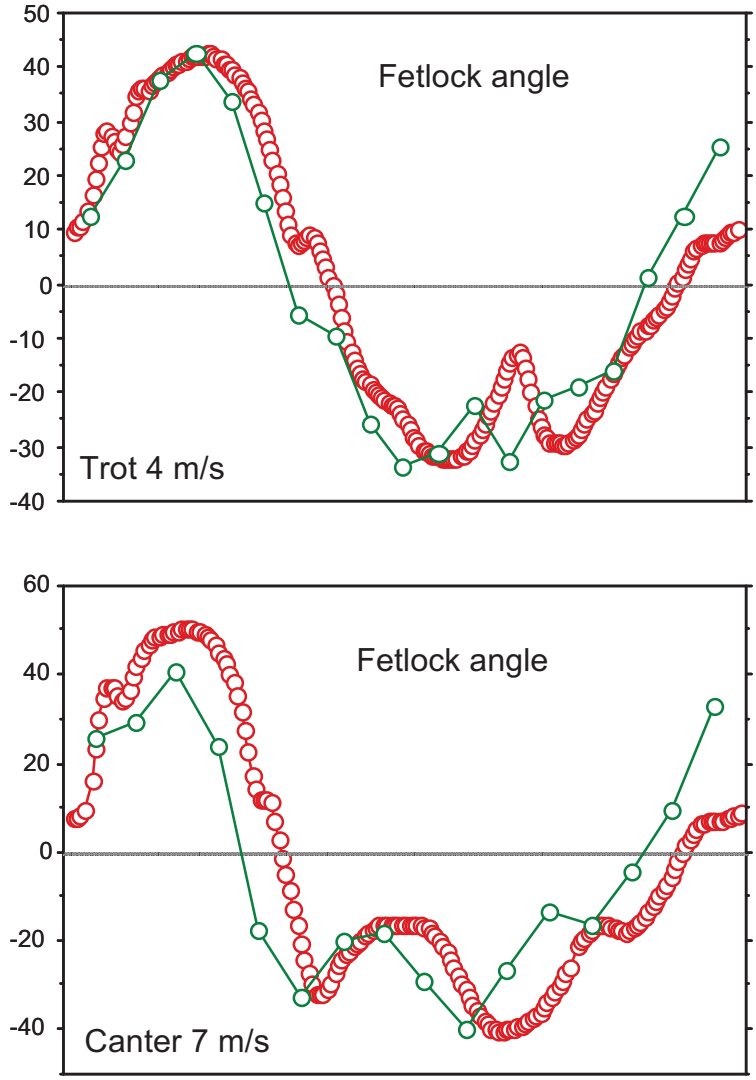

Fig. 40. Fetlock joint angle of the hindlimb at each gait type

5.7.1.2. Temporal variables

Temporal variables were compared to check the ability of the video user to detect several moments of strides. First and most important was the detection of impact (Table 9.). Time resolution of VHS devices is 40 msec, so the difference between data of the two systems was not allowed to be higher than this 40 msec (0.04 sec) unit in both positive and negative directions.

Table 9. Detection of impact

Number of stride	Measure of shift (sec)
1	0.003
2	0.053
3	0.026
4	0.013
5	0.03
6	0.02
7	0.043
8	0.016
9	0.05
10	0.03
11	0.013
12	0.026
13	0.043
Average	**0.028 (0.015)**

Duration of stance and swing phases were also compared (Table 10). On video recordings duration of these phases was calculated form the number of frames divided. The time unit is also 40 msec like at impact detection. Separation of phases on CODA recordings was assisted by accelerometer fixed on the hoof.

Table 10. Temporal data describing phases of stride from both systems. (n=13)

Speed	1.6 m/s (sd)	4 m/s (sd)	7 m/s (sd)
Mac			
Stride duration (secs)	1.04 (0.03)	0.70 (0.02)	0.59 (0.02)
Stance duration (%)	59.41	34.67	27.38
Stance duration (secs)	0.62 (0.02)	0.24 (0.01)	0.16 (0)
Swing duration (secs)	0.42 (0.02)	0.46 (0.02)	0.43 (0.02)
Coda			
Stride duration (secs)	1.03 (0.02)	0.69 (0.01)	0.58 (0.01)
Stance duration (%)	63.18	37.05	30.21
Stance duration (secs)	0.65 (0.01)	0.26 (0.01)	0.17 (0.003)
Swing duration (secs)	0.38 (0.02)	0.44 (0.01)	0.40 (0.007)

5.7.1.3. Test of accuracy

Table 11 describes absolute values of differences of forelimb data from each stride after synchronization with their standard deviation. Averaged differences of values belonging to the scapular curves showed rather high difference before data transformation, but the standard deviation of them was almost the same. Around 5 degrees of difference seemed to be acceptable at the elbow and carpal joints.

Their similar level of difference was remarkable. Fetlock data produced the highest deviation. The same level of standard deviations at elbow, carpus and fetlock joints was expressed.

Table 11. Averaged absolute values of differences from strides following each other at 4 m/s trot. (n=13)

	Scapula	Scap. transformed	Elbow	Carpus	Fetlock
Average	5.952	1.213	5.052	5.662	8.502
Standard dev.	1.498	1.296	7.039	7.446	7.358

5.7.1.4. Averaged angle - time diagrams of strides

Average stride of 13 strides from CODA and video recordings was also calculated and compared. According to non-averaged video data, oscillations were smoothed. Scapula rotation more or less followed CODA data except for the end of swing phase (Fig. 41). Despite the absolute values of this part were not correct, the position of peaks could be recognized. After correction of scapular data intersections occured much more often.

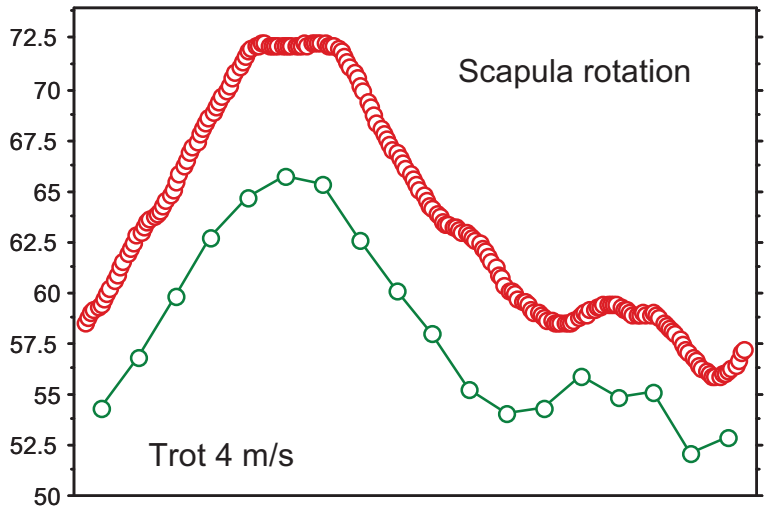

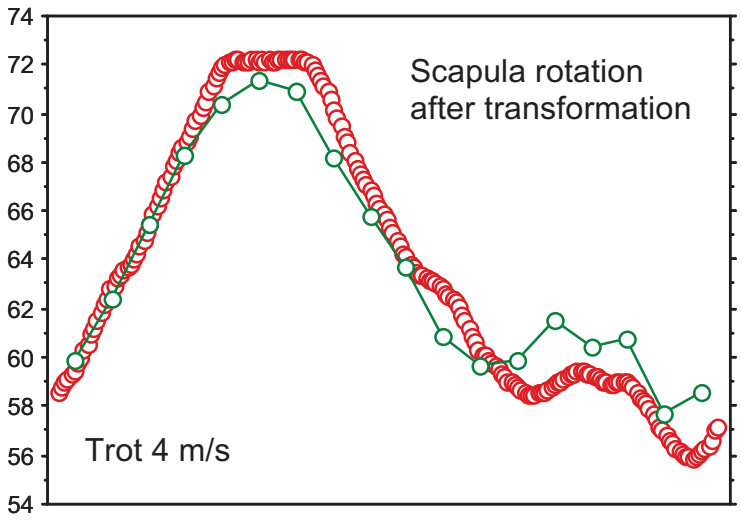

Fig. 41. Averaged scapula rotation before and after data transformation

Smaller peaks, specially at the begining of the stance phase - closer to each other than a video time unit (40 msec) - were flattened on elbow angle curves (Fig. 42).

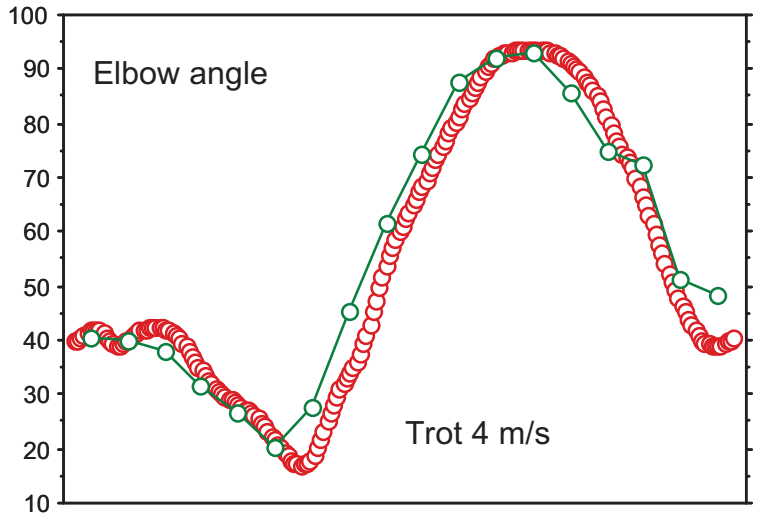

Fig. 42. Averaged data of the elbow joint angles

The double two-directional peak of the carpal cureve following impact had been smoothed (Fig. 43). Values of data were approximately equal. The maximum value of flexion remained below CODA values.

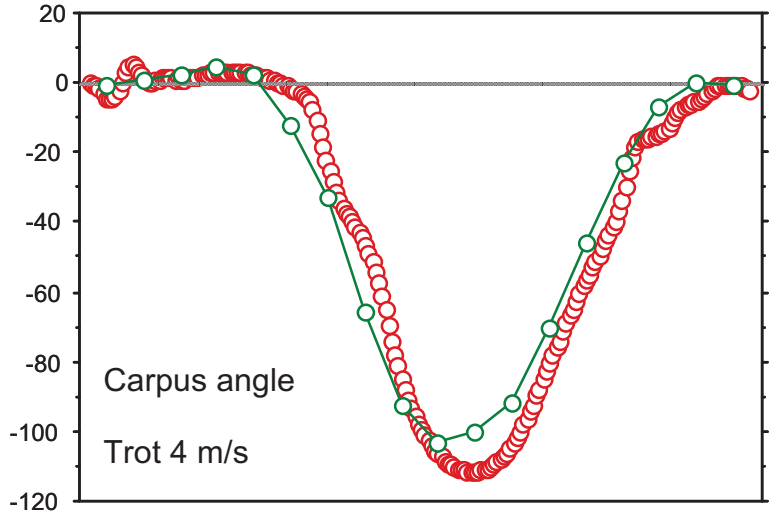

Fig. 43. Averaged data of the carpal joint angles

After some correct data the fetlock curve seemed to be shifted (Fig. 44). Deviations of data occurred at the descending branch of the stance and swing phases. Trend of peaks could be recognized in a shifted position.

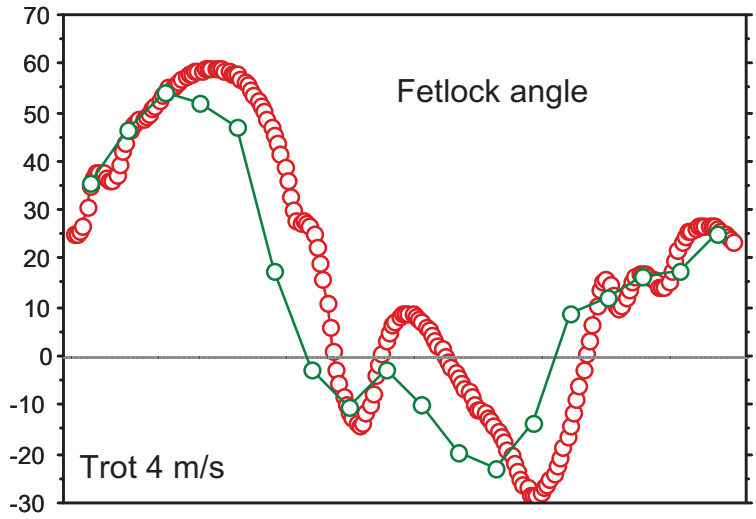

Fig. 44. Averaged data of the fetlock joint angles of the forelimb

5.7.2. Motion of the foal

5.7.2.1. Temporal data collected from motion of a foal at the walk and the trot

Lateral video recordings of a 2-month-old foal were taken at 4 m distance using no extra light sources. Motion of the foal was recorded on treadmill at 1.6 m/s and 4 m/s belt speed at pace and trot, respectively. Visual identification of most of the markers was sufficient but in some phases of the stride the outlines of the hoof marker were not clear.

Since the foal was only 2-months-old and being trained for treadmill actions only the two belt speeds were applied mentioned above. The foal performed smooth and uniform strides at both gait types. Altogether 13 strides were analyzed at each speed. Their temporal results are summarized in Table 12.

Table 12. Temporal data describing phases of stride in a foal (n=13)

Speed	**1.6 m/s (sd) (pace)**	**4 m/s (sd) (trot)**
Stride duration (secs)	0.7 (0.03)	0.46 (0.02)
Stance duration (%)	48.52	47.82
Stance duration (secs)	0.48 (0.02)	0.22 (0.01)
Swing duration (%)	51.42	52.17
Swing duration (secs)	0.36 (0.02)	0.24 (0.02)

As comapared to the adult, strides were shorter and the distribution of proportions between stance and swing phases was equalized in both gait types.

5.7.2.2. Angular data collected from forelimb motion of a foal at the walk and the trot

Alike in the adult horse, the same joints were observed and measured in the foal for a 13 strides long period. Curves derived from the walk and the trot were different of course in length due to their different durations. Therefore there was no overlap between the curves while their shape could be similar.

In the curves of the scapula rotation the first half was shorter in the trot than at the walk. The same phenomenon can be recognized in Fig. 45 at the elbow, carpus and fetlock joints. The elbow had a shorter resting phase before the

moment of take-off, the extended positions of the carpus and the fetlock were also shorter. It should be noticed that the features of the second half of the strides of both the walk and trot were preserved at each joint.

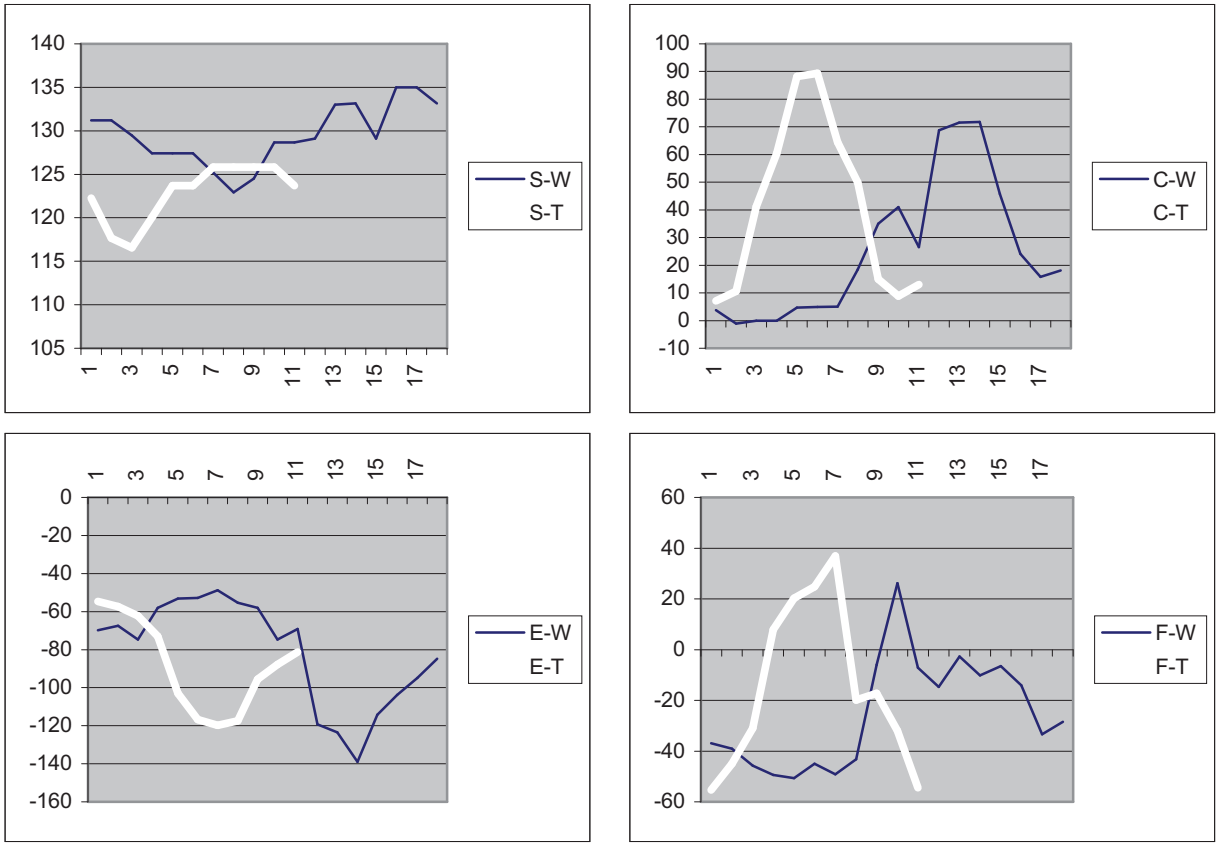

Fig. 45. Angle-time diagrams of the forelimb of the foal at walk and trot

Abbreviations:

S-W: Scapula rotation at walk

S-T: Scapula rotation at trot

E-W: Elbow angle at walk

E-T: Elbow angle at trot

C-W: Carpal angle at walk

C-T: Carpal angle at trot

F-W: Fetlock angle at walk

F-W: Fetlock angle at trot

5.7.2.3. Angular data collected from hindlimb motion of a foal at the walk and the trot

The shortening of the line at trot was similar to the forelimb data (Fig. 46). At the hip movements less oscillations could be observed during the flexion and extension. At the second phase of stance a plateau was seen in both gait types, even the values were smaller at the trot.

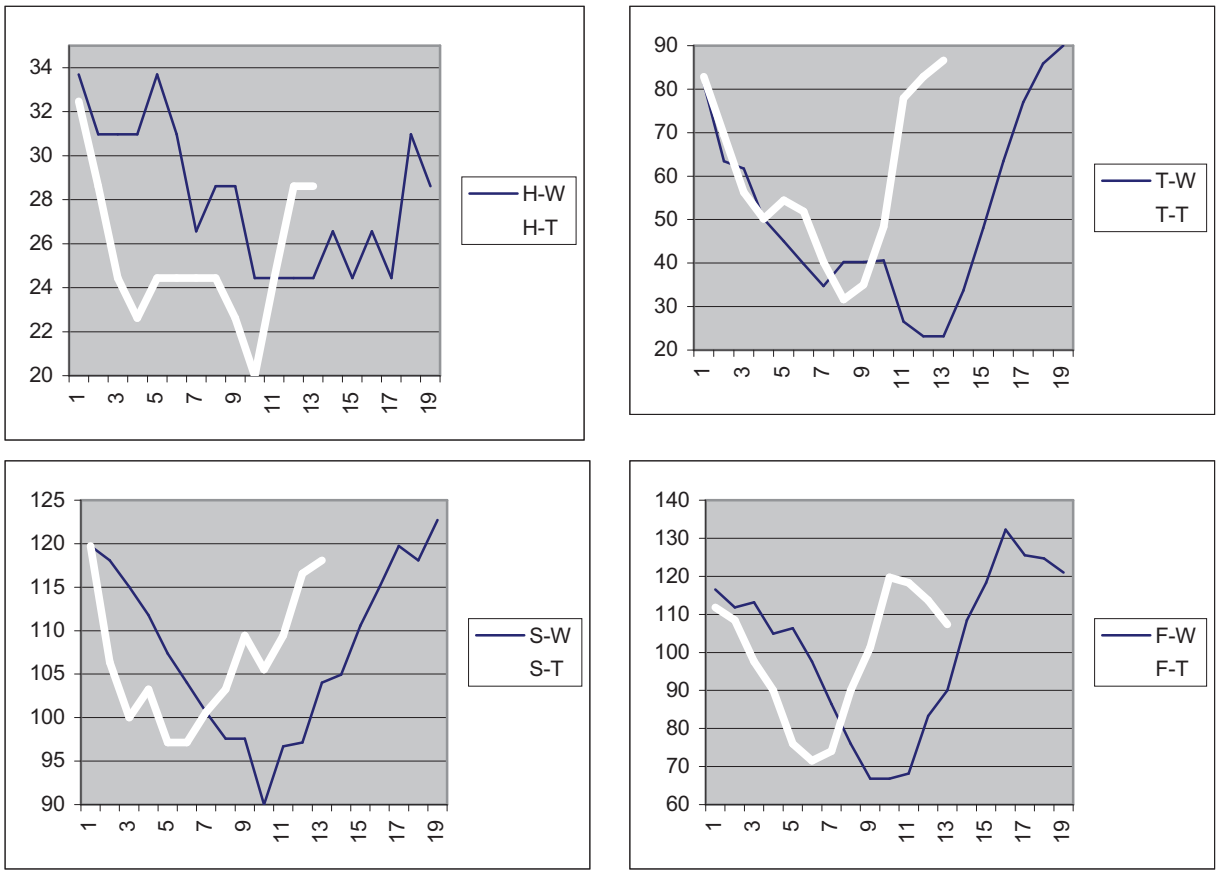

Fig. 46. Angle-time diagrams of the hindlimb of the foal at walk and trot

Abbreviations:

H-W: Hip angle at walk
H-T: Hip angle at trot
S-W: Stifle angle at walk
S-T: Stifle angle at trot
T-W: Tarsal angle at walk
T-T: Tarsal angle at trot
F-W: Fetlock angle at walk
F-W: Fetlock angle at trot

The values of the stifle joint varied within a narrower range at the trot than at the walk, otherwise their shape was similar. Similarities could be explored in the case of the tarsal and fetlock joints, too: the values of the trot gave less information but the shapes of the curves were the same. The smaller maxima and minima values should be noted at the trot in the stifle, tarsus and fetlock joints.

5.7.3. Comparison of motion of the adult to the foal

5.7.3.1. Temporal data analysis

Thirteen strides of the adult and the foal were studied at walk (1.6 m/s) and trot (4 m/s). Strides were defined from impact to impact and stance and swing phases were observed. Table 13 summarizes the percentage of the to phases. In the strides of the foal the deviation between the two phases remains small in both at the walk and the trot. The motion of the adult shows a definite decrease in the duration of the stance phase with speeding up the locomotion of the animal.

	Walk		**Trot**	
	stance (%)	**swing (%)**	**stance (%)**	**swing (%)**
Foal	48.57	51.42	47.82	52.17
Adult	59.41	40.59	37.67	62.33

Table 13. Temporal distribution of phases of strides at walk and at trot in the foal and the adult

5.7.3.2. Agle-time diagrams of the forelimb

As it was demonstrated in Table 13, duration of stance and swing phases within a single stride is equalized in the foal than in the adult. This makes a forward-shift in the curves when comparing angular data of the joints. This observation is in a good correlation with the overlap of curves in Fig. 47. Since video data of the movement of the adult horse were mathematically adjusted to data collected from CODA the same transformation was applied with video data of the motion of the foal.

The forward-shift of curves was spectacular when scapula, elbow and fetlock joints are compared but less pronounced in the carpus. The curves of the foal vary

within a narrower ranges, in other words, minima and maxima are less than in the adult. In the scapula rotation, the second phase of the curve (protraction) is less smooth and regular as compared to the adult.

In the elbow joint angle-time diagram the similarity is conspicouos. The turning over through the vertical position seems to be “synchronized” with the adult. The minimum value which corresponds to the beginning of flexion arrives earlier then expected.

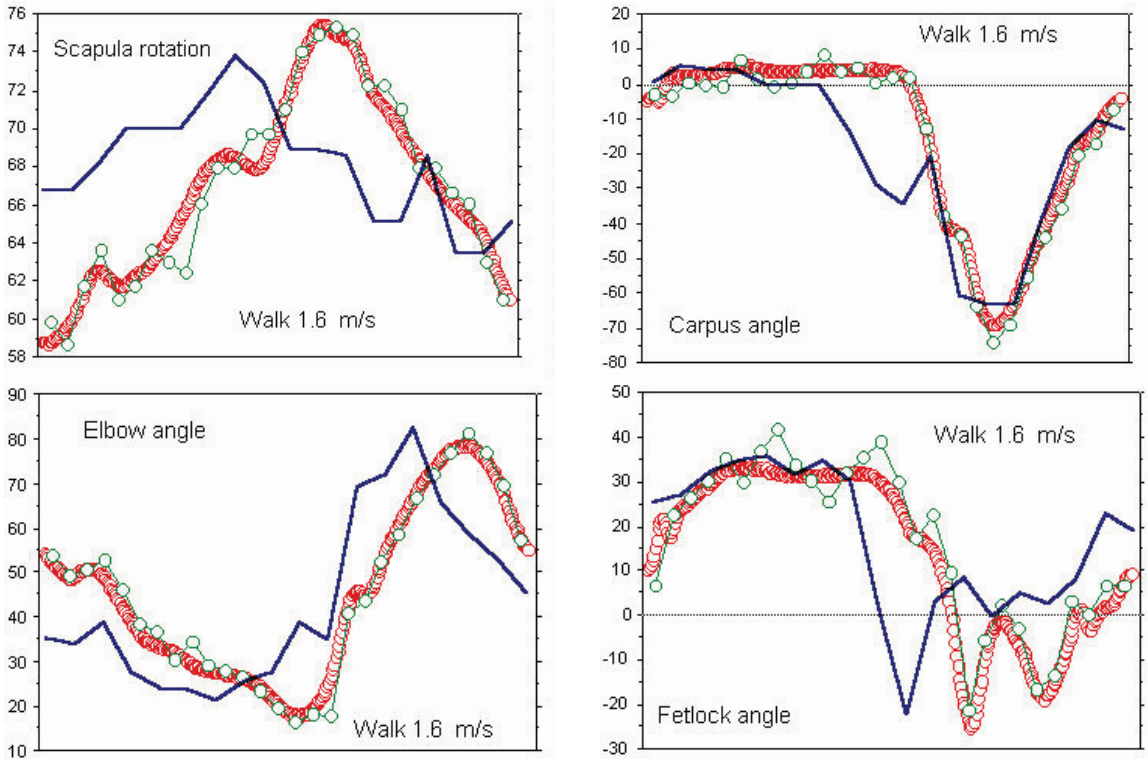

Fig. 47. Angle-time diagrams demostrating the forelimb move ments at walk. The compact circles correspond to data collected from CODA of the adult, the singular circels correspond to video data od the adult and the thick line represents video data of the foal

The carpal angle-time diagram shows a relatively good overlap between the foal and the adult, but some features should be considered in this anaylsis: some of the first values are similar, therefore the beginning of the shift cannot be detected reliably and descence in the foal’s curve starts earlier. Keeping these facts in mind the forward-shift can be recognized in this examination also at the beginning of

flexion. The flexion phase of the the carpus, however, seems to be more extended than in the adult.

The fetlock analysis shows also a good correlation between the motion of young and adult. The maximum of hyperextension in the foal is almost as high as in the adult, but the flexion follows it immediatelly with less oscillation.

5.7.3.3. Angle-time diagrams of the hindlimb

Since the same strides were analysed for forelimb and hindlimb, comparison of the distribution of the stance and swing phases were similar. Thus the same forward-shift appeared in these curves, too.

The hip movement was less intense in the foal than the adult (Fig. 48). Both in the descending and the ascendingphase of the curve positive and negative peaks appeared which suggest a less coordinated movement. The minima values of the foal remained also below the adult hip joint.

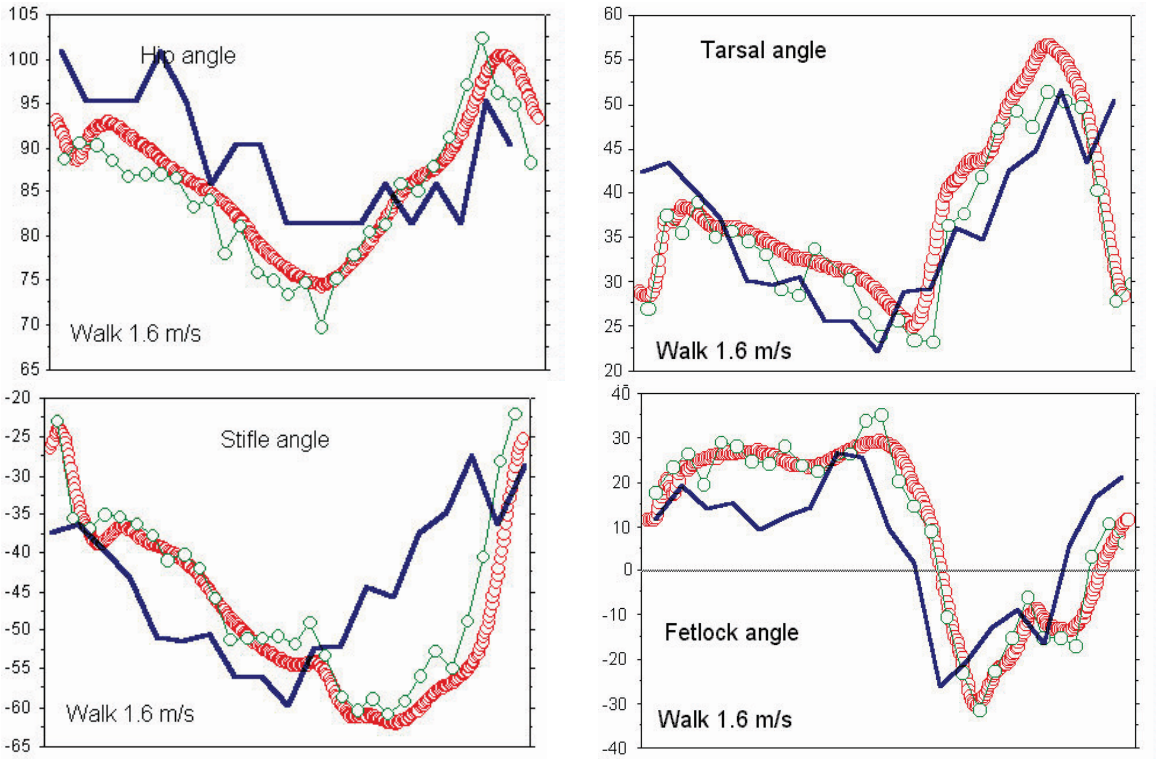

Fig. 48. Angle-time diagrams demostrating the hindlimb movements at walk. The compact circles correspond to data collected from CODA of the adult, the singular circels correspond to video data od the adult and the thick line represents video data of the foal

The motion of the stifle joint was also within a smaller range because its minimum and maximum values were smaller in the foal than in the adult. In the stance phase the similarity was more obvious than in the swing phase. In this second phase the movement of flexion seemed to be less coordinated in thefoal.

In the tarsal curve the first peak showing a slight flexion shortly after the moment of impact due to initial weight bearing could be easily dected in both ages. The extension of the foal's tarsal joint was larger and the following flexion is smaller: the extension started from a higher value and ended with a lower value than in the adult, while in the flexion the maximum value remained below the adult.

The fetlock joint curves were similar with the exception of the introduction phase. While in the adult the wieght bearing followed by the impact resulted a gradual increase in hyperextension with a double peak before and after the perpendicular position, the hyperextension of the foal was less massive and smooth. On the other hand the swing phase was in both cases similar.

6. DISCUSSION

6.1. Qualitative analysis

Owing to the fact that hardly any knowledge is available on the cytoarchtectonics and its development in the equine brain, one must rely on analogous events in better investigated species. Even this is rather uncertain since it is well established that there are great interspecies variations in cellular and pathway maturation of the brain (Noetzel and Rox, 1964; Korr, 1980). In the foal, the almost immediate standing up and hopping after birth make it obvious that this species is born with a fairly developed motor system which, however, lacks the economy of function and target-oriented coordination. Our findings relevant to cellular maturation and the development of myelinated areas of the central motor system support this assumption: the main motor centres and pathways are present already prenatally. Nevertheless, we could observe a spectacular maturation of these areas regarding both cytology and fibre quality up to postnatal day 45 from where growth rather than maturation became the leading phenomenon. This statement is based on a staining representative of the granular (rough) endoplasmic reticulum, an organelle responsible for massive protein synthesis on one hand, and on the gross histologic demonstration of myelination as a measure of impulse conducting capability on the other.

6.1.1. Cellular maturation

The sequence of neural cell maturation is proliferation, migration and differentiation (Jacobson, 1978). The precursors of nerve cells are generated in the subventricular layer of the developing brain vesicles. They undergo repeated mitoses and then start to migrate. Positioning of neurons to the final locations is guided by the processes of the radial glia (Hajós and Bascó, 1984) spanning the entire width of the neural tube and its early derivatives. The differentiation of motor neurons begins at different time intervals after they have finished their migration and occupied a final position in the brain (Altman, 1963; Atsumi, 1971). This comprises, as a next step the outgrowth of neuronal processes as indicated by ther multitude of growth cones and other cytologic and biochemical signs of axonal

pathfinding observed in this period (Landis, 1983; Pfenninger, 1983). Axonal and dendritic growth require an intensive protein synthesis for which only the cytoplasm of the cell body possesses the proper synthetic apparatus.

A second wave of protein synthetic activity is coupled to synapse formation (Balázs, 1971; Kornguth et al., 1968; Larramendi et al., 1969; Buchs et al., 1993). Our findings support the view that in the equine, the outgrowth of neuronal processes, particularly in the motor system takes place prenatally. Whether these processes are already capable to establish specific contacts, remains to be elucidated. Nevertheless, as it can be implicated from the incoordinated movements immediately after birth, there seems to be a rather diffuse flow of impulses along the motor pathways.

Looking at our findings at the cellular level, it is evident that the cytoplasmic organelle primarily associated with protein synthesis, i.e. the granular endoplasmic reticulum, hypertrophizes greatly at postnatal day 45. This is reflected by a significant increase in the intensity of Nissl-staining within the cytoplasm of motor nerve cell perikarya to such an extent that it masques all other cytoplasmic details which cannot be distinguished under the massive Nissl-substance staining. In the previous and following periods studied, the Nissl-substance of the motor neurons is present in the cytoplasm in the form of scattered large granules (Nissl-bodies) showing the typical stacks of cresyl violet-stained endoplasmic reticular cisterns. This suggests a burst-like up-regulation of in protein synthesis around postnatal day 45.

If viewed on a larger scale, all the motor areas showed a similar time course of changes in the amount of Nissl-substance. This is particularly conspicuous in areas such as the striatum where digitized images of Nissl-stained serial sections could readily be identified even at low magnifications on the basis of their cellular structure. The Nissl-pattern was prenatally poor, showing hardly any cells, whereas in the early postnatal period the cellular architecture of the striatum became evident: the caudate nucleus was distinguishable from the putamen and the typical stripes crossing the internal capsule were also revealed. A similar trend was observed in other motor regions as well.

The cerebellum deserves special attention since it is thought to be an important centre of motor coordination. It should be therefore emphasised that in the

prenatal equine cerebellum an external granular layer was hardly present indicative of an advanced cerebellar development alrerady in the late fetal period. This is particularly notable if we consider the persistence of this layer in other species over long postnatal periods (Markstrahler, 1947; Larsell, 1954; Kaufmann, 1959; Halmos, 1961; Lange, 1978).

On the basis of the present overall findings we can only specubte on the significance of the above peak in the amount of granular endoplasmic reticulum throughout the motor system. Supposed that this increase takes place up to a time (postnatal day 45) when neuronal processes have reached or at least approached their targets, we suggest that increased protein synthesis may reflect massive synaptogenesis, as a next phase of pathway maturation. Comparison with other species is not really relevant since there are extreme variations in the maturity of the motor system at birth. If the protein synthetic peak is assumed to correspond to synaptogenesis, the coincidence between this peak and the increase in the level of gait coordination observed in this postnatal period can be explained. This assumption, however, requires further cytochemical and electron microscopic support.

The decrease of Nissl-staining between early postnatal age and adulthood seems to be due to an expansion of the brain volume within this period not followed by an additional increase in Nissl-substance. As shown at higher power, cell bodies, but particularly the area of motor nuclei grow substantially. This may result in an apparent reduction of staining which is getting scattered over a larger territory.

6.1.2. Myelination

The functional significance of the myelin sheath is that by its internodal structure it enables the fastest velocity impulse conduction, the so-called saltatory conduction (Lillie, 1925; Tasaki and Takeuchi, 1941, 1942; Huxley and Stämpfli, 1949). At the nodes of Ranvier the axon is practically exposed to the extracellular space so that ionic changes take place in a sequence of 'bouncing' from one Ranvier node to the other skipping thereby the distance of the internodal segment of the axon.

It has been realized in classical strudies (see for references: Jacobson, 1978) that the development of the myelin sheath is a final step in the maturation of the

neuron. With regard to what was said above it is concievable that in the motor pathways normal velocity, target-oriented impulse conduction can happen only after the formation of a myelin sheath along the full length of the axon. In several developmental or neurological disorders myelination is either delayed or a demyelination occurs (Szalay et al., 2001). It is also well documented that the primary target of the so-called neurodegenerative diseases is the myelin sheath (Toews, 1999)

The time of myelination shows wide interspecies variations but in all cases it is marked by events such as an increase of protein synthesis in the parent cell body of the axon, and by a proliferation of oligodendroglia responsible for the formation of the myelin sheath (Río Hortega, 1930). In the present work the maturation of the neuronal cytoplasm, particularly of its main protein synthetic organelle was followed (see above), while subsequent sections were stained for myelin. Data on oligodendroglia proliferation could not be obtained from our material due to technical reasons arising from a long post mortem period elapsing prior to fixation of the brains.

Our results obtained with myelin staining show that the amount of myelin increases parallelly with the intensity of Nissl- staining, i.e. it is the highest at postnatal day 45. Here it should be noted that as a measure of myelin, its staining density over unit area was looked at. Therefore, it has to be mentioned that not only the staining density of myelinated pathways but also the area occupied by them increased substantially between the prenatal and early postnatal periods studied.

It also appeared that, at least with the method used, no regional differences could be detected in the advancement of mylination. Of course there were regions and structures such as the corpus callosum, septum, ansa lenticularis which underwent a spectacular growth between prenatal and early postnatal periods. This growth was apparently due to an increase in myelinated fibres. However, by postnatal day 45 the motor areas and tracts of the brain showed an equally advanced myelination. It is noteworthy that the area occupied by myelinated fibres also increased substantially, in other words, the white matter areas that contain the motor pathways expanded. This could be particularly well documented in the

white matter of the primary motor cortex and the internal capsule but the increase in other areas was also obvious.

6.1.3. Growth of the brain and myelination

Measurements of brain size in the different age groups clearly shows that if outer parameters are regarded, there is no net increase in size between th brains of the prenatal (-14-day-old) fetus and the 45-day-old foal. It is remarkable that this is the period when the bulk of internal changes occur either in cellular and cytoarchitectonic maturation or in myelin sheath formation. This discrepancy between overall growth and internal maturation is a novel finding.

Our observations suggest that the period between postnatal day 45 and adulthood brings about a significant growth of the overall size of the brain but adds little to the already formed myelin. It is most likely that the growth subsequent to the early postnatal period is due to the further ramification of dendritic trees, the development of the astroglial system and the increase in vascularization.

It is also suggested that the most important events of cytoplasmic maturation in the motor cell bodies are concluded by postnatal day 45.

All these stress the unusually early maturation of the equine motor system which appears to have a critical period of development up to the third months after birth. This means that future developmental, morphological, and functional analyses should concentrate on this period to understand more about the mechanisms of emergence of a coordinated gait in the foal.

6.1.4. Brain mass in relation to body size

The values of brain mass at various developmental stages suggests that the growth of the brain is not parallel to the growth of the entire body mass. While there is no increase in brain mas in the period between prenatal day 14 and postnatal day 45, the entire body mass of the foal increases 3-fold during the same time. In the following period up to adulthood, the increase in the mass of the brain is 1.8-fold, whereas that of the body 10-fold.

This again shows that foals are born with a relatively well developed brain which, after an intensive perinatal internal maturational process, grows moderately to reach the appr. 600 g mass typical for the adult. This growth is not comparable

to the growth of the entire body mass which greatly supersedes the growth of the brain.

6.2. Quantitative image analysis

Beside general growth of the brain, length, coronal section areas and diameters were measured and analysed. Results obtained from the qualitative study of histological preparations and of computer plots of large series of coronal sections were substantiated by the image anaylsis of digitized specimens.

6.2.1. Dimensions of the brain

Among major parts of the brain such as the hemispheres, cerebellum and the brainstem the longitudinal growth of the hemispheres was the most prominent. There was no difference between the left and right side as revealed in parallel sections. Within the perinatal age the change of this dimension follows the growth of the head but grows to a lesser extent than the head. When the coronal area measurements are regarded the cerebellum appears to be the fastest developing part which means that the cerebellum develops rather in the transverse direction by the development of its hemispheres. Since differences within the perinatal age were definitely smaller than the differences between data of perinatal and adult, mean of the perinatal and the adult groups could be created. It is known (Latshaw, 1987) that the vermis starts its development earlier than the hemispheres. In the perinatal age the histological maturation of the cerebellar cortex takes place and probably this causes the bulk of cerebellar growth. When the maxima of the transverse diameters were examined, a similar temporal change could be observed, as in growth of longitudinal dimensions. These data suggest that the growth of the equine cerebral hemispheres from the perinatal age to the adulthood is most pronounced longitudinally, while the cerebellum grows mainly in the transverse direction.

6.2.2. Gyrifiaction index

The amount of the cortical convolution numerically expressed by gyrifiaction index (Wosinski et al., 1996) seems to be high already in the late prenatal age. The change of GI is small within the range of examined ages. This also supports the hypothesis that the equine brain is well developed by birth. An increase can be observed, however, at the day of birth which indicates the dynamism of the cortical structures at this time. This phenomenon is underlined by the data of thickening of the cortex, too. From the youngest to the eldest (2 years period) the cortical thickness increases 1.8 times while from the youngest to 45-day-old (2 months period) 1.46 times. This disproportional distribution of thickening shows an intense cellular development found in the primary motor cortex.

6.2.3. Myelination

The proportion of myelin to the entire area of the sections (white/gray matter ratio) is outstanding in the first two months. From the last period of the prenatal age to postnatal day 45 an intense myelination was observed in the hemispheres and the cerebellum. This is in a good accordance with the development of the coordinated locomotion during this period of life. In section from the adult brain, the myelin occupies a relatively smaller territory in addition to the cellular elements. This is also supported by the values of cortical thickness.

Based on our findings territorial and temporal distribution of myelination among the major motor pathways and their temporal distribution it can be concluded that the internal capsule does not develop significantly while the pyramidal and extrapyramidal tracts grow 1.5-fold within the perinatal age. The necessary amount of myelinated motor pathwyas for basic locomotion during the weeks following birth are already present along the entire length of the pyramidal system. The thickening of the pyramidal tract at the medullary portion indicates that additional bundles join this tract deriving from the mesencephalon and the cerebellum. Similar developmental course was seen in the extrapyramidal system. By the end of the investigated period the internal capsule increase 1.5-fold, the pyramidal tract to twice, the extrapyramidal tract 2.5-fold and the corpus callosum 3.5-fold. In the perinatal period the development of corpus callosum, the major interhemispherial commissure is 1.7-fold. These data indicate that the

commissural relationships are not of primary significance around the day of birth but intensely develop afterwards. The function associated with this commissural pathway is coupled to that of similar areas between the hemispheres synchronizing this way the concurrent actions of the represented muscles.

6.2.4. Measurements in the cortex

In our histological inspections the number of Purkinje cells was high from the 7th day before birth to the 45th day following birth. Though these cells develop among the first ones in the cerebellum, their position in the piriform cell layer is not finalized by birth (Altman and Bayer, 1985). Due to this post embryonic migration the Purkinje cell count varies in the perinatal period. In the adult cerebellum, however, the cell count appears lower and its variability is definitely less which reflects the settlement of Purkinje cells by adulthood.

The presumed migration of postmitotic cells from the external germinative layer through the piriform cells to the final internal granular layer was hardly recognized in the early postnatal stage. The higher number of cells in a migratory phase in the molecular layer was encountered only in prenatal cerebella. In the 45-day-old foal the cell-count was also high but the reason of high cell number is obscure. One possible explanation is an increase in the number of “native” cell types (stellate and basket cells) of the molecular layer. Due to the cell migration emptying of the molecular layer and increase of the internal granular layer appears concurrently as we observed it at the perinatal age. The highest value of coefficient of molecular/IGL was found at the day of birth but it decreased in later stages.

For observations of cortical thickening of the motor cortex the cingulate gyrus was selected because the represenatation of the limbs in the primary motor cortex corresponds to this territory (Breazile et al., 1966). Results of this sampling cannot be applied to the entire brain but are in a tight correaltion with the development of the control of locomotr apparatus. By the end of the 2nd month of perinatal term the majority of thickening (1.45-fold) is already completed. The further thickening (0.2-fold) up to adulthood lasts for almost 2 years which indicates a disproportional growth of the motor cortex. We can state that the overwhelming share of development in the primary motor cortex takes place in the perinatal period.

6.3. Gait analysis

6.3.1. CODA-VHS parallel recordings

In our parallel recordings of the fore- and hindlimbs at walk, trot and canter of the adult horse sufficiently matching data were obtained. Reference curves of the adult joints from CODA and VHS recordings were well fitting. In spite of less details collected by the video system its curves seem to be useful in gait analysis (Clayton, 1988).

Theoretically, the more strides give the more information about events between two recorded video frames. However, these data are representing different moments, averaging them in a single curve can be misleading in comparisons. Averaging of data causes smoothed curves, but hides smaller characteristic peaks.

In the general stride analysis scapula rotation, after data transformation, shows satisfactory results in each gait type. The elbow angle is also acœptable, despite the “vibration” folowing impact has been smoothed at canter. Comparing the joints studied the carpus produces the best fitting curves in general. Although oscillation around zero degree during stance phase (Merkens and Schamhardt, 1994) looked slightly incorrect when studying single strides, examining successive series of strides average curves gave better results.

Video data of the fetlock angles in the forelimb are sufficient at walk but do not follow reliably CODA results at higher speed. It is interesting to note that the deviations between video and CODA data appear at constant phases of the stride. It is seen in the video recordings than in the lifted forelimb the antebrachium shades the distal part of the leg, especially close to the flexion point of the curve. This problem could be avoided by usage of well directed lights. Based on the consideration that the more distal segment has the higher angular speed and acceleration the higher deviations from CODA curves of the fetlock angles could be explained theoretically. Analysing more strides reveals that there are some phases of the stride when deviations periodically occur. The plateau, e.g., in the middle of the the stance phase shows oscillation even it suppose to be smooth according to the same portion of the CODA curve. Such a high deviation cannot be recognized in other joints at the same phase of the stride, so the difference

derives from such coordinates which are not used in calculations of other joint angles. The only similar coordinate is found on the hoof. The probable reason is inadequate light reflexion at the level of hoof due to poor illumination because of usage of CODA at the same time.

Hindlimb data show a slight deviation as compared to the forelimb. Since the forelimb and hindlimb recordings were taken in different strides, change of illumination circumstances could also influenced results. Hip angle as well as stifle and hind fetlock shows have acceptable results at walk and trot, but not at canter. Surprisingly, the tarsus gave the best results at all gaits. It is an interesting coincidence that the best results on the forelimb and the hindlimb are at the same horizontal level rather distally. This level seemed to be the best illuminated area.

Among temporal variables measured with both systems the differences fell into the range of the video measurement unit (0.04 s). Detection of impact based on video recognition gave inaccurate results in 15 % of 13 strides but never exceeded the theoretical 0.08 s error level calculated from one frame before and after the moment of impact.

The same frame counting method was applied for deterimation of describing of phases of stride. Percentage of stance and swing phases within the stride could be detected with ± 1.5 % of deviation.

Summarizing results of temporal data analysis, it can be concluded that all the video maesurements remained below error level. Considering that this measuring method can be readily applied by frame-by-frame playback of video recordings usage of this analysis is advanageous in practical work. In order to assist better recognition of impact enhacement of contrast between the hoof and the soil is suggested by painting or glueing the capsule with vivid colours.

6.3.2. Testing of accuracy

Results of comparison of averaged data show smaller deviation but less details, too. Scapular curves of CODA and video recordings are rather similar. Deviation of absolute values at the end of swing phase were influenced by the side bar on the treadmill. On the lifted forelimb the antebrachium shades the distal part of the leg especially close to the flexion point of the carpus which causes some deviation at the maximum flexion. This problem can be probably avoided by the use of well-

oriented lights and sufficient illumination. After some correct data, the fetlock curve seems to be shifted. On the other hand, differences occur at moments when fetlock joint is mostly accelerating and getting shaded, so the phenomenon of being pushed leftwards is not obviously caused by time shifting.

It is surprising, however, that the standard deviations of data from successive strides show similar pattern to this single stride devation and the occurrence of coincidences is rather constant.

Summarizing the test of accuracy it can be stated that the VHS recordings and the following image analysis described in our studies are suitable for purposes of gait analysis. The potential technical errors do not exceed the level of acceptance if circumstances such as good illumination are ensured.

6.3.3. The motion of the foal

When observing the locomotion of the young horse in the early postnatal age an early capability of locomotionis evident as compared to other domestic species. Still, coordinated, economic, purpose oriented movement develop somewhat later. Certain individual characteristics in the motion pattern are already present in the first some months which remain detectable throught the life-time of the animal (Back et al., 1994a). After the 4th month these characteristics can be applied in prediction of the sport performance of the foal (Back, 1994b).

The most prominent anatomical features of the foal's body are the relatively long limbs (Green, 1961). In the first some months the longitudinal growth of the limb segments is unequal, e.g. the femur elongates more rapidly than the tibia (Krüger, 1939). Due to these alterations the locomotor pattern in the age of the foal somewhat different to the adulthood (Drevemo et al., 1987). On the other hand, our examinations were made on a 2-month-old foal, therefore the incoordination of movements in the first days after birth were already eliminated.

Based on practical observations, the more or less equal distribution of the stance and swing phases within the stride was not surprising at walk (Leach and Cymbaluk, 1986; Muir et al., 1991). As it was demonstrated in our previous experiments with adult horse, the duration of the stance phase shortens with the increase of speed of the motion. At the trot of the foal similar shortening was expected but there was no significant alteration to the walk in the stance/swing

proportion. In other words, when dynamics of the walk and trot are concerned almost the same pattern is seen. Considering that the walk is thought to be a natural gait type while the trot is trained locomotion (especially at higher speed) it seems that in the early postnatal age the dynamics of the trot shows closer relationship to the walk of foal than to the trot of adulthood. This recognition is purely based on temporal data analysis.

When the distance of the peaks (on the time-axis) between walk and trot are compared in the agle-time diagrams the closest position is displayed by the fetlock joint. This means that the stance/swing proportion at the walk and trot is similar in the case of fetlock while the other joints show pronounced alterations. In our opinion the duration of stance and swing phases determines the position of the peak at the fetlock joint and as well as the characteristics of the curve before and after it, in other words the characteristics of the stance and swing phases. The effect of stance/swing proportion is less intense in the joints more proximally. While at the carpal and fetlock angles the peak represents the moment of lift-off the minima of the scapula and elbow curves are situated elsewhere. At the scapula rotation curve the proportion of the part before and following the peak is different at the two gait types. At the trot the proportion of the second part is elongated which means that the forwarding force arising in the shoulder joint acts longer. The longer the action the more exhausting the movement and this is indicating less coordination of muscle contractions acting on the shoulder joint.

The distance between the minima and maxima of the single curves measured on the angle-axis of the angle-time diagrams gives the maxima of flexion and extension during the pendular movement of the limb. Wider range of flexion and extension can be seen at walk in the shoulder and elbow joint and at trot in the carpus and fetlock. The expansion of the angular range reflects the larger force invested into movement. Our data suggest that at the walk of foals the shoulder and the elbow joints, while at trot the carpus and fetlock joints take more of the forwarding force. This means that the action point of force is shifted distally with the increasing speed of velocity, thus more energy is required for the movements (Holmström et al., 1994).

In the angle-time diagrams of the hindlimb joints the temporal shift along the time-axis between the walk and trot is approximatelly the same at each joint. The

distance between the minima and maxima measured on the angle-axis shows narrower range at the trot in each joint except for the hip. This suggests that the musculature of these joints can perform satisfactory forwarding within a smaller angular range at higher speed gait. Relating to the forelimb data, the fact becomes evident that the forelimb takes the major share from the force needed for forwarding the entire body. In the hip joint, however, the increase of the angular range with the frequent oscillation indicates a less coordinated movement.

6.3.4. Comparison of the motion of the foal and adult

The temporal data analysis in the foal-adult comparison reflects a slower limb motion of the adult at the same belt speed. This is due to the longer stance phase at both gait types. The 1.6 m/s belt speed was the base of comparison, thus both the foal and the adult had to approximate their convenient walk speed to this given parameter. Based on practical considerations we suppose that the stance/swing proportion of the stride does not change substantially during free motion of the animals and is in a good correlation with the data of the adult walk. This means that the walk of the foal was slightly forced up to the 1.6 m/s belt speed. Even visually the foal gave the impression of a normal walk. According to this, the stance/swing proportion at walk had a little swing predomination, but this did not change at 4 m/s speed of trot. The classical 1/3 stance : 2/3 swing proportion of the adult trot remained at ~fifty-fifty in the foal. This suggests that the foal prefers the rhythm of walk even at higher velocity speed which is certainly out of the range of convenience. This is in a good accordance with the experience of trainers that during the trot courses the foals "jump into canter" very often.

The analysis of forelimb angle-time diagrams of the foal and the adult shows surprisingly good correlations. Even fine details of CODA data lines remain hidden in the comparison of both VHS curves, characteristic peaks of angle-time profiles can be recognized at each joint. Despite the different stride frequency which causes a forward shift at each joint the data oscillation at the beginning of fetlock plateau and at the ascending end phase are similar, only the amount of oscillation is smaller. This means that at the level of this joint the motion pattern is similar in the foal and adult (Herring et al., 1992). Similar coincidences occur at the elbow joint but here - unlike to the fetlock - the minimum and maximum values of peaks

fall into the same range, too. At the carpus, the flexion following the hyperextension comes earlier, due to the forward shift mentioned above, but its absolute values are fitting the best. The scapular rotation gives the largest deviation. While the ascending half similar profile the descending slope is zigzagging at the foal. It is also remarkable that the angular range is definitely narrower in the foal than in the adult. This less extensive movement of the shoulder joint accompanied by almost the same range at the other joints and its uncertain protraction suggest a lower degree of coordination of its musculature (Wentink, 1978).

For the hindlimb the curves of the hip joint showed similar alterations between the foal and the adult as in the shoulder for the forelimb. On the descending half of the curve, large peaks appeared in the foal which was absent at the adult. The oscillation of the second half was also uncertain. Since the minimum and maximum values were also in different range in the foal than in the adult, the hip curve couple can be regarded as an indicator of a poorly coordinated joint. The angular ranges at the joints distal to the hip were similar in both ages. Despite the forward shift, the fetlock joint seems to be the best fitting. Even at the plateau of hyperextension, video data of the foal remain below that of the adult but this can be explained by the fact that this is the portion where the illumination was insufficient. Small differences can be seen at the tarsus and the extension of the stifle but the flexion of the stifle is less exponential and smooth with different minima and maxima. This way the stifle can be classified as a less coordinated joint at the perinatal age.

Taken together, the more muscles act on a joint, the higher is its incoordination.

7. CONCLUSIONS

Our findings obtained by qualitative and quantitative investigations suggest that the overall brain size does not increase between 14 days prior to expected birth to postnatal day 45, meanwhile significant internal changes take place:

- there is an increase in the amount of Nissl-substance, even if viewed at the level of single neurons;
- the amount of myelin increases involving the intensification of myelin staining and the appearance of newly formed myelin. This results in the enlargement of the areas of myelinated motor tracts.

Between postanatal day 45 and adulthood the overall size of the brain, as indicated by external parameters is almost doubled. This is not followed by an equal degree of myelin and Nissl-substance formation showing that the main events of motor pathway maturation occur between prenatal and early postnatal periods, whereas growth in size of the brain follows only after this maturation process.

Concerning locomotion of the horse, a new method of gait analysis was introduced and tested as to accuracy and applicability. The method is based on recordings made by a home video camcorder. It was found that it yields results comparable to those obtained by a specially developed unifunctional device (CODA).

With the help of the home video assisted method of gait analysis we were able to compare the curves of different stages of various gaits relevant to limb joints. Moreover, analytic curves were compared between the young foal and the adult. Comparison allowed to define the characteristics of ’immature’ and ’mature’ types of curve for each joint studied. This result may serve as a reference in further analyses. As a general feature, the the proximal joints equipped with large groups of muscles yield ’immature’ curves for longer postnatal periods than distal joints that in the horse are operated by a reduced musculature.

Temporal data analysis revealed that in foal the duration of phases within a stride is different from that in the adult. In the foal, the characteristcs of stride phases do not change from walk to trot, while in th adult these are conspicuously different.

Gait analysis pointed out in quantitative terms the increase of coordination in limb movements which was shown to be parallel to the maturation of the motor centres and tracts within the brain. It is assumed that there is a causal relationship between the maturation of structural and functional components of the equine locomotion. The verification of this assumption requires further studies.

Acknowledgements

I would like to express my great gratitude to Professor Ferenc Hajós for his support and efforts made as my supervisor and colleague.

Thanks are due to Dr. Willem Back at the Department of Large Animal Surgery of the Utrecht University for guidance during the treadmill measurements and to Prof. Karl Zilles at the Institute for Brain Research of the Düsseldorf University for consultations on quantitative methods and providing facilities for large-area sectioning and MRI imaging.

8. REFERENCES

Althouse, C.G. and Auer, J.A. (1987) The description of a treadmill and its uses in clinical equine research. Southwest Vet. 38. 40-46.

Altman, J. (1963) Autoradiographic investigation of cell proliferation in the brains of rats and cats. Anatomical Record 145, 573-591.

Altman, J. and Bayer, S. (1985) Embryonic development of the rat cerebellum I., II., III. J. Comp. Neurol. 231, 1-65.

Atsumi, S. (1971) The histogenesis of motor neuron with special reference to the correlation of their endplate formation. Acta Anat. 80, 161-182.

Back, W., Bogert, A.J. van der, Weeren, P.R. van, Bruin, G. and Barneveld, A. (1993) Quantification of the locomotion of Dutch Warmblood foals. Acta Anat. 146, 141-147.

Back, W., Barneveld, A., Schamhardt, H.C., Bruin, G. and Hartman, W. (1994a) Longitudinal development of the kinematics in 4-, 10-, 18- and 26-month-old Duch Warmblood horses. Equine Vet. J. Suppl. 17, 3-6.

Back, W. (1994b) Development of equine locomotion from foal to adult. Theses, Utrecht, The Netherlands.

Back, W., Schamhardt, H.C., Savelberg, H.H.C.M., Bogert, A. J. van den, Bruin, G., Hartman, W., and Barneveld, A. (1995a) How the horse moves: 1. Significance of graphical representations of equine foredlimb kinematics. Equine Vet. J. 27 (1) 31-38.

Back, W., Schamhardt, H.C., Savelberg, H.H.C.M., Bogert, A. J. van den, Bruin, G., Hartman, W., and Barneveld, A. (1995b) How the horse moves: 2. Significance of graphical representations of equine hindlimb kinematics. Equine Vet. J. 27 (1) 39-45.

Balázs, R.: Biochemical effects of thyroid hormones in the developing brain. In Pease, D.C. ed. Cellular Aspects of Neural Growth and Differentiation. Univ. Calif. Press, Los Angeles, 1971 pp. 273-311.

Baumeister, W.: Anleitung zur Kenntniss des Außeren des Pferdes für Tierärtze, Gestütsbeamte und Pferdebeseitzer jeden Standes. 6te Auflage von Rueff umgearbeitet. Ebner & Seubert, Stuttgart, 1870.

Beck, R.J., Andriacchi, T.P., Kuo, K.N., Fermier, R.W. and Galante, J.O. (1981) Changes in the gait pattern of growing children. J. Bone Joint Surg. 63a, 1452-1456.

Breazile, J.E., Swafford, B.C. and Biles, D.R. (1966) Motor cortex of the horse. Am. J. Vet. Res. 27, 1605-1609

Breter, M. Beitrag zur Gehirnentwicklung des Schweines. Diss. med. vet. München (1960).

Buchs, P.A., Stoppini, L. and Müller, D. (1993) Structural modifications associated with synaptic development in the area CA1 of rat hippocampal organotypic cultures. Devl. Brain Res. 71, 81-91.

Clark, J.E., Whitall, J. and Phillips, S.J. (1988) Human interlimb coordination: the first 6 months of independent walking. Develop. Psychobiol. 21, 445-456.

Clayton, H.M. (1988) Gait evaluation: Making the most of your home video system. Proc. 34th Ann. Conv. AAEP 4-7 dec, San Diego, California, 447-455.

Clayton, H.M. (1989) Gait analysis as a predicitve tool in performance horses. J. Equine Vet. Sc. 6, 335-336.

Clayton, H.M. (1991) Advances in motion analysis. Vet. Clin. NA 7, 365-382.

Corley, J.M. and Goodship, A.E: (1993) Treadmill training induced changes to some kinematic variables measured at the canter in Thoroughbred fillies. Equine Vet. J. Suppl. 17, 20-24.

De Lahunta, A.: Veterinary Neuroanatomy and Clicnical Neurology. Saunders Co., Philadelphia, London, Toronto (1977).

Drevemo, S., Fredericson, I., Hjertén, G. and McMiken, D. (1987) Early development of gait asymmetries in trotting Standardbred colts. Equine Vet. J. 19, 189-191.

Fredericson, I., Drevemo, S., Dalin, G., Hjertén, G., Björne, K., Rynde, R. and Franzen, G. (1983) Treadmill for equine locomotion analysis. Equine Vet. J. 15, 111-115.

Froriep, A. (1891) Über die Entwicklung des Sehnerven. Anat. Anz. 6, 155-166.

Grant, B.D. (1989) Performance prediction. Equine Athlete 2, 1-2.

Grant, B.D. (1992) Performance prediction. Equine Vet. Data 13, 226-227.

Green, D.A. (1961) A review of studies on the growth rate of the horse. Brit. Vet. J. 117, 181-191.

Hajós, F. and Bascó, E.: The surface-contact glia (monograph). Advances in Anatomy, Embryology and Cell Biology, Vol. 84. Springer-Verlag, Berlin, Heidelberg, New York, Tokyo (1984).

Halmos, G.: Entwicklung des Kleinhirns beim Rind unter besonderer Berüvksichtigung lokaler Hyperplasien des Kleinhirnwurmes. Diss. med. vet. Hannover (1961).

Herring, L., Thompson, K.N. and Jarret, S. (1992) Defining normal three-dimensional kinematics of the lower forelimb in the horse. J. Equine Vet. Sc. 12, 172-176.

Holmström, M., Fredericson, I. and Drevemo, S. (1994) Biokinematic differences between riding horses with good and poor trot. Equine Vet. J. Suppl. 17, 51-56.

Houston, M.L. (1968) The early brain development of the dog. J. Comp. Neurol. 134, 371-384.

Huxley, A.F. and Stämpfli, R. (1949) Evidence for saltatory conduction in peripheral myelinated nerve fibres. Journal of Physiology 108, 315-339.

Ingen Schenau, G.J. van (1980) Some fundamental aspects of the biomechanics of overground versus treadmill locomotion. Med. and Sc. in Sports and Exerc. 12, 257-261.

Jacobson, M.: Developmental neurobiology. Plenum Press, New York, London, 1978.

Kaufmann, I. (1959) Untersuchungen über die Frühentwicklung des Kleinhirns beim Rind. Schw. Arch. Tierheilk. 101, 49-75.

Kobluk, C.N., Schnurr, D., Horney, F.D., Sumner-Smith, G., Willoughby, R.A., Deekler, V. and Hearn, T.C. (1989) Use of high-speed cinematography and computer generated gait diagrams for the study of equine hindlimb kinematics. Equine Vet. J. 21, 48-58.

Kornguth, S.E., Anderson, J.W. and Scott, G. (1968) The development of the synaptic contents in the cerebellum of *Macaca mulatta*. J. Comp. Neurol. 132, 531-546.

Korr, H.: Proliferation of different cell types in the brain. Advances in Anatomy, Embryology and Cell Biology, Vol. 61. Springer-Verlag, Berlin (1980).

Krüger, W. (1939) Über Wachstumsmessungen an den Skelettgrundlagen der Gliedmaßen- und Rumpfabschnitte beim lebenden Trakhener Warmblut- und Mecklenburger Kaltblutpferd mittels eines eigenen Meßverfahrens. Zeitschr. für Tierz. und Züchtungsbiol. 43, 145-163.

Landis, S.C. (1983) Neuronal growth cones. Ann. Rev. Physiol. 45, 567-580.

Lange, W. (1978) The myelination of the cerebellar cortex in the cat. Cell Tissue Res. 188, 509-520.

Lanyon, L.E. (1971) Use of an accelerometer to determine support and swing phase of a limb during locomotion. Am. J. Vet. Res. 32, 1099-1101.

Larramendi, L.M.H.: Analysis of the synaptogenesis in the cerebellum of the mouse. In Llinas, R. ed. Neurobiology of Cerebellar Evolution and Development. AMA Educ. and Res. Found. Chicago, Ill. 1969, pp. 803-843.

Larsell, O. (1954) The development of the cerebellum of the pig. Anat. Rec. 118, 73-107.

Latshaw, W.K.: Veterinary Developmental Anatomy. Decker Inc. Toronto, Philadelphia, 1987.

Leach, D.H. and Cymbaluk, N.F. (1986) Relationships between stride length, stride frequency, and morphometrics of foals. Am. J. Vet. Res. 47, 2090-2097.

Lillie, R.S. (1925) Factor affecting transmission and recovery in the passive iron nerve model. Journal of General Physiology. 7, 473-507.

Magyar Imre és Győrffy-Villám András: Iskolalovaglás. Mezőgazdasági Kiadó, Budapest, 1988.

Marey, E.-J.: La machine animale, locomotion terrestre et aérienne. Germer Baillière, Paris, 1873.

Markstrahler, W.: Zur fetalen Entwicklung des Katzen Kleinhirns unter besonderer Berücksichtigung seiner Rindenstruktur. Diss. med. vet. Zürich (1947).

Martinez del Campo, L.J., Kobluk, C.N., Greer, N., Trent, A.M., Stoner, L.J., Wickstrom, L. and Loch, D. (1991) The use of high-speed videography to generate angle-time and angle-angle diagrams for the study of equine locomotion. Vet. Comp. Orthop. Traum. 4, 120-131.

Merkens, H.W. and Schamhardt, H.C. (1994) Relationships between ground reaction force patterns and kinematics in the walking and trotting horse. Equine Vet. J. Suppl. 17, 67-70.

Milart, Z.: Die Morphogenese des Gehirns beim Hausrind. 1. Mitt. Morphogenese des Rautenhirns. Arch. Exp. Vet. Med. 18 (1964) 633-648; 2. Mitt. Morphogenese des Mittel- unf Vorhirns. Arch. Exp. Vet. Med. 18 (1964) 1139-1150; 3. Mitt. Morphogenese der Furchen, Windungen und der Insel. Arch. Exp. Vet. Med. 19 (1965) 615-628.

Mitchelson, D.L. (1988) Automated three dimensional movement analysis using the CODA-3 system. Biomed. Tech. 33, 179-182.

Muir, G.D., Leach, D.H., Cymbaluk, N.F. and Dyson, S. (1991) Velocity-dependent changes on intrinsic stride timing variables of Quarterhorse foals. Equine Exerc. Phys. 3, 141-145.

Mumenthaler, M.: Neurológia. 1989. Medicina, Budapest

Noetzel, H. and Rox, J. (1964) Autoradiographische Untersuchungen über Zellteilung und Zellentwicklung im Gehirn der erwachsenen Maus und des erwachsenen Rhesus-Affen nach Injektion vom radioaktivem Thymidin. Acta Neuropathologica 3, 326-342

Pannese, E.: Neuocytology. Thieme, Stuttgart, New York (1994).

Pfenninger, K.H. (1983) Molecular biology of the nerve growth cone: A perspective. Adv. Exp. Med. Biol. 181, 1-14.

Río Hortega, P. del. (1930) Concepts histogénique, morphologique, physiologique et physio-pathologique de la microglie. Revue Neurologique 37, 956-986.

Rosenfeld, A. and Kak, A.C.: Digital Picture Processing. Academic Press, New York, 1976 p.457.

Schamhardt, H.C., Bogert, A.J. van den, Lammertink, J.L.M.A. and Markies, H. (1992) Measurements and analysis of equine locomotion with the CODA-3 kinematic analysis system. Proceedings 8th Meeting ESB, June 21-24, Rome, Italy, 270.

Schamhardt, H.C. and Merkens, H.W. (1994) Objective determination of of ground contact of the limbs of the horse at the walk and trot: comparison between ground reaction forces, accelerometer data and kinematics. Equine Vet. J. Suppl. 17, 75-79.

Stashak, T.S. Adam's Lameness in horses. 4th ed. Lea & Febiger, Philadelphia, 1987, p. 76.

Szalay, F., Zsarnovszky, A., Fekete, S., Hullár, I., Jancsik, V. and Hajós, F. (2001) Retarded myelination in the lumbar spinal cord of piglets born with spread-leg syndrome. Anat. Embryol. 203, 53-59.

Szőke Annamária és Beke László: Székely Bertalan mozgástanulányai. 1992. Magyar Képzőművészeti Főiskola – Balassi Kiadó – Tartóshullám Budapest

Tasaki, I. and Takeuchi, T. (1941) Der am Ranvierschen Knoten entstehende Aktionsstrom und seine Bedeutung für die Erregungsleitung. Pflügers Archiv für die gesamte Physiologie 244, 696-711.

Tasaki, I. and Takeuchi, T. (1942) Weitere Studienüber den Aktionsstrom der markhaltingen Nervenfaser und über die eletrosaltatorische Übertragung Nervenimpulses. Pflügers Archiv für die gesamte Physiologie 245, 764-782.

Toews, T.: Molecular Probes for PNS Neurotoxicity, Degeneration and Regeneration. In Neurodegeneration Methods and Protocols eds Harry, J. and Tilson, H.A. Humana Press, Totowa, N.J. pp. 67-88 1999.

Weeren, P.R. van, Bogert, A.J. van den and Barneveld, A. (1992) Correction models for skin displacememten in the equine kinematic gait analysis. J. Equine Vet. Sc. 12, 178-192.

Wentink, G.H. (1978) Biokinetical analysis of the movement of the pelvic limb of the horse and the rolel of muscles in the walk and trot. Anat. Embryol. 152, 261-272.

Wosinski, M., Schleicher, A. and Zilles, K. (1996) Quantitative analysis of gyrifiaction of cerebral cortex in dogs. Neurobiology, 4, 441-468.

9. APPENDIX

Source codes

GI calculations

```
macro 'Count Green Pixels  [2]';
{LUT: 255,2,greyscale,
user1, user2 only}


begin
  RequiresVersion(1.44);
    ResetCounter;
    SetForeground(2);
    DrawBoundary;
    Beep;

  SetUser1Label('Red');
  SetUser2Label('Green');
  Measure;
  rUser1[rCount]:=histogram[1];
  rUser2[rCount]:=histogram[2];
  UpdateResults;
  CopyResults;
  {SelectWindows('Data');
  Paste;}
    SelectTool('magnifier');
    SetForeground(1);
    KillROI;
end;



macro 'Count Red Pixels [3]';

begin
  RequiresVersion(1.44);
  SetUser1Label('Red');
  SetUser2Label('Green');
  Measure;
    Dispose;
  rUser1[rCount]:=histogram[1];
  rUser2[rCount]:=histogram[2];
  UpdateResults;
  CopyResults;
  SelectWindows('Data');
  Paste;
  WriteLn('');
  WriteLn('');
  SelectTool('polygon');
end;
```

```
MACRO 'Data window [D]';

BEGIN
  NewTextWindow('Data');
  WriteLn('Red(total)   Green(outer)');
  WriteLn('');
END;

MACRO 'Temp [1]';

BEGIN
  Copy;
  SetNewSize(800,800);
  MakeNewWindow('temp');
  Paste;
   KillROI;
   SetDensitySlide(69,255);
  SelectTool('wand');
END;


MACRO 'Change Tools  []';


BEGIN
   KillROI;
  SelectTool('magnifier');
END;



MACRO 'Dispose window [X]';

BEGIN
  Dispose;
END;
```

Calculations of total myelin amount

```
macro 'Count Green Pixels  []';
{LUT: 255,2,greyscale,
user1, user2 only}


begin
   ResetCounter;
  SetOptions('Area');
  Measure;
  UpdateResults;
 SetDensitySlide(188,255);
  KillROI;
end;



macro 'Myelin area [3]';
```

```
begin
  MakeBinary;
  SetOptions('Area');
{  SetUser1Label('Black');}
  Measure;
  rUser1[rCount]:=histogram[255];
  UpdateResults;
  CopyResults;
  Dispose;
  SelectWindow('Data');
  Paste;
  Write('***');
  WriteLn(' ');
  Write('***');
  WriteLn(' ');
  SelectTool('polygon');
  ResetCounter;
end;



MACRO 'Data window [D]';

BEGIN
  NewTextWindow('Data');
  WriteLn('Total - Myelin');
  WriteLn('');
END;

MACRO 'Temp [1]';

BEGIN
  Copy;
  SetNewSize(800,800);
  MakeNewWindow('temp');
  Paste;
    KillROI;
    SetDensitySlide(156,255);
  SelectTool('wand');
END;


MACRO 'Change Tools  []';


BEGIN
    KillROI;
  SelectTool('magnifier');
END;



MACRO 'Dispose window [X]';

BEGIN
  Dispose;
END;
```

Gait analysis codes

Forelimb

```
{************************************************************************
******
FILE:        Gait - fore limb

CONTENTS: A macro for manual recognition of markers and automatical
calcualtion of angles between them. The Greek letters are representing
the
angles between the bony segments and the horizontal plane.

CODED:  1995-06-01 - 1995-08-31, Utrecht

BY:            F.Szalay
Department of Anatomy & Histology
University of Veterinary Science
Budapest, Hungary
1078 Budapest, Istv‡n u. 2.  P.O.B. 2
E-mail: fszalay@ns.univet.hu
************************************************************************
*****}

 var

x1,x2,x3,x4,y1,y2,y3,y4,x5,y5,x6,y6,x7,y7,x8,y8,x9,y9,x0,y0,frame:integer
;


macro 'Angles Window [W]'

{..................
IT IS NECESSARY TO CREATE A TEXT FILE FOR DATA STORAGE. THIS MACRO MAKES
ONE CALLED 'ANGLES'
.....................}

begin

NewTextWindow('Angles');
  SetFont('Helvetica');
  SetFontSize(12);
  SetText('No background, Center');
   frame:=0;
   Writeln('Frame: ',frame);
end;

macro 'Enhance Contrast[C]'

{..................
OPTIONAL.
.....................}

begin
Sharpen;
end;

macro 'New Frame[N]'
```

```
{..................
THIS MACRO WRITES A NEW HEADER IN 'ANGLES' TEXT FILE.
.....................}

begin;
SelectWindow('Angles');
frame:=frame+1;
frame:=GetNumber('Please, enter the current frame number',frame);
Writeln('Frame: ',frame);
end;
end;

macro 'Extract the ROI [E]';

{..................
IF YOU WANT TO SEE THE MARKERS AS BINARY DOTS WITHOUT THE HORSE AND
ENVIRONMENT USE THIS MACRO. YOU MUST USE AN EXTRA COLOR (RED) TO DISPLAY
THE CENTRE OF THE MARKERS BECAUSE THIS COLOR REMAINS AFTER MAKING BINARY.
.....................}

var
  lower,upper:integer;
begin
  {lower:=GetNumber('Lower:',0);
  upper:=GetNumber('Upper:',7); }
  lower:=0;
  upper:=7;
  SetDensitySlice(lower,upper);
  MakeBinary;
end;


macro '(-'

macro 'Show  Location [1]';

{..................
THIS MACRO GIVES THE COORDINATES OF THE MARKERS WHERE YOU CLICKED.
.....................}

begin
  repeat       {The vibrating text in the Values window indicates, that
the             program is waiting for your click to enter the location
of current marker}
 SetCursor('cross');
 GetMouse(x1,y1);
 ShowMessage('Please, click at the PROXIMAL SCAPULA (1):'x1,y1);
 until button;
end;

macro 'Show  Location [2]';

begin
  repeat       {The vibrating text in the Values window indicates, that
the             program is waiting for your click to enter the location
of current marker}
 SetCursor('cross');
 GetMouse(x2,y2);
 ShowMessage('Please, click at the DISTAL SCAPULA (2):'x2,y2);
 until button;
```

```
end;

macro 'Show  Location [3]';

begin
  repeat       {The vibrating text in the Values window indicates, that
the program is waiting for your click to enter the location of current
marker}
 SetCursor('cross');
 GetMouse(x3,y3);
 ShowMessage('Please, click at the SHOULDER (3):'x3,y3);
 until button;
end;

macro 'Show  Location [4]';

begin
  repeat       {The vibrating text in the Values window indicates, that
the program is waiting for your click to enter the location of current
marker}
 SetCursor('cross');
 GetMouse(x4,y4);
 ShowMessage('Please, click at the PROXIMAL ELBOW (4):'x4,y4);
 until button;
end;

macro 'Show  Location [5]';

begin
  repeat       {The vibrating text in the Values window indicates, that
the program is waiting for your click to enter the location of current
marker}
 SetCursor('cross');
 GetMouse(x5,y5);
 ShowMessage('Please, click at the DISTAL ELBOW (5):'x5,y5);
 until button;
end;

macro 'Show  Location [6]';

begin
  repeat       {The vibrating text in the Values window indicates, that
the program is waiting for your click to enter the location of current
marker}
 SetCursor('cross');
 GetMouse(x6,y6);
 ShowMessage('Please, click at the PROXIMAL CARPUS (6):'x6,y6);
 until button;
end;

macro 'Show  Location [7]';

begin
  repeat       {The vibrating text in the Values window indicates, that
the program is waiting for your click to enter the location of current
marker}
 SetCursor('cross');
 GetMouse(x7,y7);
 ShowMessage('Please, click at the DISTAL CARPUS (7):'x7,y7);
 until button;
```

```
end;

macro 'Show  Location [8]';

begin
  repeat       {The vibrating text in the Values window indicates, that
the program is waiting for your click to enter the location of current
marker}
 SetCursor('cross');
 GetMouse(x8,y8);
 ShowMessage('Please, click at FETLOCK (8):'x8,y8);
 until button;
end;

macro 'Show  Location [9]';

begin
  repeat       {The vibrating text in the Values window indicates, that
the program is waiting for your click to enter the location of current
marker}
 SetCursor('cross');
 GetMouse(x9,y9);
 ShowMessage('Please, click at HOOF (9):'x9,y9);
 until button;
end;

macro 'Show  Location [0]';

begin
  repeat       {The vibrating text in the Values window indicates, that
the program is waiting for your click to enter the location of current
marker}
 SetCursor('cross');
 GetMouse(x0,y0);
 ShowMessage('Please, click at marker 0='x0,y0);
 until button;
end;


macro '(-'

Macro 'Angles[A]'

var
A,O:integer;
n,alpha1,alpha2,beta,gamma,delta,epsilon,scapula,elbow,carpus,fetlock:
real;


begin;

{..................
HERE YOU DEFINE HOW TO CALCULATE ANGLES FROM MARKER COORDINATES.
.....................}

if x2=x1 then alpha1:=90 else
alpha1:=arctan((y2-y1)/(x2-x1))*-180/3.1415926;
if 0 > alpha1 then alpha1:=180+alpha1;

if x3=x1 then alpha2:=90 else
```

```
alpha2:=arctan((y3-y1)/(x3-x1))*-180/3.1415926;
if 0 > alpha2 then alpha2:=180+alpha2;

if x4=x3 then beta:=90 else
beta:=arctan((y4-y3)/(x4-x3))*-180/3.1415926;
if 0 > beta then beta:=180+beta;

if x6=x5 then gamma:=90 else
gamma:=arctan((y6-y5)/(x6-x5))*-180/3.1415926;
if 0 > gamma then gamma:=180+gamma;

if x8=x7 then delta:=90 else
delta:=arctan((y8-y7)/(x8-x7))*-180/3.1415926;
if 0 > delta then delta:=180+delta;

if x9=x8 then epsilon:=90 else
epsilon:=arctan((y9-y8)/(x9-x8))*-180/3.1415926;
if 0 > epsilon then epsilon:=180+epsilon;


{..................
HERE YOU CAN CALCULATE JOINT ANGLES FROM SEGMENTAL ONES.
.....................}

scapula:=alpha2;
elbow:=beta-gamma;
carpus:=gamma-delta;
fetlock:=delta-epsilon;

{..................
THIS PART PLACES THE JOINT ANGLES, SEGMENTAL ANGLES AND MARKER
COORDINATES INTO A TEXT FILE.
.....................}

selectWindows('Angles');
Writeln(scapula:3:3);
Writeln(elbow:3:3);
Writeln(carpus:3:3);
Writeln(fetlock:3:3);

Writeln(alpha2:3:0);
Writeln(beta:3:0);
Writeln(gamma:3:0);
Writeln(delta:3:0);
Writeln(epsilon:3:0);

Writeln(x1,', ',y1);
Writeln(x2,', ',y2);
Writeln(x3,', ',y3);
Writeln(x4,', ',y4);
Writeln(x5,', ',y5);
Writeln(x6,', ',y6);
Writeln(x7,', ',y7);
Writeln(x8,', ',y8);
Writeln(x9,', ',y9);
Writeln(x0,', ',y0);

SelectWindow('Angles');
frame:=frame+1;
frame:=GetNumber('Please, enter the next frame number',frame);
```

```
Writeln('Frame: ',frame);

end;
```

Hindlimb

```
{************************************************************************
******
FILE:        Gait Hindlimb

CONTENTS: A macro for manual recognition of markers and automatical
calcualtion of angles between them. The Greek letters are representing
the
angles between the bony segments and the horizontal plane.

CODED:  1995-06-01 - 1995-08-31, Utrecht

BY:            F.Szalay
Department of Anatomy & Histology
University of Veterinary Science
Budapest, Hungary
1078 Budapest, Istv‡n u. 2.  P.O.B. 2
E-mail: fszalay@ns.univet.hu
************************************************************************
*****}

var
x1,x2,x3,x4,y1,y2,y3,y4,x5,y5,x6,y6,x7,y7,x8,y8,x9,y9,x0,y0,frame:integer
;
UserName:string;
nameofx1:string;
nameofy1:string;
nameofx2:string;
nameofy2:string;
nameofx3:string;
nameofy3:string;
nameofx4:string;
nameofy4:string;
nameofx5:string;
nameofy5:string;
nameofx6:string;
nameofy6:string;
nameofx7:string;
nameofy7:string;
nameofx8:string;
nameofy8:string;
nameofx9:string;
nameofy9:string;
nameofx0:string;
nameofy0:string;


macro 'UserName[U]'

begin;
UserName:=Getstring('You are my current user. Please, enter your name
here.','Feri');
end;
```

```
macro 'SetUp [S]'
var
   a,PWN:integer;

begin;
PWN:=nPics;
if PWN = 0 then exit;
nameofx1:=GetString('Please, enter the name of the marker 1:','TUBER
COXAE');
nameofy1:=nameofx1;
nameofx2:=GetString('Please, enter the name of the marker 2:','TROCHANTER
MAJOR');
nameofy2:=nameofx2;
nameofx3:=GetString('Please, enter the name of the marker 3:','PROXIMAL
STIFLE');
nameofy3:=nameofx3;
nameofx4:=GetString('Please, enter the name of the marker 4:','DISTAL
STIFLE');
nameofy4:=nameofx4;
nameofx5:=GetString('Please, enter the name of the marker 5:','PROXIMAL
HOCK');
nameofy5:=nameofx5;
nameofx6:=GetString('Please, enter the name of the marker 6:','DISTAL
HOCK');
nameofy6:=nameofx6;
nameofx7:=GetString('Please, enter the name of the marker 7:','FETLOCK');
nameofy7:=nameofx7;
nameofx8:=GetString('Please, enter the name of the marker 8:','CORONARY
BAND');
nameofy8:=nameofx8;
nameofx9:=GetString('Please, enter the name of the marker 9:','SOLE');
nameofy9:=nameofx9;
nameofx0:=GetString('Please, enter the name of the marker 0:','');
nameofy0:=nameofx0;

  NewTextWindow('Marker Info',220,170);
  SetFont('Helvetica');
  SetFontSize(12);
  SetText('No background, Center');
   frame:=0;
   Writeln('Marker 1: ',nameofx1);
   Writeln('Marker 2: ',nameofx2);
   Writeln('Marker 3: ',nameofx3);
   Writeln('Marker 4: ',nameofx4);
   Writeln('Marker 5: ',nameofx5);
   Writeln('Marker 6: ',nameofx6);
   Writeln('Marker 7: ',nameofx7);
   Writeln('Marker 8: ',nameofx8) ;
   Writeln('Marker 9: ',nameofx9);
   Writeln('Marker 0: ',nameofx0);
   SelectWindow('Marker Info');
   MoveWindow(0,480);
   NextWindow;

end;


macro '(-'
```

```
macro 'Enhance Contrast[C]'

{..................
OPTIONAL.
.....................}

begin
Sharpen;
end;


macro 'Extract the Horse [E]';

{..................
IF YOU WANT TO SEE THE MARKERS AS BINARY DOTS WITHOUT THE HORSE AND
ENVIRONMENT USE THIS MACRO. YOU MUST USE AN EXTRA COLOR (RED) TO DISPLAY
THE CENTRE OF THE MARKERS BECAUSE THIS COLOR REMAINS AFTER MAKING BINARY.
.....................}

var
  lower,upper:integer;
begin
  {lower:=GetNumber('Lower:',0);
  upper:=GetNumber('Upper:',7); }
  lower:=0;
  upper:=7;
  SetDensitySlice(lower,upper);
  MakeBinary;
end;


macro '(-'

macro 'Point at marker [1]';

{..................
THIS MACRO GIVES THE COORDINATES OF THE MARKERS WHERE YOU CLICKED.
.....................}

begin
  repeat       {The vibrating text in the Values window indicates, that
the              program is waiting for your click to enter the location
of current marker}
 SetCursor('cross');
 GetMouse(x1,y1);
 ShowMessage('Please, click at marker 1:'x1,y1);
 until button;
end;

macro 'Point at marker [2]';

begin
  repeat       {The vibrating text in the Values window indicates, that
the              program is waiting for your click to enter the location
of current marker}
 SetCursor('cross');
 GetMouse(x2,y2);
 ShowMessage('Please, click at marker 2:'x2,y2);
 until button;
```

```
end;

macro 'Point at marker [3]';

begin
  repeat       {The vibrating text in the Values window indicates, that
the program is waiting for your click to enter the location of current
marker}
 SetCursor('cross');
 GetMouse(x3,y3);
 ShowMessage('Please, click at marker 3:'x3,y3);
 until button;
end;

macro 'Point at marker [4]';

begin
  repeat       {The vibrating text in the Values window indicates, that
the program is waiting for your click to enter the location of current
marker}
 SetCursor('cross');
 GetMouse(x4,y4);
 ShowMessage('Please, click at marker 4:'x4,y4);
 until button;
end;

macro 'Point at marker [5]';

begin
  repeat       {The vibrating text in the Values window indicates, that
the program is waiting for your click to enter the location of current
marker}
 SetCursor('cross');
 GetMouse(x5,y5);
 ShowMessage('Please, click at marker 5:'x5,y5);
 until button;
end;

macro 'Point at marker [6]';

begin
  repeat       {The vibrating text in the Values window indicates, that
the program is waiting for your click to enter the location of current
marker}
 SetCursor('cross');
 GetMouse(x6,y6);
 ShowMessage('Please, click at marker 6:'x6,y6);
 until button;
end;

macro 'Point at marker [7]';

begin
  repeat       {The vibrating text in the Values window indicates, that
the program is waiting for your click to enter the location of current
marker}
 SetCursor('cross');
 GetMouse(x7,y7);
 ShowMessage('Please, click at marker 7:'x7,y7);
 until button;
```

```
end;

macro 'Point at marker [8]';

begin
  repeat       {The vibrating text in the Values window indicates, that
the program is waiting for your click to enter the location of current
marker}
 SetCursor('cross');
 GetMouse(x8,y8);
 ShowMessage('Please, click at marker 8:'x8,y8);
 until button;
end;

macro 'Point at marker [9]';

begin
  repeat       {The vibrating text in the Values window indicates, that
the program is waiting for your click to enter the location of current
marker}
 SetCursor('cross');
 GetMouse(x9,y9);
 ShowMessage('Please, click at marker 9:'x9,y9);
 until button;
end;

macro 'Point at marker [0]';

begin
  repeat       {The vibrating text in the Values window indicates, that
the program is waiting for your click to enter the location of current
marker}
 SetCursor('cross');
 GetMouse(x0,y0);
 ShowMessage('Please, click at marker 0='x0,y0);
 until button;
end;


macro '(-'

macro 'Angles Window [W]'

{..................
IT IS NECESSARY TO CREATE A TEXT FILE FOR DATA STORAGE. THIS MACRO MAKES
ONE CALLED 'ANGLES'
.....................}

begin;
NewTextWindow('Angles',200,400);
  SetFont('Helvetica');
  SetFontSize(12);
  SetText('No background, Center');
   frame:=0;
   Writeln('Frame: ',frame);
   MoveWindow(500,200);
   NextWindow;
   PutMessage('These data can be converted to a COMMA DELIMITED FILE in
Excel, or whatever.');
end;
```

```
Macro 'Write Angles[A]'

var
A,O,m:integer;
n,alpha,beta,gamma,delta,epsilon,pelvis,hip,stifle,tarsus,fetlock: real;
{pelvis= pelvis rotation, hip= hip joint, stifle=stifle joint,
tarsus=tarsus joint, fetlock=fetlock joint}

begin;

{..................
HERE YOU DEFINE HOW TO CALCULATE ANGLES FROM MARKER COORDINATES.
.....................}

if x2=x1 then alpha:=90 else
alpha:=arctan((y2-y1)/(x2-x1))*-180/3.1415926;
if 0 > alpha then alpha:=180+alpha;

if x3=x2 then beta:=90 else
beta:=arctan((y3-y2)/(x3-x2))*-180/3.1415926;
if 0 > beta then beta:=180+beta;

if x5=x4 then gamma:=90 else
gamma:=arctan((y5-y4)/(x5-x4))*-180/3.1415926;
if 0 > gamma then gamma:=180+gamma;

if x7=x6 then delta:=90 else
delta:=arctan((y7-y6)/(x7-x6))*-180/3.1415926;
if 0 > delta then delta:=180+delta;

if x8=x7 then epsilon:=90 else
epsilon:=arctan((y8-y7)/(x8-x7))*-180/3.1415926;
if 0 > epsilon then epsilon:=180+epsilon;


{..................
HERE YOU CAN CALCULATE JOINT ANGLES FROM SEGMENTAL ONES.
.....................}

pelvis:=alpha;
hip:=alpha-beta;
stifle:=beta-gamma;
tarsus:=gamma-delta;
fetlock:=delta-epsilon;

{..................
THIS PART PLACES THE JOINT ANGLES, SEGMENTAL ANGLES AND MARKER
COORDINATES INTO A TEXT FILE.
.....................}

if nPics = 0 then exit;
{Close;}
selectWindows('Angles');
Writeln(pelvis:3:3);
Writeln(hip:3:3);
Writeln(stifle:3:3);
Writeln(tarsus:3:3);
Writeln(fetlock:3:3);
```

```
Writeln('Segmental angles');
Writeln(alpha);
Writeln(beta);
Writeln(gamma);
Writeln(delta);
Writeln(epsilon);

Writeln('Coordinates');
Writeln(x1,',',y1);     {COMMA DELIMITED FILE !!!}
Writeln(x2,',',y2);
Writeln(x3,',',y3);
Writeln(x4,',',y4);
Writeln(x5,',',y5);
Writeln(x6,',',y6);
Writeln(x7,',',y7);
Writeln(x8,',',y8);
Writeln(x9,',',y9);
Writeln(x0,',',y0);

SelectWindow('Angles');
frame:=frame+1;
frame:=GetNumber('Please, enter the current frame number',frame);
Writeln('Frame: ',frame);
{Open('Macintosh HD: PICT 0');}


end;

macro 'New Frame[N]'

{.................
THIS MACRO WRITES A NEW HEADER IN ROWS OF 'ANGLES' TEXT FILE.
.....................}


begin;
SelectWindow('Angles');
frame:=frame+1;
frame:=GetNumber('Please, enter the current frame number',frame);
Writeln('Frame: ',frame);
NextWindow;
end;
```